

INHIBITION OF ALZHEIMER'S TYPE TOXIC AGGREGATES OF TAU WITH FUNGAL
SECONDARY METABOLITES

By

©2015

Smita Ramesh Paranjape

Submitted to the graduate degree program in Molecular Biosciences and the Graduate Faculty of
the University of Kansas in partial fulfillment of the requirements for the degree of Doctor of
Philosophy.

Chairperson Dr. Truman Christopher Gamblin

Dr. Berl Oakley

Dr. Kristi Neufeld

Dr. Erik Lundquist

Dr. Yoshiaki Azuma

Dr. Eli Michaelis

Date Defended: July 7, 2015

The Dissertation Committee for Smita Ramesh Paranjape
certifies that this is the approved version of the following dissertation:

Inhibition of Alzheimer's type toxic aggregates of tau with fungal secondary metabolites

Chairperson Dr. Truman Christopher Gamblin

Date approved: 7/21/15

Abstract

Tau is a microtubule-associated protein that is typically found in the axons of neurons. The aggregation of the tau is a significant event in many neurodegenerative diseases including Alzheimer's disease. In these disease tau dissociates from microtubules and begins to form toxic insoluble intracellular tau aggregates. The process of conversion of soluble monomeric tau to insoluble aggregates is not well understood. Differential conformational changes in pathological forms of the protein may affect its propensity for aggregation and function. Post translational modifications such as hyperphosphorylation or truncation may induce these conformational changes and alter aggregation and function. The studies described here used in vitro assays to determine how truncation affects tau conformation and how they can alter aggregation and function. This information helps to describe how intrinsic differences due to modifications of tau can manifest themselves in the varying pathologies of tauopathies. Tau aggregation is a common mode of pathogenesis in tauopathies, including Alzheimer's disease. Tau aggregation correlates with dementia and neurodegeneration and is viewed as a potential therapeutic target for AD. Fungi have historically been a good source of medicinally important compounds. We identified secondary metabolites obtained from *Aspergillus nidulans* as tau aggregation inhibitors. We identified a novel class of tau aggregation inhibitors, azaphilones. Four of the azaphilones inhibited tau aggregation and disassembled pre-formed tau aggregates without inhibiting tau's ability to polymerize microtubules. Preliminary NMR studies showed that our most potent azaphilone, aza-9 interacts with specific residues of tau protein in a dose dependent fashion. Aza-9 also disassembled tau aggregates formed by aggregation enhancing truncation mutant 1-391 in a dose dependent fashion. Azaphilones are therefore very promising lead

compounds for tau aggregation inhibitors, provide a novel scaffold for the same and represent a new class of compounds with tau aggregation inhibitor activity.

Acknowledgements

I would like to thank my mentor, Dr. Chris Gamblin for his support and guidance throughout my graduate career. He was always very approachable and helpful. I am glad to have had the opportunity to work under his guidance.

I would like to thank all my committee members. They always gave valuable suggestions and comments which helped me in my projects and also in my overall development. I would like to especially thank Dr. Berl Oakley, who served as my reader and also provided guidance in the projects involving compounds provided by his lab.

I would like to thank Dr. De Guzman and his lab members for assisting with the NMR experiments and analyzing the data. I would like to thank Andrew Riley and Dr. Tom Prisinzano, for providing the compounds used in our study. I would like to thank the Oakley lab members, especially Liz Oakley and Dr. Ruth Entwistle for their help and contributions in the projects involving *Aspergillus nidulans* secondary metabolites.

I would like to thank all my lab members past and present for their support and friendship. Dr. Ben Combs helped me in getting acquainted with the lab settings techniques during my first two years at KU. I'll like to thank Yamini Mutreja, Dr. Mythili Yenjerla, Bryce Blankenfeld, and Adam who have assisted me in my research projects, helped me prepare for presentations and were always ready to help when needed. I would like to thank Dakota Bunch, an undergraduate in our lab who specifically helped me make the tau truncation constructs.

Finally, I would like to thank my family for always encouraging me to pursue my dreams. I cannot imagine reaching this point in life without their love and support.

Table of contents

Chapter I Introduction.....	1
1.1 Tau Introduction.....	1
1.2 Tau structure.....	1
1.3 Tau function	2
1.4 Tau aggregation.....	4
1.5 Alzheimer’s disease and other tauopathies	6
1.5.1 Alzheimer’s disease.....	6
1.5.2 Frontotemporal Dementia with Parkinsonism Linked to Chromosome 17 (FTDP-17) .	9
1.5.3 Pick’s disease (PiD).....	9
1.5.4 Progressive supranuclear palsy (PSP)	9
1.5.5 Corticobasal degeneration (CBD)	10
1.5.6 Argyrophilic grain disease (AGD)	10
1.6 Post translational modifications	11
1.6.1 Phosphorylation	11
1.6.2 Glycosylation.....	11
1.6.3 Acetylation.....	12
1.6.4 Ubiquitination and Oxidation	12
1.6.5 Tau truncations	12
1.7 Inducing tau aggregation <i>in vitro</i>	13
1.8 Treatment for AD and other tauopathies.....	14
1.8.1 Currently available FDA approved drugs.....	15
1.8.2 Therapeutic strategies aimed at targeting underlying molecular mechanisms in AD ..	16
1.9 Tau based therapeutics	19
1.9.1 Inhibiting tau phosphorylation.....	19
1.9.2 MT stabilization.....	22
1.9.3 Enhancement of tau clearance mechanisms	23
1.9.4 Inhibition of tau pathology propagation	24
1.9.5 Tau aggregation inhibitors.....	25
1.10 Thesis overview.....	28
Chapter II Effects of tau truncations on Aggregation and Microtubule Interactions	31
2.1 Introduction	31

2.2 Experimental Procedures	37
2.3 Results	41
2.4 Discussion.....	51
3.1 Introduction	62
3.2 Experimental procedures	64
3.3 Results	68
3.5 Discussion.....	82
Chapter IV Azaphilones as tau aggregation inhibitors: Second generation compounds obtained from <i>Aspergillus nidulans</i>	86
4.1 Introduction	86
4.2 Experimental procedures	87
4.3 Results	92
4.4 Discussion.....	107
Chapter V: Using NMR to determine interaction between Aza-9 and tau protein.....	115
5.1 Introduction	115
5.2 Experimental procedures	117
5.3 Results:	119
5.4 Discussion.....	130
Chapter VI Aza 9 is effective against aggregation enhancing truncation mutant 1-391	132
6.1 Introduction	132
6.2 Experimental procedures	134
6.3 Results	136
6.4 Discussion.....	139
7.1 Introduction	143
7.2 Tau truncations	144
7.3 Azaphilones obtained from <i>Aspergillus nidulans</i> as tau aggregation inhibitors	146
7.4 Future directions	147
Bibliography	152

Chapter I Introduction

1.1 Tau Introduction

Tau protein was identified from brain tissue by Weingarten et al. in 1975 as a microtubule associated protein (MAP) that promoted microtubule assembly¹. Tau is one of the MAPs among the family of structural MAPs, including MAP1, MAP2, MAP4 and MAP6 which were first described as microtubule-stabilizing proteins²⁻⁴. Tau is a natively unfolded protein mainly found in neuronal axons where it binds to microtubules, is involved in their assembly and stabilization and in regulation of motor-driven axonal transport^{5, 6}. In the year 1986, several reports came out showing that tau protein was a component of the neurofibrillary tangles (NFTs) or paired helical filaments (PHFs) found in brains of patients suffering from Alzheimer's disease (AD)⁷⁻⁹. Phosphorylated tau protein was a major antigenic determinant of PHFs¹⁰. In the next few decades, tau was seen to play a major role in pathogenesis of a range of diseases, collectively called tauopathies¹¹⁻¹³. It is now known that tau aggregation plays a major role in disease pathogenesis in AD and other tauopathies. Post translational modifications of tau protein such as phosphorylation¹⁴, truncation¹⁵, ubiquitination¹⁶, acetylation¹⁷, glycosylation¹⁸, and oxidation¹⁹ may have a causative role in tau aggregation. The effects of many of these modifications on aggregation are not well-characterized as yet.

1.2 Tau structure

The human tau gene is mainly expressed in the neurons of the central nervous system and the protein itself typically localizes to the axons of the neurons but can be found in the somatodendritic compartment as well. Six isoforms of tau protein are expressed in the adult human brain. The six isoforms are the product of alternative splicing from a single gene [*MAPT* (microtubule-associated protein tau)] located on chromosome at position 17q21.31^{20, 21}. The

isoforms differ from each other by the presence or absence of exon 10 at the C-terminal creating 3-repeat and 4 –repeat isoforms of tau respectively (Figure 1). The 3R and 4R isoforms further differ by the absence of exons 2 and 3 at the N-terminal or presence of one or two of the same. The 3R and 4R isoforms are present in a 1:1 ratio in the cerebral cortex of healthy adults ²².

Tau has very little secondary structure and has been described as a natively unfolded or intrinsically disordered protein^{23, 24}. As seen in figure 1.1, the tau N-terminal domain contains exons E2 and E3. It is also called the projection domain of tau because upon binding to tubulin, the N terminal of tau projects away from the surface of the microtubule. The N-terminal domain of tau is followed by a proline-rich region. The proline rich region is relatively basic because of its high glycine and proline content. It is predicted that this region could play a role in spacing of microtubules allowing the cargo to travel through the axon by contracting and expanding the microtubule cytoskeleton to allow easier passage²⁵. The C-terminal of tau protein contains the microtubule binding repeat (MTBR) region and therefore plays a major role in binding of tau to microtubules²⁶. The presence of 3 or 4 MTBRs influences the binding affinity of tau isoforms to microtubules. These domains of tau play specific roles in the process of tau aggregation.

1.3 Tau function

Tau promotes formation of axonal microtubules, stabilizes them, and drives neurite outgrowth ²⁷. A recent study showed that tau remains highly dynamic when bound to microtubules and small groups of tau residues bind tightly to microtubules, while the intervening parts stay flexible²⁸. In neurons, microtubules act as tracks connecting the cell body and the tip of the axons, to transport cargo such as mitochondria²⁹, lysosomes³⁰, peroxisomes³¹ and many other endocytotic or exocytotic vesicles via the motor proteins, kinesins and dyneins.

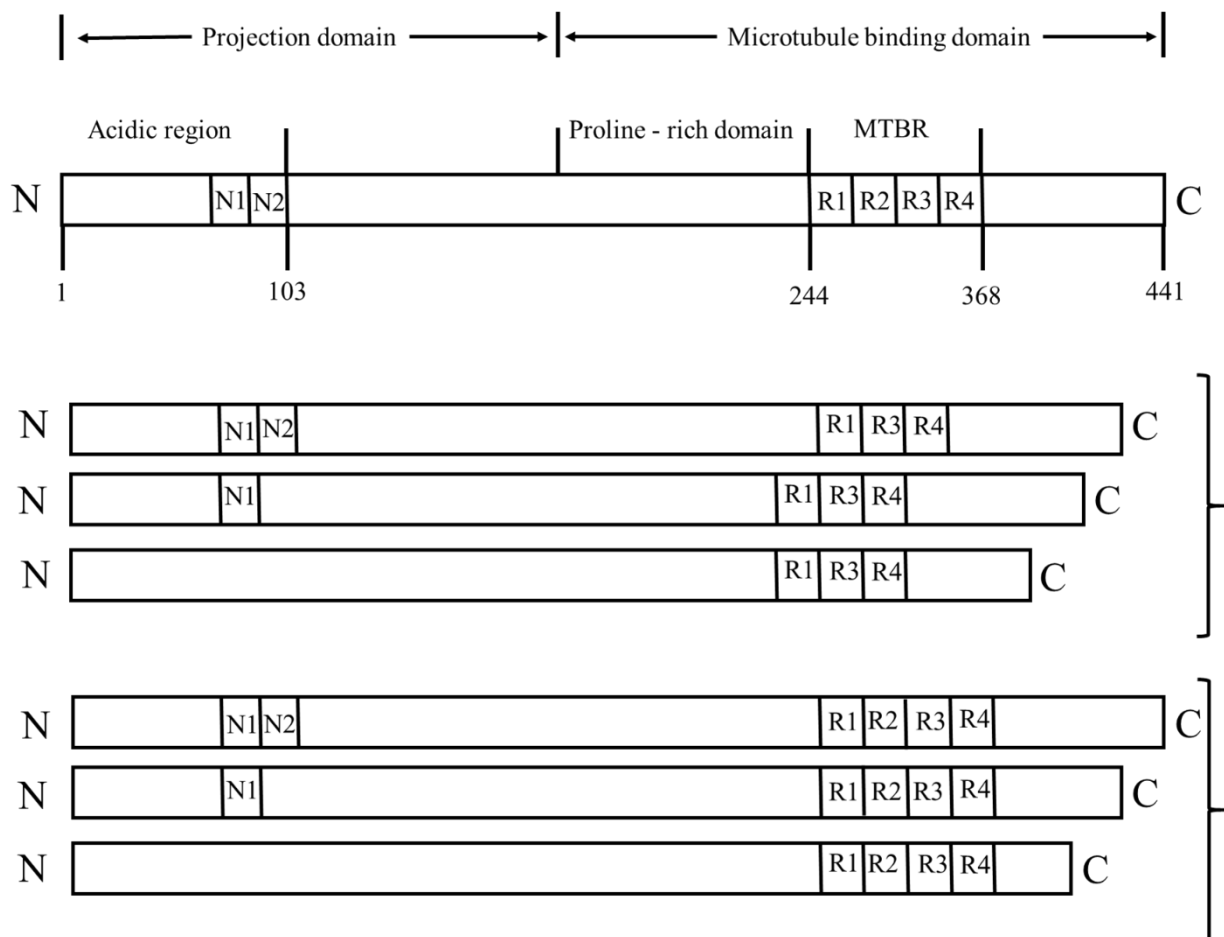
Figure 1.1

Figure 1.1 Tau protein structure. The human full length tau protein consists of 441 amino acids. The N-terminal region consists of exons 2 and 3 shown as N1 and N2 respectively in this diagram. The C-terminal region consists of four microtubule binding repeat (MTBR) domains. There is a proline-rich domain right before the MTBR region. The C-terminal domain along with the proline rich region is also called the microtubule binding domain. Exon 10 codes for the second repeat domain R2. In the human brain six tau isoforms are generated through alternative mRNA splicing of exons 2, 3, and 10 and range from 352 to 441 amino acids in length. The 3-repeat isoforms and 4-repeat isoforms have been shown in the figure.

Therefore, tau helps in maintaining axonal transport and cell shape³². Overexpression of tau preferentially slows down the plus-end directed intracellular transport mediated by kinesin motor proteins^{33, 34}. The minus-end transport involving dynein is less affected by tau expression levels. Tau also has other functions such as membrane interactions or anchoring of enzymes. The N-terminal projection domain has an important role in neuritic development and it mediates the interactions between the plasma membrane and microtubules³⁵. Tau is also involved in signal transduction pathways which could affect the spatial distribution of MTs³⁶, and also have structural interactions with phosphatases and MTs which might control the phosphorylation state of tau³⁷. Tau affects MT bundling and spacing which is known to be affected by the sizes of the tau isoforms³⁸. Tau interacts with specific chaperone proteins which affect the functions of tau such that they may suppress the formation of NFTs³⁹.

1.4 Tau aggregation

In the diseased state, tau is altered such that it loses its ability to bind to microtubules and is consequently released from microtubules. This leads to destabilization of microtubules and, in addition the unbound tau molecules form intracellular toxic tau aggregates. Therefore, conversion of soluble monomeric tau into insoluble tau aggregates, potentially results in both loss-of-function and gain-of-function toxicities⁴⁰. Tau molecules undergo a series of post-translational modifications and conformational changes in neurons to attain a pro-aggregation tau conformation⁴¹. Tau aggregation plays a major role in pathogenesis of Alzheimer's disease and other tauopathies. Tau aggregation correlates with the type and severity of cognitive impairment in Alzheimer's disease⁴², and tau aggregation can lead to cell death and cognitive defects in cellular and animal models (reviewed in⁴³).

Tau aggregates are found in different forms including paired helical filaments (PHFs), straight filaments (SF) and twisted ribbons. PHFs arise from aggregation of tau monomers and have a highly ordered β -sheet structure at their core. The tau molecules bind to each other via hexapeptide motif regions to form these β -sheet structures. The hexapeptide motifs can by themselves induce β -sheet formation leading to formation of tau aggregates and can act as seeds to induce full length tau molecules to aggregate^{44, 45}. These motifs are found in the microtubule-binding repeat region (MTBR) of tau protein. The hexapeptide motif regions are ²⁷⁵VQIINK²⁸⁰ which is referred to as the PHF6* motif, and the ³⁰⁶VQIVYK³¹¹ which is referred to as the PHF6 motif. The tau aggregation process takes place in two steps – nucleation and elongation. In the nucleation phase, tau monomers come together to form small oligomeric species of tau. Tau oligomers are known to be soluble and are more prevalent in human AD brain samples than was predicted before. Tau oligomers in human AD brain samples were 4-fold higher than those in the controls and the oligomers were seen to play a role in the frontal cortex tissue from AD brains⁴⁶. The oligomers act as seeds that incorporate more tau monomers to form larger, fibrous aggregates. This is the elongation phase of tau aggregation. Tau aggregates have a core region which mainly contains regions of the protein around the hexapeptide motifs described above, and the core is surrounded by a ‘fuzzy coat’ which includes the N- and C-terminal regions of the protein⁴⁷. Aggregates have different morphologies in different tauopathies, for example – NFTs in AD, Pick bodies in Pick’s disease and globose tangles in Progressive Supranuclear Palsy (PSP)^{48, 49}.

There are many unanswered questions about tau aggregation. We do not know the exact mechanism for the conversion of monomeric tau to aggregated tau. Several studies have been carried out trying to understand the roles post-translational modifications of tau including

phosphorylation and truncations, play in aggregation. Tau aggregates are variable in their length and morphology. They can be long filaments or small oligomers or a combination of both. We do not have conclusive evidence as to whether the long filaments, small oligomer aggregates, a combination of both or intermediate length filaments are the toxic species. Recently however finding supporting that the small oligomeric species are in fact the toxic species of tau have emerged⁵⁰.

1.5 Alzheimer's disease and other tauopathies

Tauopathies are a group of neurodegenerative diseases that are characterized by the presence of aggregates of tau, usually containing abnormally phosphorylated tau. The neurodegeneration is generally caused due to loss of tau's ability to associate with microtubules⁵¹. Tauopathies can be differentiated based on the morphologies of the tau aggregates, the cell types affected, the location of tau aggregates in the brain and the related symptoms that correlate with the specific brain regions affected. The major tauopathies include Alzheimer's disease, Frontotemporal Dementia with Parkinsonism Linked to Chromosome 17 (FTDP-17), Pick's disease (PiD), progressive supranuclear palsy (PSP), Corticobasal degeneration (CBD) and argyrophilic grain disease (AGD).

1.5.1 Alzheimer's disease

Alzheimer's disease is the most common type of dementia that typically occurs in late adult life. It mainly causes problems with memory, thinking and behavior. The symptoms get worse with time, eventually reaching a point where they start interfering with everyday tasks, and ultimately can lead to death. The main pathogenic hallmarks of AD are presence of extracellular amyloid plaques primarily containing amyloid- β ($A\beta$) peptide and intracellular tau aggregates in the

brain⁵². The presence of tau aggregates is observed before the appearance of amyloid plaques and the amount of tau aggregation correlates well with disease progression and the loss of neuronal axons⁵³. There is also a less likely possibility that tangles and plaques appear independent of each other. The tau aggregates are made up of all the six isoforms of tau and these isoforms are present in approximately the same proportions as are found in a normal brain⁵⁴.

The AD process begins in the axons and the tau lesions are mainly localized within the entorhinal region of the temporal lobe⁵⁵. The tau aggregation then spreads to, and is restricted, to a few regions in medial portions of the temporal lobe. At this stage, some patients with mild cognitive impairment are diagnosed⁵⁶. At the final stages of AD tau aggregation is seen in all cortical regions and severe lesions can be observed on Gallyas silver staining and AT8 immunoreactivity studies⁵⁷. Monoclonal antibody AT8 recognizes tau protein phosphorylated at both serine 202 and threonine 205⁵⁸. At this stage usually initial provisional clinical AD diagnosis is made. Also, there is a theory of possible disease progression of pathogenic molecules of abnormal tau or oligomeric tau aggregates from the locus coeruleus to the transentorhinal region of the cerebral cortex via neuron-to-neuron transmission and transsynaptic transport⁵⁹.

The other main component of AD is A β - amyloid plaques. The amyloid hypothesis states that the soluble A β fragments are synaptotoxic and lead to formation of plaques and subsequently also play a role in development of intracellular NFTs. The gene coding for the amyloid precursor protein (APP) is located on chromosome 21. Triplication of this chromosome leads to increased prevalence of dementia in older people with Down syndrome⁶⁰. 5% of AD cases are early-onset AD due to mutations in one of three genes: those encoding amyloid precursor protein (APP) and

presenilins 1 and 2⁶¹. Presenilins 1 and 2 are part of the protease complex that cleaves the APP to generate A β pathology in AD. The best known genetic risk factor of AD is the inheritance of the ϵ 4 allele of the apolipoprotein E (APOE), which is associated with lipid metabolism.

There have been many studies done to understand the relationship between tau aggregation and the amyloid cascade hypothesis – do these processes occur independently of each other, does tau aggregation precede amyloid plaque formation or is it the other way around? Studies using crosses of transgenic mice expressing mutant tau gene and mutant APP gene have shown that there is definite interaction between A β and tau that leads to increased NFT formation and distribution in regions of brain vulnerable to these lesions⁶². There are no tau mutations that are directly associated with AD unlike those in the APP gene. Therefore, many investigators and pharmaceutical companies believe that A β is a very promising target for disease therapy in Alzheimer's disease.

Meanwhile, there is strong evidence showing that tau plays a major role in AD disease pathogenesis. NFT accumulation more closely reflects antemortem clinical manifestations of the disease than plaque pathology^{42, 63}. Specific mutations in the tau gene have been associated with a certain type of tauopathy now recognized as frontotemporal dementia with Parkinson linked chromosome 17 (FTDP-17)^{64, 65}. Overexpression of wild-type tau or aggregation-enhancing mutant tau constructs in cellular or animal models has been shown to induce toxicity⁶⁶. In transgenic AD mouse models, the presence of tau is necessary along with A β to exert toxic effects⁶⁷. Further, reducing tau expression in these mice models leads to recovery from memory deficits⁶⁸.

1.5.2 Frontotemporal Dementia with Parkinsonism Linked to Chromosome 17 (FTDP-17)

FTDP-17 is a group of disorders caused due to mutations in the tau gene. The patients suffer from cognitive, behavioral and motor disturbances. It is characterized by superficial cortical spongiform changes, frontotemporal atrophy with loss of neuronal cells and white and grey matter gliosis. Tau aggregates are seen in the brains of these patients⁶⁹. There are 10 silent mutations and 31 missense mutations known in the tau gene that may lead to early-onset tauopathies. The FTDP-17 mutants have differential effects on tau aggregation and on tau's ability to interact with microtubules. For example, P301L mutant aggregates at a much faster rate compared to wild type full length tau protein.

1.5.3 Pick's disease (PiD)

PiD accounts for 0.4% to 2% of all the cases of dementia. The patients exhibit clinical abnormalities such as behavioral changes, language disruptions and problems with executive functions such as planning and organization. Neuroimaging shows focal cortical atrophy and hypoperfusion in the frontal and temporal lobes upon functional imaging, widespread degeneration of the white matter, chromatolytic neurons and the presence of Pick bodies (PB)⁷⁰.⁷¹ Tau proteins are the main cytoskeletal components that are modified during the neurodegenerative changes⁷². They aggregate into straight and random filaments in PBs and the aggregates are made up almost exclusively of hyperphosphorylated 3R tau isoforms with the exception of serine 262. S262 is phosphorylated in AD but not in Pick bodies^{73, 74}.

1.5.4 Progressive supranuclear palsy (PSP)

Patients suffering from PSP mainly show movement disorders along with personality changes, loss of balance, eye movement and difficulties in swallowing⁷². In PSP, globose neurofibrillary

tangles are found in the subcortical areas and occasionally in the central cortex and spinal cord. The neuritic changes are mainly displayed in the basal ganglia, subthalamus and brainstem regions but not in the frontal cortex like AD⁷⁵. In the NFTs tau forms straight filaments and tubules that are different from the paired helical filaments found in AD⁷⁵. In PSP, the levels of tau mRNA isoforms containing exon 10 are increased in the brainstem but not the frontal cortex or cerebellum. Therefore this may lead to an increase in four-repeat tau protein isoforms that may contribute to the formation of NFTs in PSP⁷⁶.

1.5.5 Corticobasal degeneration (CBD)

CBD is a rare sporadic neurodegenerative disorder that is characterized by widespread neuronal and glial accumulation of tau aggregates mainly consisting of the 4R tau isoforms. The aggregates are composed of PHF and SF-like filaments that combine to form inclusions as well as neuropil threads. Neuropil threads are a group of fibrils that are identified by tau-specific antibodies and are associated with neurite projections^{77, 78}. The clinical manifestations of CBD are diverse with progressive asymmetrical rigidity and apraxia, progressive aphasia, impaired ocular movements, and dementia⁷⁹.

1.5.6 Argyrophilic grain disease (AGD)

AGD is a sporadic late-onset dementia that usually presents in combination with other sporadic tauopathies including AD pathology. It is a 4R tauopathy characterized by abundant neuropil grains (ArGs)⁸⁰. The main constituent of ArGs is abnormally phosphorylated tau and they are mainly found in the entorhinal and transentorhinal cortices, the amygdala and the hypothalamic lateral tuberal nuclei. Additional neuropathological features include ballooned neurons and astrocytic tau pathology⁸¹.

1.6 Post translational modifications

Tauopathies are characterized by the presence of aggregated tau deposits, but the causes or mechanisms of tau aggregation in sporadic tauopathies are not fully understood. Tau undergoes post translational modifications that could play a role in making tau more prone to aggregation or in reducing tau's ability to bind to microtubules. Therefore, studying the effects of these post translational modifications may help in understanding the aggregation mechanisms. These modifications include phosphorylation, truncation, ubiquitination, acetylation, glycosylation and oxidation.

1.6.1 Phosphorylation

Full length tau has around 80 phosphorylation sites which means 20% of the molecule has the potential to be phosphorylated. Tau protein purified from AD brains has increased phosphorylation compared to that in normal healthy brains⁸². Tau is phosphorylated at 2 to 3 sites in the healthy brain but can have around 5-9 moles of phosphate per mole of tau in protein purified from AD brains⁸². Abnormal tau phosphorylation reduces microtubule binding^{83, 84} and may enhance aggregation^{85, 86}. Phosphorylation of tau in the brain is mainly regulated via kinases such as glycogen synthase kinase 3 (GSK3) and protein kinase A (PKA)^{10, 87} and phosphatases including are phosphoprotein phosphatase 2A (PP2A) and PP-1⁸⁸. Therefore changes in protein kinase and/or protein phosphatase activities could enhance tau phosphorylation causing loss-of function and/or gain-of function toxicities.

1.6.2 Glycosylation

The pathogenesis of tau in AD not only involves hyperphosphorylation but also glycosylation of tau in PHFs. Studies show a correlation between tau phosphorylation and glycosylation. The

glycosylation of tau is an early abnormality that could facilitate the subsequent abnormal hyperphosphorylation of tau in the AD brain⁸⁹. Glycosylation of tau increases the stability of the PHF structure and also might induce oxidative stress, thereby contributing to pathogenesis in AD¹⁸.

1.6.3 Acetylation

Tau acetylation is another post translational modification which has not been well characterized. It was reported that the amount of tau acetylation is enhanced in patients at early stages of tau pathology and contributes to accumulation of phosphorylated tau⁹⁰. Tau acetylation impairs tau-microtubule interactions thereby inhibiting tau function and it promotes pathological tau aggregation. The lysine residue (K280) within the microtubule-binding motif has been identified as a major site of tau acetylation¹⁷. Therefore, modulation of tau acetylation could be a potential therapeutic strategy towards tauopathies.

1.6.4 Ubiquitination and Oxidation

Ubiquitination of tau is the first line of defense against tau accumulation. Therefore, ubiquitinated tau in NFTs could indicate that the cell was unable to degrade the protein due to the presence of protease- and proteasome resistant tau aggregates^{16, 91}. Finally, oxidation of tau at Cysteine-322 affects tau conformation and aggregation as well¹⁹.

1.6.5 Tau truncations

Tau undergoes conformational changes when it transforms from its monomeric state to begin the aggregation/ polymerization process. The discovery of antibodies Alz-50 and MC-1 which identify specific conformations of tau supported this theory of conformational change. The folding of the tau molecule is accompanied by proteolytic truncation at both ends of the molecule⁹². The first evidence of truncated tau in AD brains was provided by mAb 423 that

recognized only tau proteins C-terminally truncated at Glu391 and decorated NFTs obtained from brains of AD patients⁹³. Therefore it was established that truncated tau is a part of the pathological process of tau aggregation in AD⁹⁴. In AD brains, tau truncations are known to occur at D13, E391 and D421^{95,96}. The accumulation of truncated tau correlates with disease progression therefore may be contributing to the process of tau aggregation in AD brains^{97, 98}.

The amino and carboxyl termini play an important role in the process of tau aggregation.

Portions of the N-terminus are necessary for the formation of the aggregated tau conformation and impact tau polymerization. Removal of the N-terminus leads to a decrease in the amount of tau aggregation⁹⁹. The C-terminus of tau inhibits filament formation *in vitro*. Therefore, truncation of the C-terminal domain of tau aggravates tau aggregation¹⁰⁰. The exact roles of the N- and C- termini have not been understood very well and further characterization is needed to understand their exact role in the aggregation mechanism.

1.7 Inducing tau aggregation *in vitro*

As mentioned previously, tau aggregation plays a major role in pathogenesis of tauopathies. It is therefore important to understand the molecular mechanisms that lead to abnormal aggregation of tau. It will help in development of better therapeutics targeting these underlying molecular mechanisms of pathogenesis. Monomeric tau has a very high energy barrier for aggregation. Even at very high concentrations, monomeric tau does not aggregate by itself. Therefore an inducer molecule is required to overcome this energy barrier and cause tau to aggregate. Inducer molecules such as heparin and arachidonic acid (ARA) are therefore used to drive rapid self-association of tau molecules.

Inducer molecules fall into two major groups – polyanions including heparin¹⁰¹, polyglutamate¹⁰², RNA¹⁰³ and fatty acid-like molecules including arachidonic acid (ARA)¹⁰⁴, docosahexaenoic acid¹⁰⁵ and alkyl sulfonate detergents¹⁰⁶. The exact mechanism by which these molecules induce tau aggregation is not completely understood as yet, although one hypothesis is that clustering of the negative charges on the inducers could provide a template for the positively charged tau molecule to bind to and assemble²⁵. The two most commonly used inducer molecules are ARA and heparin.

Heparin promotes polymerization of truncated tau containing mainly MTBR at a higher efficiency than polymerization of full length tau¹⁰¹. Further, elimination of a cysteine under oxidizing conditions enhances the polymerization by heparin. Heparin induced tau aggregation is enhanced by formation of tau dimers through cysteine cross-linking and inhibited via intramolecular cysteine cross-linking at position 291 and 322¹⁰⁷. The filaments formed from heparin induction have morphological characteristics similar to PHFs²⁵.

ARA induces tau aggregation of the full length tau protein at an efficient rate compared to heparin and also at physiological concentrations of tau¹⁰⁷. The filament morphology is that of straight filaments but they have a high degree of structural similarity to PHFs supported by the fact that they are recognized by antibodies and fluorescent dyes that react with autopsy-derived PHFs and those induced by heparin. Finally, ARA induced filaments can nucleate from PHFs obtained from human AD brain¹⁰⁸.

1.8 Treatment for AD and other tauopathies

The numbers of AD cases are increasing every year at a very fast rate and there are no effective treatments available currently which could actually stop or reverse the disease condition. AD is

the sixth leading cause of death in the US and it is the only cause of death in the top 10 in America that cannot be prevented or cured. Therefore, there is an urgent need for treatments for AD as well as other tauopathies. The treatment options currently available include altering the functioning of the neurotransmitters or neurotransmitter receptors. These drugs help in reducing the rate of progression of the disease, but none of them actually stop or reverse it.

1.8.1 Currently available FDA approved drugs

The U.S. Food and Drug Administration (FDA) has approved 5 drugs that can be used to treat symptoms of AD – donepezil, galantamine, rivastigmine, tacrine and memantine¹⁰⁹. **Table 1.1** summarizes the source, mechanism of action and the year the drug was approved for use by the FDA.

Donepezil, galantamine, rivastigmine and tacrine are cholinesterase inhibitors (ChEIs). In AD, the degeneration of cholinergic neurons in the basal forebrain leads to the loss of cholinergic neurotransmission in the cortex, hippocampus, and other regions of the brain therefore contributing to the impaired cognition observed in AD patients. Therefore, the concept of AD being a cholinergic deficiency condition was established which had an influence on early AD drug development eventually leading to identification, study and approval of cholinesterase inhibitors for the treatment of AD¹¹⁰. ChEIs primarily improve cholinergic neurotransmission by slowing down the degradation of acetylcholine (ACh) by the enzyme acetylcholinesterase (AChE), leading to increase in the levels of ACh which plays an important role in regulating memory, thinking, judgement and other thought processes^{110, 111}.

Memantine is the first Alzheimer's drug targeting the NMDA receptor. It is also the only drug that has been shown to be effective in the later stages of AD. In 2005, the FDA declined to

approve using memantine to treat mild Alzheimer's disease cases. Memantine works by uncompetitively binding to and blocking NMDA receptors. Excessive influx of calcium ions through NMDA receptors due to glutamergic dysfunction results in neuronal death through mechanisms not completely understood¹¹². Such excitotoxicity is seen in AD and memantine is known to prevent this NMDA receptor mediated excitotoxicity without affecting normal synaptic activity¹¹³. Apart from these drugs, alternative therapies including use of nonsteroidal anti-inflammatory drugs, vitamin E, selegiline, Ginkgo biloba extracts, estrogens, statins and behavioral and lifestyle changes have been explored as therapeutic options¹¹⁴.

The current treatments only delay the progression of symptoms associated with AD. Also, these drugs have severe side effects. Long-term use of ChEIs increases risk of bradycardia, which means the heart rate is slower than normal, and loss of consciousness (syncope) and their consequences¹¹⁵. Other common side effects include gastrointestinal anomalies including nausea and diarrhea. It also results in an overall reduction in synaptic functioning. Discontinuing these drugs may lead to loss of beneficial cognitive and functional effects that would not have been evident previously¹¹⁵.

1.8.2 Therapeutic strategies aimed at targeting underlying molecular mechanisms in AD

In an effort to find disease modifying treatments, the focus in the field of therapeutics in AD and other tauopathies has now shifted to targeting the underlying molecular mechanisms responsible for disease pathogenesis. These include the two main hallmarks of the disease – amyloid plaques and tau aggregates. Drugs targeting the components of the amyloid cascade hypothesis aim at reducing amyloid pathology¹¹⁶.

Table 1.1 FDA approved drugs for treatment of AD.

Drug	Brand name	Source	Mechanism	Approved for	FDA approved
donepezil	Aricept	Synthetic	Acetyl cholinesterase inhibitor.	All stages	1996
galantamine	Razadyne	Plant source/ synthetic	Acetyl cholinesterase inhibitor.	Mild to moderate	2001
memantine	Namenda	Synthetic	Blocks NMDA receptors	Moderate to severe	2003
rivastigmine	Exelon	Synthetic	Acetyl cholinesterase inhibitor.	Mild to moderate	2000
tacrine	Cognex	Synthetic	Acetyl cholinesterase inhibitor.	Mild to moderate	1993

1.8.2.1 Amyloid based therapeutics

The amyloid targeting therapeutics could be sorted into several classes. The first is small molecules inhibiting β - or γ -secretases that generate $A\beta$ from APP¹¹⁷. Enhancing the activity of α -secretase to enhance the nonamyloidogenic pathway of APP processing is another approach to therapy towards AD¹¹⁸. The goal is to reduce the $A\beta$ plaque load. The concern with these is that several γ -secretase inhibitors block the same step in Notch processing and could interfere with Notch signaling pathway proteins and other cell surface receptors. Signaling through Notch is involved in crucial cell-fate decisions during development and therefore targeting γ -secretases for the treatment of AD may risk toxicity caused by reduced Notch signaling¹¹⁹. The second attempts to prevent oligomerization of $A\beta$ or enhance the plaque clearance from the cerebral cortex^{120, 121}. This is mainly attempted by active $A\beta$ clearance by promoting microglial activity¹²². The third is the use of anti-inflammatory drugs, which is based on the observation that progressive accumulation of $A\beta$ causes an inflammatory response in the cerebral cortex¹²³. The fourth approach is regulation of cholesterol homeostasis. Prolonged use of cholesterol-lowering drugs is associated with lower incidence of AD¹²⁴ and has been shown to reduce pathology in APP transgenic mice¹²⁵. $A\beta$ aggregation is partially dependent on metal ions Cu^{2+} and Zn^{2+} ¹²⁶. Therefore the fifth approach involves chelation of these ions, which could prevent $A\beta$ deposition. APP mice treated with a known Cu^{2+}/Zn^{2+} chelator showed a reduction in $A\beta$ deposition¹²⁷.

AD drug development has been dominated by amyloid-based therapeutic approaches. Around 19 drugs targeting amyloid have failed at randomized clinical trials or their development has been stalled¹²⁸. Therefore alternative therapeutic strategies now need to be explored.

1.9 Tau based therapeutics

Based on the results from all the clinical trials it is evident that targeting only the amyloid pathway is not effective in stopping or reversing disease pathology. In fact, clearance of A β using active immunization did not prevent tau pathology or neurodegeneration in human AD patients¹²⁹. Therefore, it is important to develop alternative tau mediated therapies. The mechanisms of tau pathology are not clear but tau aggregation, phosphorylation and propagation are likely pathological mechanisms that lead to loss of function or gain of function of tau eventually causing neurodegeneration. There are a number of therapeutic strategies aimed at reducing tau- caused pathology such as inhibiting tau phosphorylation (Figure 1.2), enhancing MT stabilization, clearance of extracellular tau through tau immunotherapy, enhancing the protein degradation pathways, attenuation of inflammatory responses caused by tau pathology, inhibiting/regulation of other post translational modifications such as glycosylation, nitration and acetylation and finally inhibiting the tau aggregation process. A few of the currently popular therapeutic strategies are discussed in more detail below.

1.9.1 Inhibiting tau phosphorylation

Tau protein has around 80 potential phosphorylation sites and the phosphorylation state of the protein is regulated by the activities of tau protein kinases and phosphatases. Hyper phosphorylation of tau is an important step in neurodegeneration in tauopathies¹³⁰. Therefore regulating activities of tau kinases and phosphatases are, potentially, good therapeutic approaches for treatment of AD and related dementias.

1.9.1.1. Inhibiting tau kinases

There are many kinases for tau phosphorylation including glycogen synthase kinase 3 (GSK3), protein kinase A (PKA), mitogen activated protein kinases (MAPKs), cyclin dependent kinase 5 (CDK5), cyclin dependent kinase1 (CDK1) and MT affinity regulating kinase 1 (MARK1).

GSK-3 and CDK5 phosphorylate tau at many sites, have high expression levels in the brain and are associated with NFT pathology in AD¹³¹. Therefore, these are the most obvious targets for treatment.

Lithium chloride which is a GSK-3 inhibitor prevented tau hyperphosphorylation and NFT formation in a mouse model but did not disassemble pre-formed tau aggregates¹³². Tideglusib is a novel GSK-3 inhibitor which reduced tau phosphorylation, A β amyloid deposits and prevented memory deficits in transgenic mice expressing APP and tau¹³³. Recently, phase II trial of tideglusib for AD and PSP has been carried out. The results showed no clinical benefit over a short term but further dose- finding studies are yet to be done in the early disease stage¹³⁴. Other than GSK-3 inhibitors, no other tau protein kinase inhibitors have entered clinical trials. This could be because these kinases have multiple substrates and therefore are more prone to causing other side effects¹³⁵.

Figure 1.2

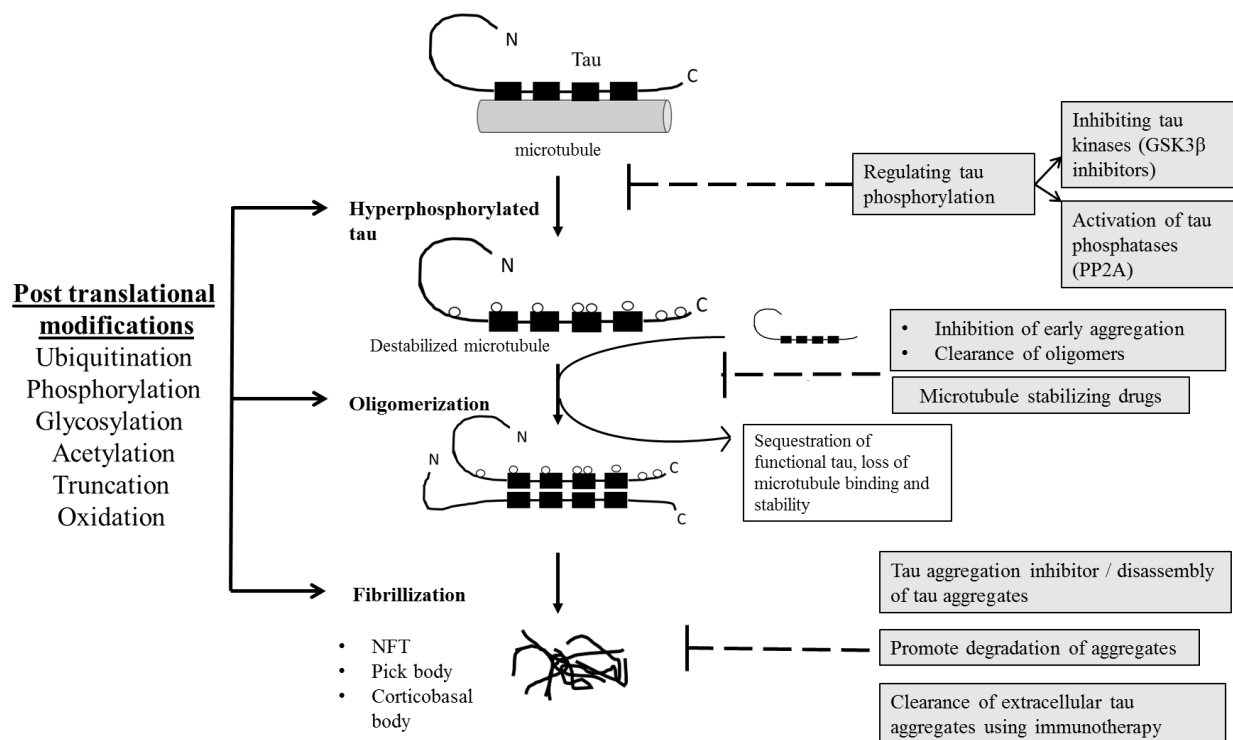


Figure 1.2 Tau-based therapeutics. In an adult human brain, tau is bound to microtubules through MTBR regions (4 repeat). When in diseased state, tau is altered such that it loses its ability to bind to MTs. The altered unbound tau monomers sequester functional tau monomers to form oligomers and eventually toxic tau aggregates. Due to loss of tau binding, microtubule structure is also destabilized. One of the most frequent and studied reasons for loss of microtubule binding is hyperphosphorylation. A number of other posttranslational modifications such as ubiquitination, glycosylation, phosphorylation, acetylation, oxidation or truncation due to caspases may potentiate the dynamics of oligomerization or aggregate formation. There are different types of pathological tau lesions that differ in appearance or content such as NFTs, Pick bodies, which contain only 3-repeat isoforms, or other forms. Potential therapeutic strategies are shown in grey boxes and the black dashed lines show potential stages of therapeutic intervention.

1.9.1.2 Activation of phosphatases

The two important phosphatases that are affected in AD are phosphoprotein phosphatase 2A (PP2A) and PP-1¹³⁶⁻¹³⁸. PP2A accounts for more than 70% of all phosphoseryl/phosphothreonyl activity in the human brain¹³⁹. In the adult human brain, PP2A regulates the phosphorylation of tau that suppresses MT assembly activity and this suggests that PP2A might be a good target for therapeutics¹⁴⁰. PP2A is a part of multiple signal transduction pathways regulating normal cellular homeostasis, however, and targeting it for therapeutics might cause many unwanted side effects. Sodium selenite has shown to stabilize PP2A-tau complexes. In transgenic AD mice models treated with sodium selenite, there was reduced tau pathology making it a promising lead compound for therapeutics¹⁴¹. Memantine has also shown the ability to enhance PP2A activity indirectly, therefore attenuating tau hyperphosphorylation *in vitro*¹⁴². Further, it was seen that treatment with memantine for one year results in significant decrease in the levels of phosphorylated tau in CSF of AD patients¹⁴³.

Tau protein function is regulated by a balance in activities of phosphatases and kinases and therefore targeting the same raises the concern of affecting the normal tau regulation.

1.9.2 MT stabilization

The main function of tau is to promote MT assembly. Post translational modifications like hyperphosphorylation alter tau such that it no longer binds to microtubules, leading to MT destabilization and aggregation of unbound altered tau molecules¹⁴⁴. This impairs MT stability, axonal transport and accumulation of tau aggregates. MT stabilizing drugs could therefore rescue these functional impairments. Paclitaxel is a MT stabilizing drug used for cancer treatment.

When an AD mouse model was treated with paclitaxel, there was improvement in fast axonal

transport, MT density and overall increase in motor function¹⁴⁵. Paclitaxel has poor blood-brain barrier permeability however, and therefore is not suitable for treatment. Davunetide is another MT stabilizing drug which reached phase II clinical trials for treatment of tauopathies. The main mechanism of action of davunetide is to stabilize MTs, but the drug does not appear to be directly involved in polymerization or dynamics of reconstituted neural MTs¹⁴⁶. Epophilon is another MT stabilizing drug which showed reduction in tau pathology in the forebrain and an increase in the hippocampal neuronal integrity in a PS19 tauopathy mouse models¹⁴⁷. In another study in a different tau transgenic mouse model, rTg4510, there was an improvement in cognitive function and reduction in tau pathology upon treatment with very low doses of a drug similar to epithilone, BMS-241027¹⁴⁸. Therefore, MT stabilizing drugs are potentially good therapeutic drugs for treatment of tauopathies. Clinical trials of these drugs are currently going on. Microtubules are involved in many regular cell processes such as cell division, and use of MT stabilizing drugs can impair the dynamic nature of the MTs therefore leading to cell death.

1.9.3 Enhancement of tau clearance mechanisms

The Hsp70/CHIP chaperone system plays an important role in selective degradation of altered tau species including phosphorylated tau, and in regulation of tau turnover¹⁴⁹. Dysregulation of such ubiquitin-proteosomal pathways could be responsible for tau aggregation. Therefore, enhancing degradation of pathological tau, including tau oligomers or fibrils, is yet another strategy for tau based therapeutics. Hsp90 plays an important role in maintaining the degenerative phenotype of tau in the diseased state. Hsp90 could be binding to tau inducing a conformational change making it more accessible for phosphorylation by GSK3 and its aggregation. In a tauopathy mouse model, JNPL3, use of an Hsp90 inhibitor resulted in reduction of hyperphosphorylated tau and tau aggregates in the brain¹⁵⁰. On the other hand, inhibiting

Hsp90 also leads to upregulation of heat shock transcription factor, which causes increases expression of multiple different heat shock proteins (Hsps), which leads to unintended side effects that could negate the effects of inhibition of Hsp90. Therefore, cochaperones of Hsp90 are also now being targeted to yield more specific effects. For example, Withaferin A is a compound that inhibits cochaperone of Hsp90, Cdc37. Withaferin A was shown to decrease tau aggregates in mice and also leads to increase of Hsp70 and Hsp27 levels (reviewed in¹⁵¹).

The autophagy-lysosomal system also plays an important role in degradation of tau aggregates, especially the larger aggregates which use three different pathways¹⁵². Trehalose is an activator of autophagy. When Trehalose was administered to transgenic mice expressing a P301S human tau mutant, it reduced tau phosphorylation in neurons and also the amount of insoluble tau protein and also improved neuronal survival¹⁵³. This pathway potentially makes a very good therapeutic target because it specifically targets abnormal tau. A study showed that a caspase cleaved form of tau, which is more toxic than full length tau, is preferentially degraded via autophagy with a faster turnover than wild type tau¹⁵⁴. This strategy of tau based therapeutics would not affect the physiological functions of tau and therefore could be of tremendous therapeutic value.

1.9.4 Inhibition of tau pathology propagation

It is now known that tau pathology can spread from one cell to another via extracellular tau aggregates¹⁵⁵. The hypothesis is that these aggregates can enter the cell cytoplasm and interact with normal endogenous tau and induce tau fibrillization by acting as a template for nucleation or seeding¹⁵⁶. If this hypothesis is correct, removal or degradation of extracellular tau aggregates is a promising therapeutic strategy to stop disease progression. Immunotherapy to remove

extracellular tau aggregates looks promising based on a number of studies conducted in transgenic tau mouse models using passive immunization or active immunization¹⁵⁷⁻¹⁵⁹.

1.9.5 Tau aggregation inhibitors

Tau aggregation is caused when natively unfolded sequences in the MTBR region of tau monomers undergo a conformational change due to post translational modifications like phosphorylation, to form β -sheet structures and to form NFTs. It is believed that small molecules could interact with the β -sheet structures to inhibit tau aggregation. Recently, a tau aggregation inhibitor, a stable, reduced form of methylthioninium chloride has reached three phase-3 clinical trials, one for the treatment of Pick's disease and two studies for AD¹⁶⁰. Tau aggregation inhibitors (TAIs) identified to date belong to many different chemical classes as will be discussed below.

1.9.5.1 Polyphenols

Polyphenols are often biosynthesized by plants and are known for their potential antibiotic, antidiabetic and neuroprotective properties¹⁶¹. These are characterized by the presence of one or more hydroxyl groups (-OH) bound to an aromatic benzene ring. Many polyphenols have been identified in high throughput screens (HTS) for amyloid-aggregation inhibition and these inhibit a variety of amyloidogenic aggregates like those of α -synuclein, A β 40 and tau among others¹⁶²⁻¹⁶⁴. Oleuropein aglycone is a natural phenolic derivative which inhibits tau aggregation at low micromolar concentrations¹⁶⁵. This compound was found to be more active than methylene blue on both wild-type tau and aggregation enhancing mutant tau protein P301L¹⁶⁵. Myricetin is another polyphenol with an IC₅₀ of 1.2 μ M and which may be interfering with the elongation

phase in fibril assembly¹⁶². (-)-Epi-gallocatechine (EGCG) is a polyphenol which has an IC₅₀ value of 1.8 μ M for tau aggregates¹⁶².

1.9.5.2. Anthraquinones

Anthraquinones are close analogues of polyphenols. Several anthraquinones sharing a tricyclic aromatic ring system with some modifications have shown tau aggregation inhibition abilities and are known for their intercalating capabilities. Emodin, Daunorubicin, Adriamycin, PHF016 and PHF005 are anthraquinones which have shown the ability to inhibit tau filament assembly and also induce aggregation of preformed aggregates of tau¹⁶⁶. Several anthraquinones are A β aggregation inhibitors and molecular modelling suggests that these compounds have the common ability to adopt a specific three-dimensional pharmacophore conformation with aromatic rings bound to hydrophobic regions and prevent it from forming fibrils¹⁶⁷.

1.9.5.3 Rhodanine- based inhibitors

Rhodanines were identified as tau aggregation inhibitors (TAIs) in a screen, and the scaffold was further explored via the synthesis of a focused library¹⁶⁸. These compounds could inhibit tau aggregation and also promote filament disassembly at 100-600 nM concentration. They showed activity in cellular assays without cytotoxicity and didn't interfere with tau's ability to promote MT assembly¹⁶⁸. bb14, an inhibitor from the rhodanine class showed a reversal of toxicity caused by tau aggregation when used in cell culture models (N2a cells expressing mutant tau), in a *C.elegans* model expressing proaggregant tau species¹⁶⁹ and in an organotypic slice model derived from inducible tau-transgenic mice¹⁷⁰.

1.9.5.4 Phenylthiazolyhydrazide (PTH) inhibitors

PTHs were obtained as hits against tau aggregation in an initial ligand-based virtual screen of 200 000 compounds¹⁷¹. BSc3094, an inhibitor belonging to the PTH class, inhibited tau aggregation with an IC₅₀ of 1.6 μM and for filament disassembly a DC₅₀ of 0.7 μM for a 10 μM K19. Further, NMR studies indicate that BSc3094 binds to monomeric tau, therefore maybe shifting tau conformation to form off-pathway tau species¹⁷². These compounds are potential producers of radical oxidative species (ROS). The formation of reactive acyl radicals has been reported in other studies using these compounds and therefore would require further testing¹⁷³.

1.9.5.5 N- Phenylamine inhibitors

N-phenylamine derivatives were identified as TAIs in a screen. These compounds inhibited tau aggregation in cell models of tauopathy as well¹⁷⁴. The effects were investigated on an inducible N2a cell model of tauopathy. Upon incubation with 10 μM of B4A1, a phenylamine inhibitor, for a minimum of 5 days, the Thioflavin S (ThS) signal in cells decreased by 70% compared to untreated control and the cell viability returned to normal as well.

1.9.5.6 Benzothiazoles

Benzothiazoles are heteroaromatic structures with a 1, 3-thiazole ring and are known to display high affinities for β-sheet structures¹⁷⁵. Cyanine dyes which are characterized by a polymethine chain linking two benzothiazoles have been identified as TAIs. N744 is an inhibitor belonging to this group of compounds which inhibits tau aggregation *in vitro* with an IC₅₀ of 380 nM and further also drives the endwise disaggregation of tau filaments¹⁷⁶.

1.9.5.7 Aminothienopyridazines (APTZs)

APTZs were identified in a quantitative HTS of approximately 292000 compounds to inhibit tau assembly. APTZs inhibited tau aggregation at IC_{50} values in the range of 5-7 μ M and did not interfere with tau-mediated MT assembly¹⁷⁷. APTZs act by a mechanism that differs depending on the tau isoforms. Active APTZs were found to promote oxidation of the two cysteine residues in 4R tau isoforms by a redox recycling mechanism. This results in formation of disulfide-containing compact monomeric tau molecules which were resistant to aggregation. But, in 3R tau isoforms, APTZs facilitated intermolecular disulfide formation leading to dimers which act as seeds for tau aggregation¹⁷⁸. This could affect their viability as a therapeutic agent.

1.10 Thesis overview

Tauopathies are one of the greatest health concerns currently and there are no prevention strategies or effective treatments in sight. It is therefore crucial that researchers find a safe and successful therapeutic treatment soon. As shown in figure 1.2, there are several strategies being tested to stop or reverse the disease progression. The studies are in preliminary stages of development and a small number of compounds have reached the final stages of clinical trials. At this stage I cannot comment upon whether one treatment strategy is better than the other.

Tauopathies are a very complex group of neurodegenerative diseases and we do not have enough knowledge about what initiates tau aggregation, why the pathologies are so varied, or what is the mechanism linking tau aggregation to its toxicity. There is a need to conduct research on both the fronts – 1) Understanding tau aggregation and 2) finding an effective treatment for the same.

The first part of the study described here was designed to characterize how the aggregation and functions of tau are affected by the site of truncation. Characterizing these differences will assist

in elucidating the mechanisms of initiation of tau aggregation as well as how it may be exerting its toxic effects. We characterized the tau aggregation and function *in vitro*. Truncation of tau is known to occur in tauopathies. Truncated tau is seen in NFTs obtained from human AD patients. Truncation clearly plays a role in disease pathogenesis by affecting tau's function and aggregation. Eight truncation mutants were generated in the full length tau isoform. I determined the differences within the truncation mutants through several assays designed to measure and characterize the aggregation of the protein, as well as its ability to stabilize microtubule polymerization.

In the second part of the study, secondary metabolites obtained from *Aspergillus nidulans* containing aromatic ring structures were screened for their ability to inhibit tau aggregation. We chose seventeen compounds based on their structural similarity to previously identified tau aggregation inhibitors (TAIs). The effect of the compounds was measured through assays designed to measure the tau aggregation and examine filament morphology after treatment with the compounds. We identified three compounds which inhibited tau aggregation. One of the compounds was an intermediate in the azaphilone biosynthesis pathway. Dr. Berl Oakley and his colleagues generated a small library of azaphilones obtained from asperbenzaldehyde. We sought to determine whether these eleven azaphilones retained any tau aggregation inhibition activity observed in asperbenzaldehyde. We carried out several *in vitro* assays designed to test the activity of the compounds on tau filament assembly process and pre-formed tau aggregates. We characterized the aggregates formed after compound treatment to assess their toxicity. We determined the effect of the compounds on tau's ability to stabilize microtubule polymerization. Finally I began a project where I started characterizing the interaction between the compounds and tau protein using NMR. I obtained preliminary results regarding the possible residues

involved in the interaction. Further, I tested the most potent compound for its activity against an aggregation enhancing tau truncation mutant. This was to test whether the compound would be effective against tau modified in disease conditions, which would be therapeutically beneficial.

Chapter II Effects of tau truncations on Aggregation and Microtubule Interactions

2.1 Introduction

Aggregation of the microtubule-associated protein tau is a significant event in the progress of certain neurodegenerative diseases termed tauopathies. A large portion of the current research in the field is focused on trying to understand the mechanisms and factors affecting tau filament formation, which should eventually help in finding better therapeutic strategies for tauopathies. Tau undergoes many post translational modifications which alter the conformation of tau protein such that it is more prone to aggregation. Tau phosphorylation has been studied extensively and is known to play a major role in tau pathogenesis¹⁷⁹. Truncation of tau is another post translational modification that is known to cause conformational changes that induce a misfolding cascade in Alzheimer's disease (AD) and other tauopathies¹⁸⁰. Truncated tau is seen in the NFTs obtained from human AD patients. In fact, protein truncations are known to play a major role in pathogenesis of many other human degenerative disorders such as α -synuclein in Parkinson's Disease PD¹⁸¹, TDP-43(TAR DNA-binding protein 43) in FTLD (Frontotemporal Lobar Dementia)¹⁸² and huntingtin in HD(Huntington's Disease)¹⁸².

Tau is a substrate for many caspases. Caspase-6 and caspase-3 cleaved tau fragments are associated with early as well as late development of NFTs and correlate well with cognitive decline^{97, 98, 183}. Truncated tau can be identified using specific antibodies such as MN423 and TauC3⁹⁵. MN423, generated in mice immunized with morphologically intact pronase-resistant PHF core, recognizes the compact fold of the PHF core tau truncated at Glu391⁹³. TauC3 recognizes tau truncated at Asp 421, which has a different conformation from that of normal tau. DC11 is a truncation-dependent conformational antibody that recognizes altered tau in AD

brains¹⁸⁴. DC11 recognizes neither native healthy tau nor its full length recombinant counterpart. However, this monoclonal antibody showed strong immunoreactivity with truncated tau (residues 151-421). This antibody revealed that a range of truncated tau species including N- and C-terminal truncations possess pathological conformations of tau. A specific sequence of events for truncations has been suggested⁹². Alz50 conformation is first formed and is seen in pre-tangle neurons¹⁸⁵. Alz50 has a discontinuous epitope consisting of a.a. 2-10 from the amino terminal of tau and a.a 312-342 from the MTBR, and therefore is conformation dependent (Figure 2.1). After NFT formation, truncation occurs at both the amino- and carboxyl-termini. Alz50 positive tau aggregates are reactive to Tau-C3 which means they are truncated at D421¹⁸⁶. They are also reactive to Tau-66 antibody, which is also a conformational antibody dependent on the proline-rich region of tau interacting with MTBR. Once tau is in the tau-66 conformation, it is cleaved more extensively in NFTs and becomes positive for MN423 that detects the truncation at E391. It has been shown in *in vivo* studies that activation of executioner caspases in neurons in transgenic mice, led to cleavage at D421, followed by formation of thioflavin-S positive NFTs and tangle-related conformational epitopes¹⁸⁷. Thioflavin S is a dye which binds to amyloid structures and can be used to identify tau aggregates. When truncated tau proteins were expressed in brains of transgenic animal models, neurodegeneration was observed. Truncated tau induced hyperphosphorylation and formation of tau aggregates that were characteristic of AD¹⁸⁸. The expression of truncated-tau activated inflammatory responses such as activation of microglia and leukocyte infiltration¹⁸⁹. It further induced oxidative stress as well¹⁹⁰. Further, when human a truncated tau transgene was expressed in a rat model, it resulted in sequestration of endogenous rat tau proteins and in their fragmentation and aggregation. It is therefore believed that few forms of truncated tau may have the potential to initiate and drive the tau truncation cascade¹⁹¹.

Figure 2.1

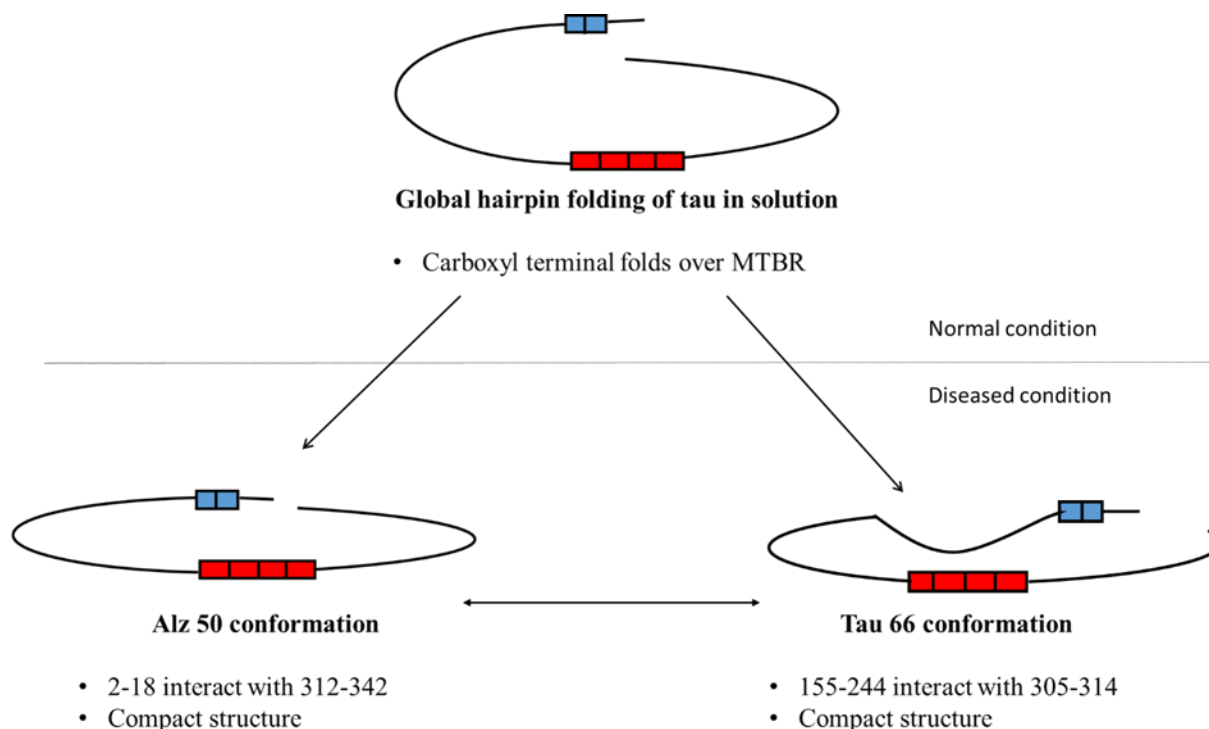


Figure 2.1 Conformations of monomeric tau. In the figures, the red squares are the microtubule binding repeats (MTBR) of tau. The blue squares are the exons in the N terminal. In a normal condition tau attains a global folding conformation, where the C-terminal folds over the MTBR. In a diseased state two conformations of tau have been identified. The Alz50 and the Tau66 conformations are shown in the figure above. They form a more compact structure making tau prone to aggregation. Antibodies recognizing these conformations do not show reactivity against tau obtained from normal healthy brains.

It is important to study the isolated effects of tau truncations on aggregation mechanisms and tau function. The N-terminal and C-terminal regions of tau protein are involved in maintaining the global hairpin conformation of tau as well as the Alz 50 and tau 66 conformations that are found in the diseased condition. Removal of a.a. 2-18 from the amino-terminal portion of tau that overlaps with the Alz 50 epitope, inhibits tau polymerization *in vitro*⁹⁹. Interaction of the N-terminal region with the MTBR region of tau may be required for aggregation. Removal of amino acids from the C terminus of tau greatly increases the rate and extent of tau polymerization¹⁰⁰. Therefore the C-terminus plays an inhibitory role in tau aggregation. There are unanswered questions regarding which stretches of amino acids in the N- and C-termini of tau play a crucial role in tau aggregation and MT stabilization. N-terminal and C-terminal truncation mutants will affect tau conformations and therefore affect aggregation and MT stabilization. Understanding the effects of tau truncations on tau conformation and MT stabilization will help in understanding their roles in aggregation mechanisms.

We constructed eight truncation mutants in the background of full-length tau *in vitro*, which included five N-terminal truncations, two C-terminal truncations and one mutant with both N and C terminal truncations (Figure 2.2). The truncation mutants used in the study are shown in Table 2.1. We chose these mutants because prior studies have shown that some of these truncations or similar truncations can influence tau aggregation (Table 2.1). We found that the truncations had different effects on the aggregation and MT interactions of tau. The differences in aggregation amounts, kinetics and filament morphologies helped in our understanding of pathology resulting from the truncations.

Figure 2.2

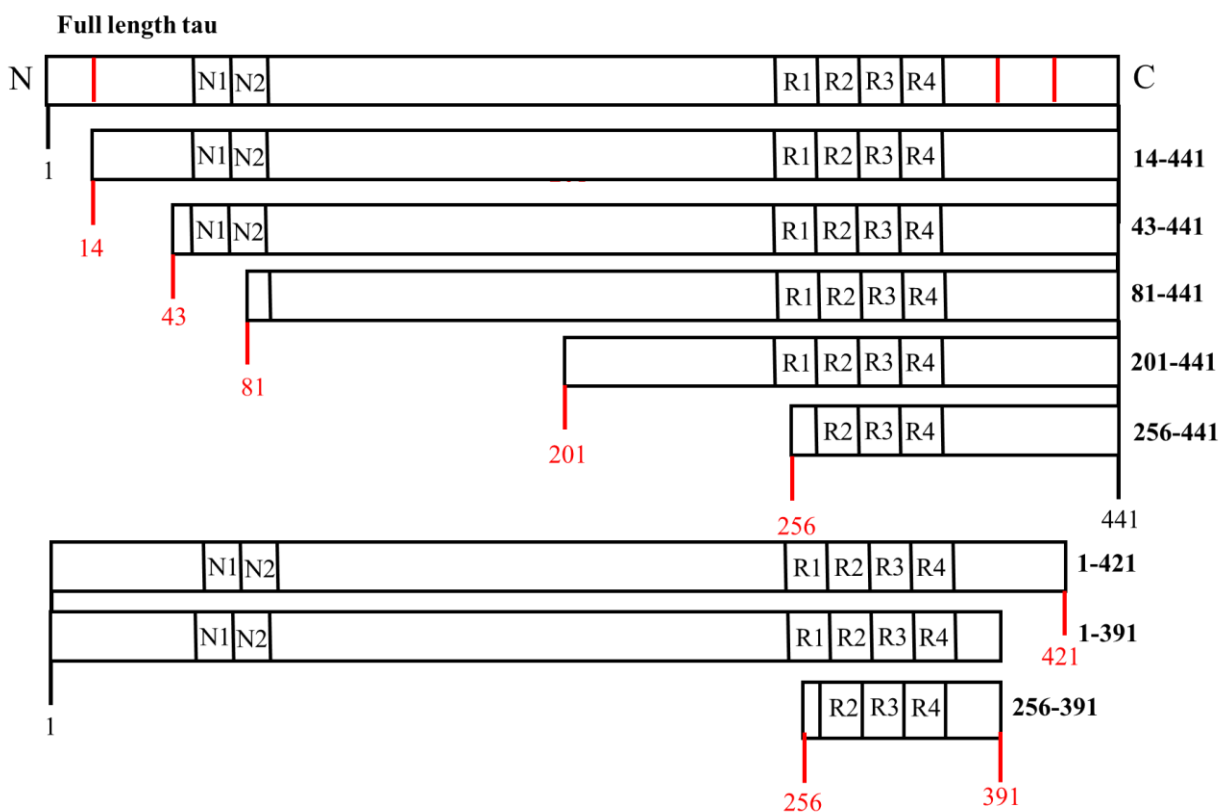


Figure 2.2 Truncations used in this study. All truncations constructs were derived from full length tau construct (labelled). The N and C terminals of each construct are labelled in the diagram. The two N-terminal exons, e2 and e3, have been labelled as N1 and N2 respectively. The four MTBR regions are R1-R4. The respective truncations have been labelled with their specific names. The five amino terminal truncations are 14-441, 43-441, 81-441, 201-441 and 256-441. The two carboxyl terminal truncations included are 1-391 and 1-421. One mutant construct with truncations at both the N and C terminals was made, 256-391.

Table 2.1: Tau truncations used in this study

C-Truncation Mutants	
1-421	C-terminal Caspase 3 cleavage site, elevated in Alzheimer's disease ⁹⁷
1-391	MN423 antibody site, elevated in Alzheimer's disease ⁴⁷
N-Truncation Mutants	
14-441	N-terminal Caspase 6 cleavage site ⁹⁶
43-441	Removes N-terminal region that binds inhibitory N-terminal peptides ¹⁹²
81-441	Removes N-terminal hydrophobic region (amino acids 75-80) (predicted)
201-441	Removes the majority of the N-terminal region of tau, but leaves a hydrophobic region involved in tau binding to microtubules (predicted)
256-441	Complete removal of N-terminal region and proline-rich region of tau (predicted)
N- and C –truncation mutant	
256-391	Approximates the PHF core ¹⁹³

2.2 Experimental Procedures

2.2.1 Protein expression and purification. All wild-type (WT) and truncation constructs were expressed and purified as described previously¹⁹⁴. The mutagenesis was done using the Quikchange site-directed mutagenesis kit from Stratagene (La Jolla, CA). The following truncations were generated in a full-length 2N4R tau background contained in a pT7C vector: 14-441, 43-441, 81-441, 201-441, 256-441, 1-391, 1-421 and 256-391.

2.2.2 Arachidonic acid-induced polymerization. Recombinant WT and truncated tau proteins, at a concentration of 2 μM , were incubated in buffer containing 0.1 mM EDTA, 5 mM dithiothreitol, 10 mM Hepes buffer (pH 7.64), 100 mM NaCl, and 3.75% ethanol in a 1.5 mL microcentrifuge tube. The polymerization inducer molecule was arachidonic acid (ARA) at a concentration of 75 μM . Reactions were allowed to proceed overnight at 25 °C.

2.2.3 Thioflavin S fluorescence. The total amount of aggregation was measured utilizing the thioflavin S (ThS) Sigma-Aldrich (St. Louis, MO) fluorescence assay. Thioflavin S binds amyloid structures in tau aggregates. Upon binding, thioflavin S undergoes a characteristic blue shift in its emission spectrum. It will not produce this blue shift upon binding to monomeric tau. 150 μL of each reaction was added to separate wells in a 96-well, white, flat-bottom plate. ThS was diluted in water and added to the well to a final concentration of 20 μM . The fluorescence shift was measured with a Cary Eclipse Fluorescence Spectrophotometer (Varian Analytical Instruments, Walnut Valley, CA) with an excitation wavelength of 440 nm and an emission wavelength of 520 nm. PMT voltage was set to 650 V. Readings from a reaction with 2 μM protein and 0 μM ARA were used as a blank and subtracted from the reading for each reaction¹⁹⁴.

2.3.4 Right-angle laser light scattering. Laser light scattering is a useful indirect method for measuring tau polymerization *in vitro*, in that under our conditions the intensity of scattering is proportional to the mass of polymerized tau filaments¹⁹⁵. Aggregation of the protein was read by adding 180 μL of the reaction to a 5 mm x 5 mm optical glass fluorometer cuvette (Starna Cells, Atascadero, CA). A 12 mW solid state laser, with a wavelength of $\lambda=532$ nm and operating at 7.6 mW, was aimed at the cuvette. The amount of light scattered by particles in the reaction was measured by capturing the amount of light perpendicular to the angle of the beam using a SONY XC-ST270 digital camera. The images were captured at varying aperture settings (from f4 to f11) and analyzed using the histogram function of Adobe Photoshop¹⁹⁵.

2.3.5 ARA-induced polymerization kinetics. ARA was added to our polymerization buffer (0.1 mM EDTA, 5mM dithiothreitol, 10 mM Hepes buffer (pH 7.64), 100 mM NaCl) to a final concentration of 75 μM and 3.75% ethanol in a 5 mm x 5 mm optical glass fluorometer cuvette. Tau polymerization was measured by collecting images of the right-angle scattered light at specific time points beginning from the initiation of the reaction upon addition of protein, at a final concentration of 2 μM , and the ending once the reaction had reached a steady-state. The data were fit to the Finke-Watzky 2-step equation designed to describe the nucleation and elongation of protein aggregation¹⁹⁶. The mechanism assumes simplified nucleation ($A \xrightarrow{k_1} B$) and elongation ($A + B \xrightarrow{k_2} 2B$) steps to yield the following equation:

$$[B]_t = [A]_0 - \frac{\frac{k_1}{k_2} + [A]_0}{1 + \frac{k_1}{k_2[A]_0} \exp(k_1 + k_2[A]_0)t}$$

The k_1 and k_2 rate constants are used to qualitatively compare the rates of nucleation and elongation, respectively, of our protein aggregation reactions. $[B]_t$ is the aggregates formed over time t , $[A]_0$ is the amount of monomeric tau at time zero and t is time in minutes.

2.3.6 Transmission electron microscopy. The ARA-induced polymerization reactions were diluted 1:10 in polymerization buffer and 2% glutaraldehyde. After five minute incubation, a formvar-coated copper grid (Electron Microscopy Sciences, Hatfield, PA) was placed on top of a 10 μ L drop of the diluted sample for 1 minute. The grid was then blotted on filter paper, placed on a drop of water, blotted with filter paper, placed on a drop of 2% uranyl acetate, and blotted dry. The grid was then placed on another drop of 2% uranyl acetate for 1 minute and blotted dry for a final time. For all tau variants a single grid was prepared and examined from each of three separate reactions. The grids were examined using a TECNAI G2 20 electron microscope (FEI Co., Hillsboro, OR). Images were collected with the Gatan Digital Micrograph imaging system at a magnification of 3600X. Five images were collected from each grid and analyzed. The aggregated tau in each of the 15 images was quantified by using Image-Pro Plus 6.0. The macro was designed to recognize filaments with a total perimeter of greater than 30 nm. This eliminated background noise. The perimeter of each filament was measured and divided by two in order to estimate the filament's length. These values were totaled in order to estimate the total amount of aggregated material in each image. The total polymerization/image was calculated by taking the mean of all total polymerization values. The mean of all filament lengths was also determined by calculating the mean length of all filaments in a given image and reported as a mean of those values with the error bars representing standard deviation.

2.3.7 Tubulin polymerization assay. Microtubule polymerization was monitored by recording the DAPI fluorescence enhancement due to the incorporation of a fluorescent reporter into

microtubules as polymerization occurs. The Tubulin Polymerization Assay kit from Cytoskeleton, Inc. (Denver, CO) was used to measure the polymerization of tubulin. The reaction conditions included WT tau or one of the tau variants at 1 μ M, or a control compound, added along with 1 mM GTP, 2 mg/ml (~36 μ M dimerized) tubulin, 2 mM MgCl₂, and 0.5 mM EGTA in 80 mM PIPES buffer at a pH of 6.9. The reaction proceeded in a black, flat-bottomed polystyrene 96-well plate. Paclitaxel was used at 3 μ M in one reaction to serve as a positive control for tubulin polymerization, as well as a way to normalize separate reactions. One well containing no compound served as a negative control. After addition of the compounds the plate was inserted into a FlexStation II Fluorometer (Molecular Devices Corporation, Sunnyvale, CA) set at a temperature of 37 °C and the reactions were mixed by shaking for 5 seconds. The fluorescence was measured with an excitation wavelength of 355 nm and an emission wavelength at 455 nm at 1 minute intervals for 1 hour. The data were fit to the Gompertz equation

$$y = ae^{-e^{-(t-t_i)/b}}$$

as described previously⁸⁶. y is the value of laser light scattering measured at time t ; a is the maximum amount of light scattering; t_i is the point of inflection where the increase in scattering is at its maximum and b is equal to $1/k_{app}$. K_{app} is proportional to the rate of polymerization. These values were averaged and reported \pm standard deviation^{14, 86}.

2.3.8 Statistical analysis. An unpaired two-tailed Student's t-test was used to compare means of WT values to mean values of each tau truncation mutant for Thioflavin S fluorescence, right-angle laser light scattering, quantitative electron microscopy, kinetics parameters and for the microtubule assembly assay. P-values less than or equal to 0.05 are indicated with one asterisk

(*), less than or equal to 0.01 with two asterisks (**), and less than or equal to 0.001 with three asterisks (***)).

2.3 Results

2.3.1 Selection of truncation mutants. Tau is known to be truncated at both its termini during the progression on Alzheimer's disease. We generated eight different tau truncation mutants consisting of two carboxyl-terminal truncation mutants, five amino-terminal truncation mutants and one mutant with truncations at both the amino and carboxyl termini. The truncations are shown in figure 2.2.

2.3.2 Tau truncation mutants have variable effects on the total polymerization *In vitro* experiments were done to examine the effects of the truncation mutants on the ARA-induced polymerization of tau at 2 μ M protein and 75 μ M ARA. After the reactions proceeded overnight, the total amount of aggregation was measured by ThS fluorescence and right-angle laser light scattering (LLS). In the ThS assay, most of the truncations decreased the total amount of tau aggregation compared to the WT except for 43-441. Among those which showed a decrease, truncation 81-441, 201-441, 256-441 and 256-391 showed a significant decrease in polymerization compared to WT (Figure 2.3 A).

Figure 2.3

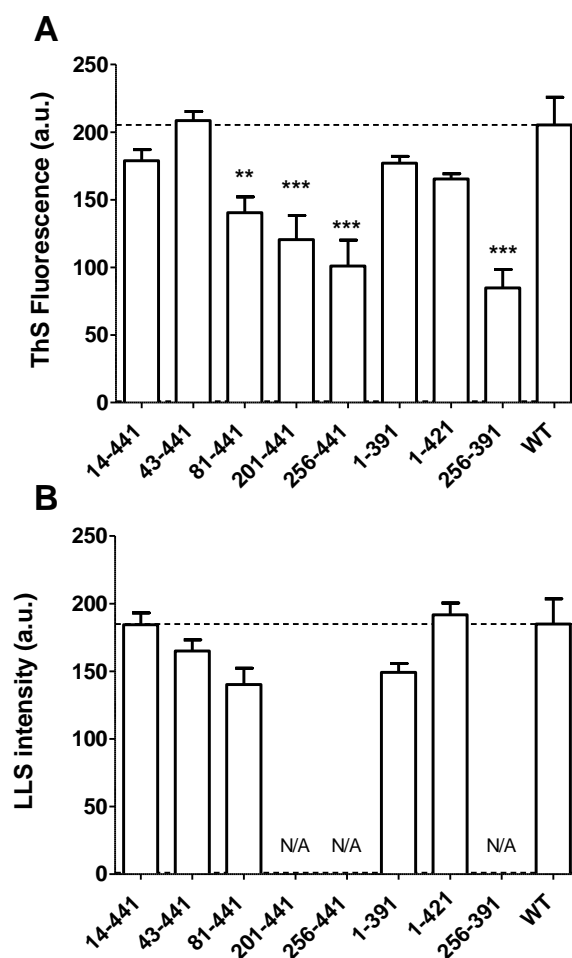


Figure 2.3: Polymerization of wild-type and tau truncations measured by Thioflavin S binding and right-angle laser light scattering. Polymerization reactions contained 2 μ M of WT or one of 8 tau truncations and 75 μ M ARA. Reactions were incubated overnight at 25 $^{\circ}$ C. The final extent of polymerization was measured by (A) ThS fluorescence and (B) right-angle LLS. Data represent the mean from 5 experiments \pm SD. Stars represent P-value results from Student's unpaired t tests comparing means from each mutant to WT. (*), $P < 0.05$; (**), $P < 0.01$; (***), $P < 0.001$.

In the LLS assay, 14-441, 43-441, 81-441, and 1-391 showed a decrease in the amount of polymerization compared to WT (Figure 2.3 B). We were unable to quantify the LLS values for aggregation by 201-441, 256-441 and 256-391 because the aggregates did not scatter light evenly (Figure 2.4). Upon doing electron microscopy, there were no detectable filaments on the electron microscopy grids of mutants 201-441, 256-441 and 256-391. We therefore speculate that the light scattering could be due to micelles formed by ARA due to its interaction with the constructs. This does not rule out the possibility of presence of very large aggregates which could be affecting the light scattering. Also, the protein could be precipitating and forming amorphous clumps of the protein and not be forming ordered filaments as in the case of tau aggregates. Further investigation to determine the exact nature of interaction between ARA and these constructs would help in explaining the uneven light scattering observed.

Based on the LLS and ThS results, we believe that N- terminal truncations with more than 80 residues truncated, are reducing the total amount of aggregation and the C-terminal truncations are not causing a decrease in the total amount of aggregation. While the removal of the N- and C- termini of tau together, leaving only the PHF fragment, leads to a significant decrease in the total tau aggregation based on ThS results.

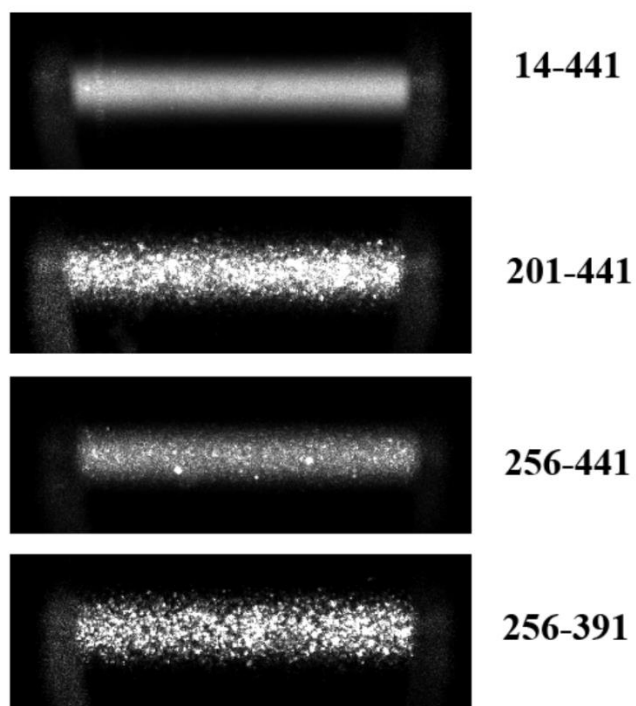
Figure 2.4

Figure 2.4 LLS images. These are images of LLS assay for 14-441, 201-441, 256-441 and 256-391. The light is scattered evenly for 14-441. This can be quantified using the histogram function in Adobe Photoshop. The light is scattered in an uneven fashion for 201-441, 256-441 and 256-391 as seen in the images above. This is not quantifiable.

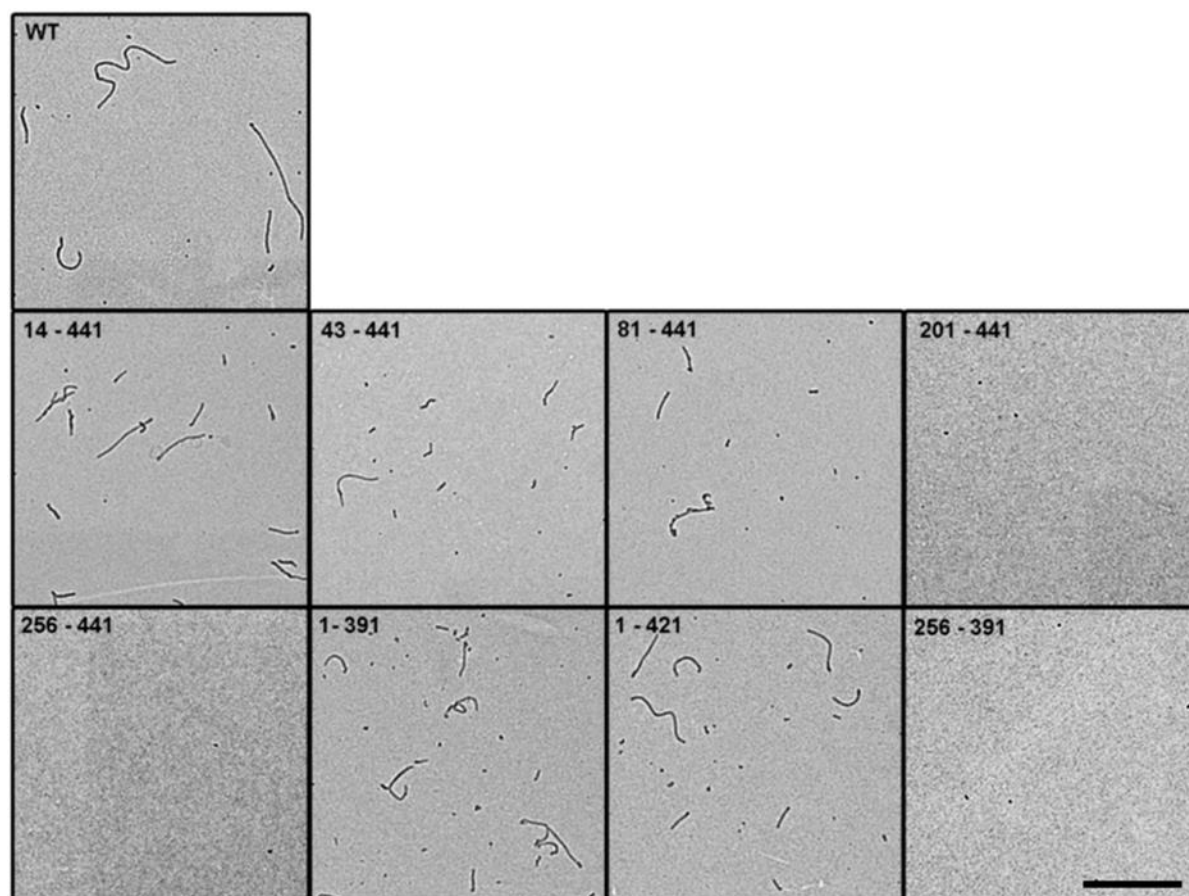
Figure 2.5

Figure 2.5 Electron micrographs of polymerization reactions containing 2 μ M protein and 75 μ M ARA. Representative electron micrographs for WT, 14 – 441, 43 – 441, 81 – 441, 201 – 441, 256 – 441, 1 – 391, 1 – 421 and 256 – 391. The scale bar in the lower right panel represents 1 μ M and is applicable to all images.

Figure 2.6

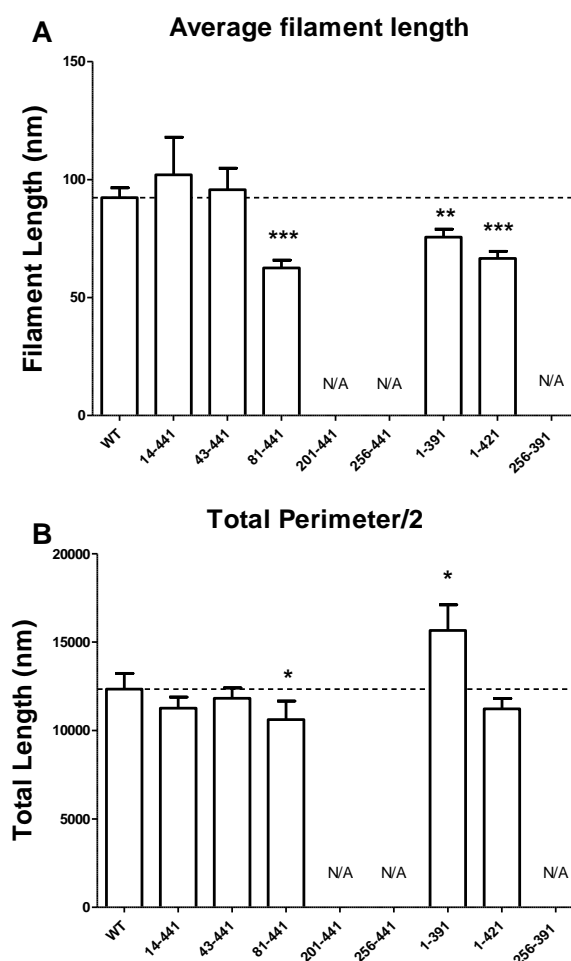


Figure 2.6: Quantitation of polymerized tau protein in electron micrographs. Images in the electron micrographs from Figure 2 were quantified using Image-Pro Plus 6.0. **(A)** The graph displays the total length (nm) of polymerized tau filaments/image. **(B)** The graph displays the average filament length (nm) of polymerized tau filaments/image. Data in both graphs represent the mean of 5 images from each of 2 separate reactions \pm SD for a total of $n=10$. Stars represent P-value results from Student's unpaired t tests comparing means from each truncation mutant to WT. (*), $P < 0.05$; (**), $P < 0.01$; (***), $P < 0.001$.

2.3.3 Tau truncation mutants have little effect on tau filament morphology.

LLS and ThS are both very informative assays but are indirect methods of quantifying tau aggregation. The LLS results are affected by the length distribution of the aggregates and the structure of tau recognized by ThS is not known as yet. Therefore, we viewed the filaments directly by electron microscopy (Figure 2.5). The morphology of the filaments of the 14-441, 43-441, 81-441, 1-391 and 1-421 truncation forms looks similar to the WT filaments. There were no detectable filaments on the electron microscopy grids of mutants 201-441, 256-441 and 256-391. Earlier, we saw a significant decrease in ThS staining for these three truncations (Figure 2.3A).

We quantified the total filament lengths (total tau aggregation) and the average filament lengths of the aggregates on the grids (Figure 2.6). The total tau aggregation by the N-truncation mutant 81-441 was significantly lower than that of WT tau. The average filament length of 81-441 was also significantly lower than that of WT. The 1-391 truncation caused an increase in the total tau aggregation compared to WT tau and a decrease in the average filament length.

1-421 did not have an effect on the total amount of tau aggregation compared to the WT but showed a significant decrease in the average filament length. The other mutants, 14-441 and 43-441 caused an overall slight decrease in filament length compared to WT. 14-441 made filaments which were slightly longer than the wild type tau filament lengths.

2.3.4 Kinetics of polymerization varies with the tau truncation mutants. The morphology of the tau aggregates could be influenced by the rate of polymerization. We therefore sought to determine if the tau truncations are affecting the rate of polymerization. The polymerization was followed using LLS and the numbers were then fit to a two-step model of polymerization to determine the nucleation and the elongation rates (Figure 2.7). As mentioned earlier, the

aggregates of tau truncations 201-441, 256-441 and 256-391 did not scatter light evenly and therefore it was not possible to carry out aggregation kinetics study on these.

We compared the nucleation rates of these mutants (Figure 2.8). 1-391, 1-421, 43-441 and 81-441 truncation mutants showed a significantly higher nucleation rate than the WT. While the nucleation rates of 14-441 did not differ much from that of the WT. The elongation rates of the truncations 1-391, 1-421, 43-441 and 81-441 were significantly higher than that of the WT.

The N truncation mutants had an overall lower amount of tau aggregation at the end of 6 h compared to the WT, while the C-truncation mutants were closer to the WT in terms of total amount of aggregation after 6 h.

Figure 2.7

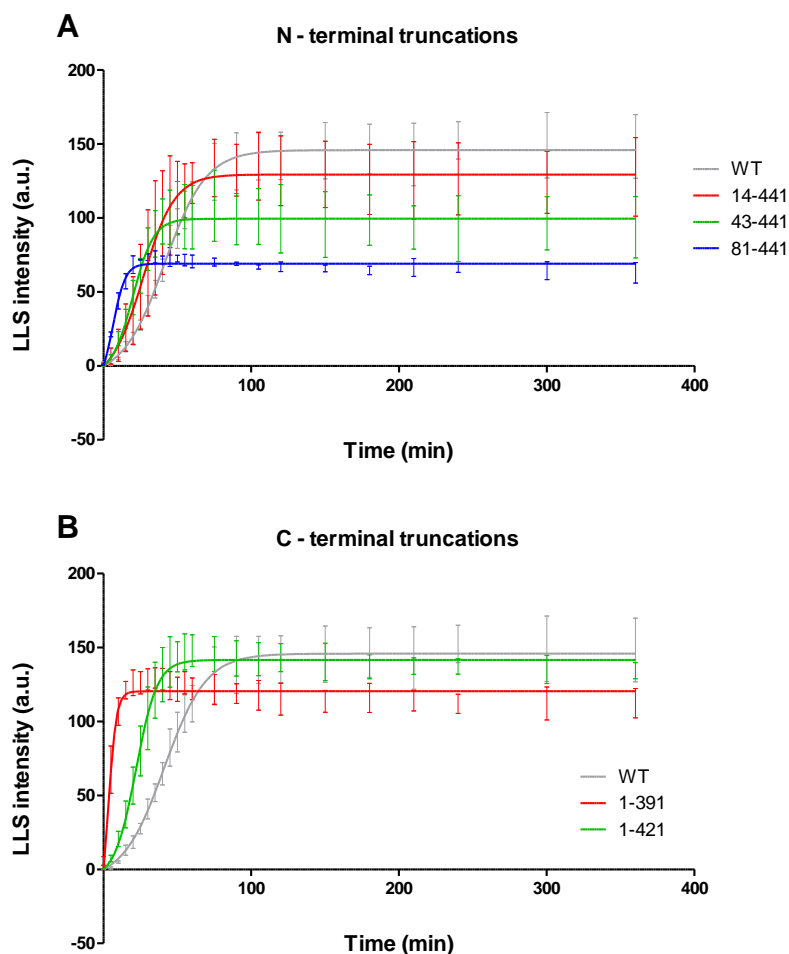


Figure 2.7 Comparison of tau polymerization kinetics. The parameters describing the tau polymerization kinetics curves fit to the Finke-Watzky mechanism are displayed. The first parameter is (A) k_1 , representing the rate of nucleation or formation of oligomers. The second parameter is (B) k_2 , the rate of elongation or extension of the oligomeric tau aggregates into filaments. Data represent means of values for fits of at least 3 separate reactions \pm SD. Stars represent P-value results from Student's unpaired t tests comparing means from each mutant to WT. (*), $P < 0.05$; (**), $P < 0.01$; (***), $P < 0.001$.

Figure 2.8

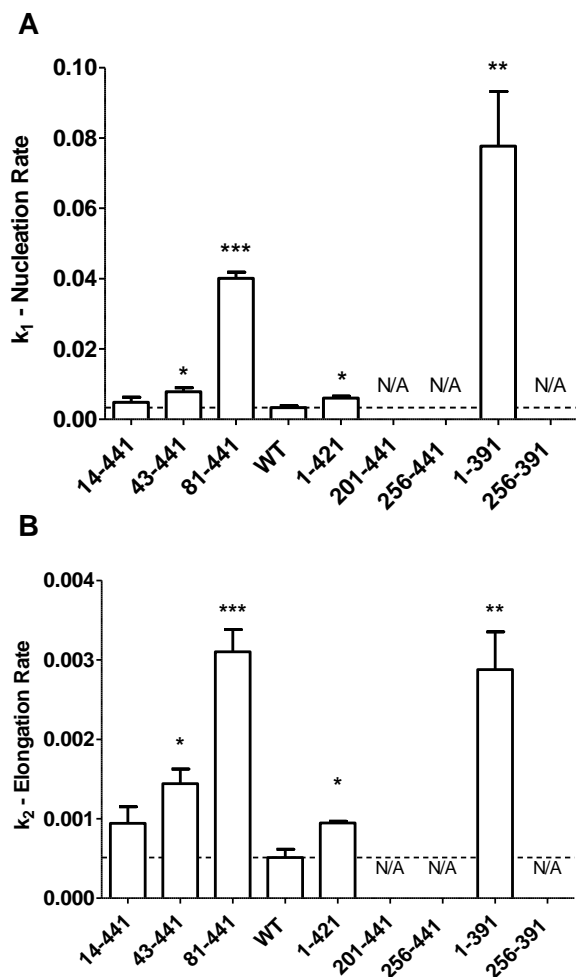


Figure 2.8: Comparison of tau polymerization kinetics. The parameters describing the tau polymerization kinetics curves fit to the Finke-Watzky mechanism are displayed. The first parameter is (A) k_1 , representing the rate of nucleation or formation of oligomers. The second parameter is (B) k_2 , the rate of elongation or extension of the oligomeric tau aggregates into filaments. Data represent means of values for fits of at least 3 separate reactions \pm SD. Stars represent P-value results from Student's unpaired t tests comparing means from each mutant to the WT. (*), $P < 0.05$; (**), $P < 0.01$; (***), $P < 0.001$.

2.3.5 Tau truncations have differing effects on tau's ability to stabilize microtubule

assembly. We sought to determine whether the tau truncations would affect tau's normal function of stabilizing microtubules. Microtubule polymerization was monitored using a fluorescence-based assay and the resulting curves (Figure 2.9) were fit to a Gompertz function in order to determine maximal extent of microtubule polymerization, the rate of elongation, and lag time in the presence of the tau truncations (Figure 2.10). Most of the proteins stabilized microtubules (MTs) to levels similar to WT tau. 256-441 and 1-391 stabilized MTs to a lesser extent compared to WT tau. 256-391 reduced the overall MT stabilization significantly. 256-391, 1-391 and 256-441 induced MT elongation at a slower rate. The lag time for tubulin polymerization was increased in the presence of 256-391 and 256-441 while 14-441 and 81-441 slightly decreased the lag time.

2.4 Discussion

In AD, monomeric tau undergoes a complex series of posttranslational modifications such as phosphorylation, acetylation etc. followed by enzymatic cleavages, and conformational changes that lead to transformation of monomeric soluble tau to an insoluble accumulation of misfolded protein. Truncation is an important post-translational modification having an etiological role in tau pathology. The truncation state of tau protein affects many of tau's normal and pathologic characteristics such as its ability to bind to microtubules, to assume specific conformations and its ability to self-assemble to form tau filaments. We sought to directly compare aggregation and function of WT tau against a wide range of tau truncation mutants under the same experimental conditions.

The first evidence of tau's change in conformation was obtained when the discontinuous epitopes of the Alz50 and tau-66 monoclonal antibodies were discovered⁴¹.

Alz50 identifies the conformation of tau when its amino terminus comes in contact with the MTBR region, making a compact conformation which converts the soluble random coil configuration of tau into a more compact conformation which facilitates aggregation. The Alz50 conformation as mentioned earlier, is seen in early pre-tangle tau. Later in AD, tau molecule in Alz-50 conformation can shift to the tau-66 conformation which basically depends upon the proline-rich region (155-244) of tau interacting with a region of the MTBR (305-314), which partially overlaps the putative N-terminus binding site in the Alz-50 conformation¹⁹⁷ (Figure 2.1).

We made five truncation mutants of tau with varying lengths of N-terminal truncations (Figure 1). The removal of portions of the N-terminal will affect the Alz-50 and tau 66 conformations and therefore should have an impact on tau aggregation. Truncation at N –terminal a.a. site 13, did not change the tau aggregation kinetics compared to WT tau. The N –terminal epitope involved in Alz50 is a.a.2-18. Therefore, the truncation at D13 site does not completely eliminate this epitope and therefore a weakened Alz50 conformation can be formed.

Upon truncating larger portions of the N-terminus by making truncations at 42 and 80 we observed an increase in the rate of tau aggregation. The elimination of larger portions of tau N – terminus may be driving the tau monomers to form the tau-66 conformation, without going through the transition from alz50 to tau66 conformation.

Figure 2.9

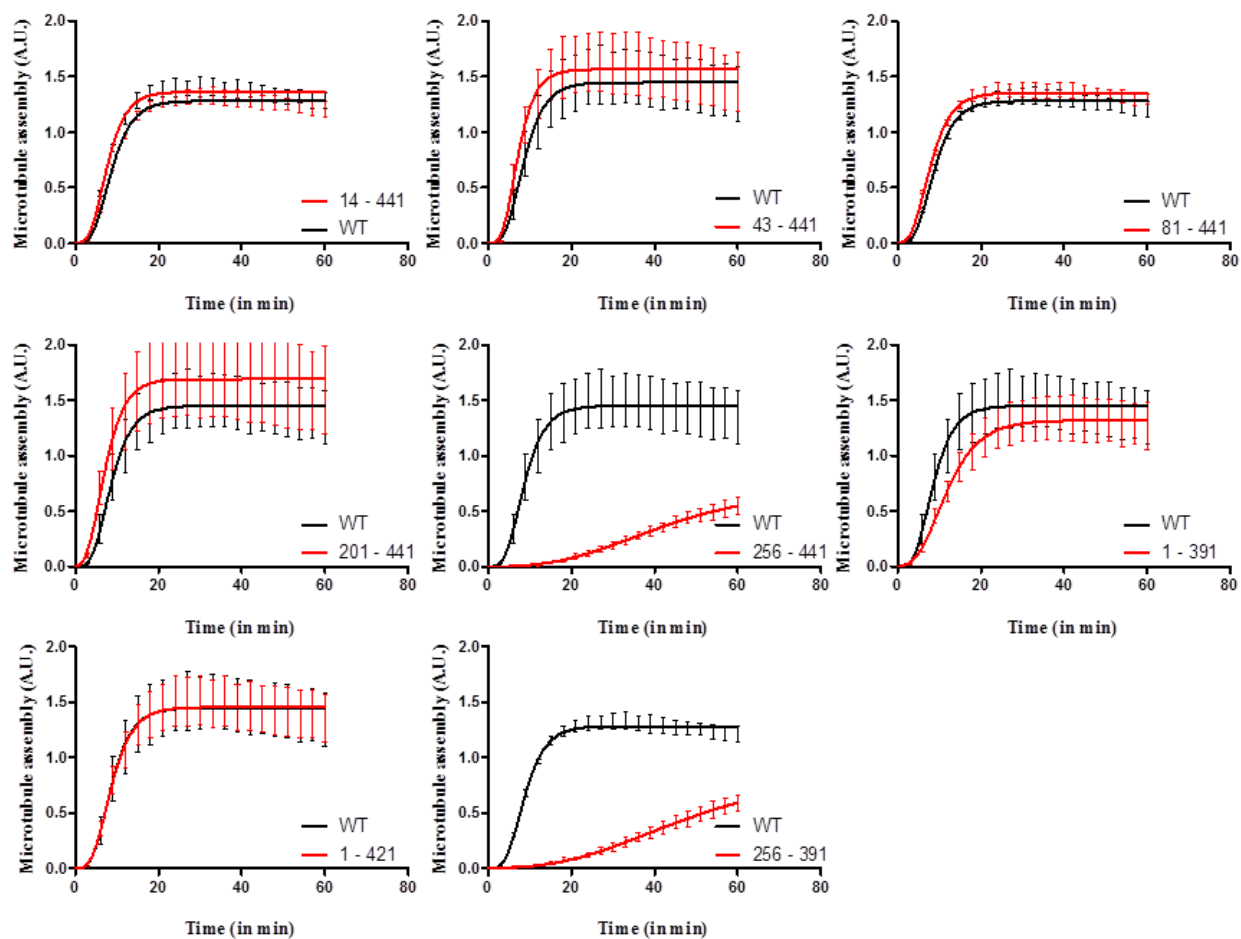


Figure 2.9: Microtubule assembly curves in presence of tau. Each point represents a mean value of the amount of tubulin polymerized into microtubules in the presence of wild-type tau (black) or tau truncations of (A) 14-441, (B) 43-441, (C) 81-441, (D) 201-441, (E) 256-441, (F) 1-391, (G) 1-421 and (H) 256-391. The values are fluorescence readings normalized to paclitaxel-stabilized polymerization of microtubules.

Further truncations at a.a. 200 and a.a. 256 eliminates the proline-rich region of tau molecule required for the formation of tau 66 conformation. These mutants may therefore not form either of the two Alz50 and tau66 conformations. We observed that these truncation mutants were unable to form tau filament when observed under electron microscope. Based on these results we may infer that formation of either the alz50 or the tau 66 conformation may be required for formation of tau filaments.

The 81-441 truncation gets rid of the N-terminal hydrophobic region (a.a. ⁷⁵VTAPLV⁸⁰). This truncation reduced the overall amount of aggregation and increased the filament nucleation and elongation rates significantly. This could mean the fast nucleation is taking up large amounts of monomeric tau quickly and leading to a drop in the protein level below the critical concentration of aggregation required for the elongation step. This was reflected in the significant reduction in the average filament lengths compared to the WT tau filament lengths.

The N-terminal and the proline-rich domains play a major role in the conformational changes in tau required for formation of tau filaments. We observed that none of the N-terminal truncations in our study cause an increase in aggregation. Therefore N-terminal truncations may not be initiating aggregation but may be playing a role in the later stages of pathogenesis after formation of tau aggregates. We have included only five N –truncation mutants in our study. A recent study has identified 21 new N –terminally truncated tau species that occur in the human brain. Their findings suggest that the N-terminal part of tau could be directly involved in regulation of microtubule stabilization¹⁵¹. It would be interesting to test whether these truncations affect tau aggregation properties.

Figure 2.10

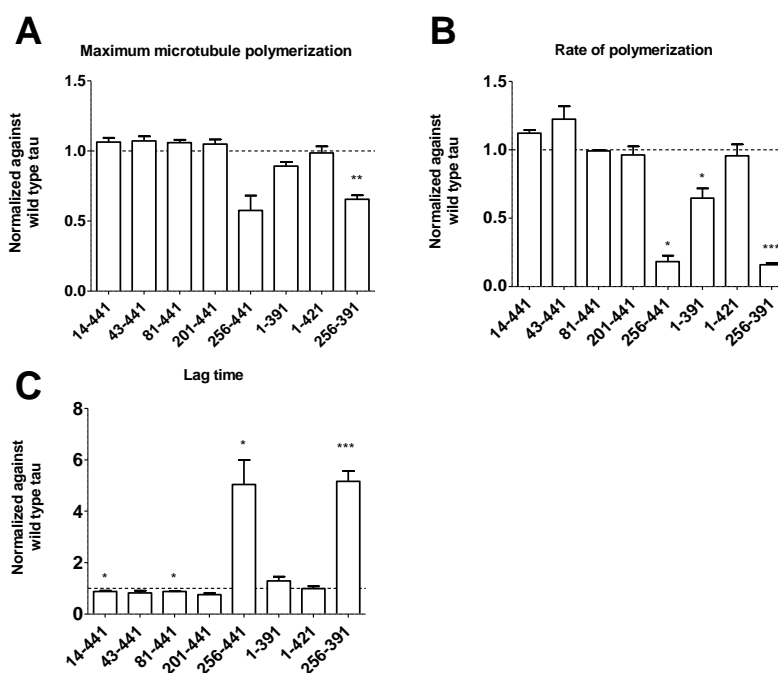


Figure 2.10: Stabilization of microtubule assembly by tau protein. The tau truncation mutants were incubated with tubulin and its polymerization was measured via a fluorescence assay. Numbers were normalized to values of polymerization in the presence of paclitaxel. The relative fluorescence units (y-axis) were plotted vs. time (x-axis) and fit to the Gompertz equation. From the parameters describing these curves, the values normalized against that of WT for the (A) maximum amount of microtubule polymerization in presence of each protein, (B) k_{app} or rate of microtubule polymerization, and (C) lag time, the time before microtubule polymerization is detected. The values in (A–C) are mean values of the changes from WT in three separate experiments \pm SD. Stars represent p-value results from Student's unpaired t tests comparing means from each mutant to WT. (*), $p < 0.05$; (**), $p < 0.01$; (***), $p < 0.001$.

We made two constructs with truncations at the carboxyl terminal 1-391 and 1-421. Truncations at D421 and E391 allow for the formation of alz50 and the tau66 conformations. In our experiments, both these truncations reduced the average filament length compared to those formed by WT full length tau. The nucleation and elongation rates for both the truncations were significantly higher than that of WT. The 1-391 truncation showed a significant increase in the total amount of aggregation and showed a significant reduction in average filament lengths. We have used the Finke-Watzky mechanism and feel it is a good way to calculate the nucleation and elongation rates in a simplified manner to accurately represent the differences in aggregation mechanisms for the truncation constructs. Tau truncations at the C-terminal assemble at a faster rate than WT tau¹⁰⁰. Truncations at E391 and D421 are known to occur in AD. Truncation at E391 is known to occur fairly late in AD. The D421 truncation is brought about by caspase 6 after the formation of NFTs⁹⁷. The expression of a truncated tau molecule consisting of a.a. 151-421 in hippocampal neurons induced apoptosis suggesting that caspase cleavage at D421 turns tau into an apoptosis effector molecule. The longest fragment with full apoptotic capacity is tau 1-422, which only lacks the 19 C-terminal residues¹⁹⁸. The relationship between tau aggregation and its apoptotic properties is presently unclear.

C-terminal truncations therefore have the ability to induce aggregation and therefore may occur at the early stages or the later stages of tau aggregation. Our data does not provide evidence that truncation initiates tau aggregation. It would be interesting to conduct experiments to test the same by doing tau aggregation reactions without ARA but using a small amount of 1-391 or 1-421 aggregates which may sequester full length tau protein to form aggregates.

In AD, tau is eventually truncated at both its N- and C- terminal. Therefore we created a construct with only 256-391, which approximates the PHF core region¹⁹³. There was a

significant decrease in the total amount of tau aggregation and the EM grids didn't show any filaments formed. The LLS assay could not be quantified for the same reason as for 201-441 and 256-441 constructs discussed previously. In previous studies, K19 tau construct has been used to accelerate tau filament formation drastically. K19 also approximates the PHF core region, but it is made from 3-repeat tau isoform and therefore is missing the second microtubule binding repeat (exon 10)¹⁹⁹. Tau filament assembly proceeds at a more rapid rate if the protein subunits are cross-linked into dimers, for example by an oxidized disulfide bridge by Cys 322. In the case of K19 construct, there is a single Cys 322. This will form dimers with other K19 monomers easily and therefore form dimers which will help accelerate aggregation. In our construct, we have two cysteine residues at positions 291 and 322. Therefore, there is a greater possibility of intramolecular bonds being formed between these cysteine residues, which would make them unavailable for dimerization. This would limit the formation of tau dimers and therefore will inhibit tau filament formation. This could explain the decrease in tau aggregation for 256-391 truncation mutants we saw in our assays. It would be interesting to have a mixture of K19 and 256-391 mutants and observe the tau aggregation kinetics and filament morphology.

The other effect of tau aggregation is loss of MT binding. We therefore, tested the ability of the truncated tau species to polymerize MT assembly. The N-terminal truncations did not differ from the WT full-length tau in their ability to polymerize MTs. The 256-441 showed a decrease in the total amount of MT polymerization. There was a significant decrease in the rate of MT polymerization and an increase in the lag time, which is basically the nucleation time for tubulin in MT assembly process. This could be because the 256-441 truncation eliminates the proline-rich region as well as part of the first MTBR region. The C-terminal truncations had different effects on MT polymerization compared to WT. The maximum amount of MT polymerization

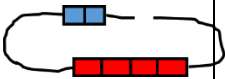
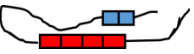

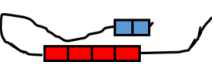

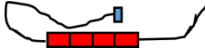




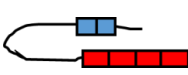
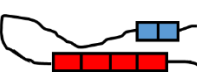
was not different from that in presence of WT tau. 1-391 had a reduced rate of MT polymerization compared to WT. This can be explained by the possibility of masking of the MTBR region by the N terminal. The 256-391 truncations significantly decreased the maximum amount of MT polymerization, the rate of MT polymerization and showed an increase in lag time. **Table 2.11** summarizes the observed results and the predicted effects on tau conformations.

FTDP-17 mutants like R5L have shown to enhance tau aggregation under similar experimental conditions²⁰⁰. They aggregate into longer tau filaments compared to WT and a lack of oligomeric tau species. The first 25 amino acids of tau protein carry a charge of -4 while the charge on the third MTBR is +3. Due to the R5L mutation, the overall charge of the amino region changes from -4 to -5, and possibly increases the electrostatic interaction between the N –terminus and MTBR. This means that changes in the charge of specific amino acids placed at strategic positions on tau protein involved in conformational changes required for aggregation affect the protein aggregation properties to a larger extent than making changes like truncation of a stretch of 14 to 50 residues at once.

Extensive studies on the effects of C-terminal tau truncation *in vivo* have been done⁹⁵. We now know that the tau truncation at the N-terminal is a regulated process with several preferential cleavage sites within the tau molecule and is not a random process¹⁹¹. Studies using rat brain tissue have shown that transgenic truncated tau is sufficient to initiate and drive the tau truncation cascade. These truncation models have been studied individually and their effects have been studied *in vitro* and *in vivo*. This is the first study where in a wide range of tau truncations including N-terminal, C-terminal as well as a construct with truncations at both the termini have been compared and studied under similar experimental conditions.

We saw a clear difference in the effects of N-terminal truncations compared to those of C-terminal truncations on tau aggregation and MT assembly. These effects correlated well with the ability of the truncations to form alz50 and/or the tau 66 conformations. Truncations which inhibited formation of both these conformations were unable to form tau filaments. The site of truncation on either of the terminals also affects the aggregation kinetics and MT assembly parameters. Further characterizing of truncation mutants and their effects in animal models or other *in vivo* systems may help explain the role played by tau truncations in tauopathies and how these mechanisms are affecting the progression of sporadic tauopathies.

Table 2.2: Effect of truncations on tau conformation (predicted) and tau aggregation

	Alz 50	Tau 66	Tau aggregation (Compared to full length tau)	Microtubule Polymerization (Compared to full length tau)
14-441			No change	No change
43-441			Faster aggregation kinetics	No change
81-441			Reduction in aggregation. Smaller filament lengths. Faster aggregation kinetics	No change
201-441			Decrease in aggregation. No filaments seen on electron microscopy grids.	No change
256-441			Decrease in aggregation. No filaments seen on electron microscopy grids.	Decrease in rate and total amount of MT polymerization. Increased lag time.
1-391			Increase in aggregation. Faster aggregation kinetics. Smaller filament lengths	Decrease in rate of MT polymerization

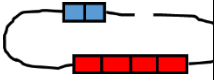
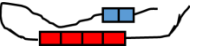
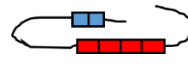
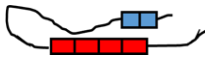
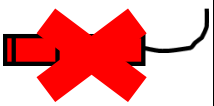

	Alz 50	Tau 66	Tau aggregation	Microtubule Polymerization
			(Compared to full length tau)	(Compared to full length tau)
1-421			Faster aggregation kinetics. Smaller filament lengths	No change
256-391			Decrease in aggregation. No filaments seen on electron microscopy grids.	Decrease in rate and total amount of MT polymerization. Increased lag time.

Table 2.2 This table summarizes conformational possibilities for each of the truncation mutants. The effect of the truncations on tau aggregation and MT polymerization has been summarized as well.

Chapter III Tau aggregation inhibitors obtained from *Aspergillus nidulans*: First generation compounds

3.1 Introduction

Alzheimer's disease (AD) is the most common form of dementia. It is a neurodegenerative disease characterized by pathological markers – mainly intracellular tau aggregates and extracellular amyloid plaques. The physiological role of tau protein is to regulate microtubule stability by binding to microtubules. In the diseased state however, tau undergoes post translational modifications and undergoes conformational changes which result in its dissociation from microtubules²⁰¹. The dissociated tau aggregates into different types of inclusions such as neurofibrillary tangles, neuropil threads and neuritic plaques. These inclusions are found in AD and in several other neurodegenerative tauopathies⁹². Mutations in the tau gene have been associated with tauopathies such as FTDP-17 (Frontotemporal dementia with parkinsonism linked to chromosome 17)²⁰⁰. Tau aggregation correlates well with the type and severity of cognitive impairment in AD⁴² and tau aggregation can lead to cell death and cognitive defects in cellular and animal models⁴³. Therefore, tau aggregation is a viable therapeutic target for treatment of AD and other tauopathies.

Tau aggregation involves conformational changes in tau molecules and these tau molecules interact with each other to form tau filaments. The core of the tau filaments is made of β -sheet structures and it is believed that small molecules that interact with these β sheet structures inhibit tau aggregation by potentially preventing further addition of tau molecules to the growing aggregate^{44, 202}. Compounds belonging to the class of polyphenols¹⁶², cyanine dyes¹⁷⁶, phenothiazines¹⁶², rhodanine¹⁶⁸, N-phenylamines²⁰³, thienopyridazines¹⁷⁷, quinoxalines²⁰⁴ and

anthraquinones¹⁶⁶ have been previously identified as tau aggregation inhibitors. These compounds belong to different classes but share the common feature of having multiple aromatic fused-rings in their structure. These compounds are in their initial stages of discovery and therefore it is not known whether they would be effective *in vivo* or whether they have the required pharmacokinetic properties and can cross the blood brain barrier. Is it necessary to find more lead compounds which could inhibit tau aggregation and would be suitable for further development.

Fungi have historically been a good source of medicinally important compounds such as antibiotics, antioxidants and antimicrobials. Using efficient gene targeting systems, Dr. Berl Oakley's lab along with their collaborators have identified many biosynthetic pathways²⁰⁵⁻²⁰⁷ in *Aspergillus nidulans* that produce compounds with a wide range of chemical structures²⁰⁸⁻²¹⁵. Some of these compounds share structural similarities with previously identified tau aggregation inhibitors such as the presence of fused ring structures. We decided to determine if these compounds also inhibited tau aggregation. We chose 17 compounds which included anthraquinones, xanthenes and other metabolites and assessed their ability to inhibit tau aggregation *in vitro*. Several compounds affected tau filament assembly at various levels. Amongst these three compounds, asperthecin, asperbenzaldehyde and 2, ω -dihydroxyemodin were potent and gave reproducible results in inhibiting tau aggregation in a dose dependent fashion. The compounds did not completely inhibit tau's function of stabilizing microtubules. These compounds are therefore good candidate compounds for further development. Two of the compounds – asperthecin and 2, ω - dihydroxyemodin belong to the anthraquinone class of compounds. Some of the compounds belonging to this class have previously been identified as tau aggregation inhibitors (TAIs)¹⁶⁶. Asperbenzaldehyde was an interesting compound because it

has a novel structure compared to previously identified TAIs. Further, it is an intermediate in an azaphilone biosynthesis pathway. Azaphilones are compounds with interesting biological activities which includes lipoxygenase inhibitor activity, which is a beneficial property for treatment of AD²¹¹.

3.2 Experimental procedures

3.2.1 Compounds. Compounds were purified from *Aspergillus nidulans* as described previously^{211, 213-217} from a single peak of HPLC chromatography, and purity was estimated by NMR (Table 3.1).

3.2.2. Tau polymerization reactions. 2 μ M recombinant tau protein was incubated in polymerization buffer which contained 10 mM HEPES (pH 7.64), 5 mM DTT, 100 mM NaCl, 0.1 mM EDTA, and 3.75% ethanol. Compounds dissolved in DMSO were added to the tau solution at final concentrations of 200 μ M, 100 μ M, 50 μ M, or 25 μ M as described in Results. Compounds were allowed to incubate with tau for 20 min before the addition of 75 μ M arachidonic acid to initiate tau filament formation²¹⁸. The reactions were allowed to proceed at room temperature for 16 h before analysis.

Table 3.1. Purity of tested compounds from ^1H NMR spectra (Prisinzano lab, KU)

Compound name	Integration of impurity in ^1H NMR	Estimated purity
A. Emericellin	0.17	> 85 %
B. Varietoxanthone	0.08	> 92 %
C. Emodin	0.06	> 94 %
D. 2, ω -Dihydroxyemodin	0.06	> 94 %
E. Endocrocin	0.05	> 95 %
F. Sterigmatocystin	0.04	> 96 %
G. F9775A	0.13	> 88 %
H. F9775B	0.05	> 95 %
I. Asperthecin	0.04	> 96 %
J. Crysophanol	0.06	> 94 %
K. Aloe emodin	0.06	> 94 %
L. Shamixanthone	0.07	> 93 %
M. Demethylsterigmatocystin	0.02	> 98 %
N. ω -Hydroxyemodin	0.06	> 94 %
O. Monodictyphenone	0.24	> 80 %
P. 3'-hydroxyversiconol	0.03	> 97 %
Q. Asperbenzaldehyde	0.01	> 99 %

3.2.3. Filter trap assay. Tau polymerization reactions, as described above, were diluted to 20 ng/300 μ L in TBS and passed through a pre-wetted nitrocellulose membrane (Bio-Rad Laboratories) using vacuum force in a dot-blot apparatus (Bio-Rad Laboratories). The membranes were washed thrice with TBS-0.05% Tween20 (TBST) and then blocked in 5% nonfat dry milk in TBST for 1 h. The membranes were then incubated with a mixture of three primary antibodies overnight at 4°C [Tau 5 antibody²¹⁹ at 1:50000 dilution, Tau 12 antibody⁹⁶ at 1:250000 dilution, and Tau 7 antibody¹⁹² at 1:250000 dilution; antibodies were a kind gift from Dr. Lester I. Binder]. Membranes were washed thrice in TBST and incubated with secondary antibody, [HRP-linked goat anti-mouse IgG (Thermo Scientific)], for 1 h. at room temperature. The membranes were washed twice in TBS-Tween buffer, and a final wash was made with TBS. The blot was developed using an ECL (enhanced chemiluminescence) Western blotting analysis system (GE Healthcare). Images were captured with a Kodak Image Station 4000R and were quantified using the histogram function of Adobe Photoshop 7.0. Statistical analyses were performed using 1-way ANOVA with Dunnett's multiple comparison test to compare the triplicate values to control values.

3.2.4 Transmission electron microscopy. Polymerization reaction samples were diluted 1:10 in polymerization buffer and fixed with 2% glutaraldehyde for 5 min. 10 μ L of each sample was added to a Formvar carbon-coated grid for 1 min. The grid was blotted on filter paper, washed with water, blotted, washed with 2% uranyl acetate and blotted before staining with 2% uranyl acetate for 1 min. followed by a final blotting on filter paper. The grids were examined with a Technai F20 XT field emission transmission electron microscope (FEI Co.). Images were taken with the Gatan Digital Micrograph imaging system. The images were collected at a magnification of 3600 \times . The filaments were quantified using Image-Pro Plus 6.0 software²¹⁸.

The perimeter of the filaments was determined, and the length was obtained by dividing the perimeter in half. For quantitative analysis, filament lengths were placed into bins as described in Results. Statistical analyses were performed using two-way ANOVA with Bonferroni post-tests to compare replicate means for each bin size with the no compound data serving as reference values.

3.2.5 Tubulin polymerization assay. Polymerization of tubulin was measured using a tubulin polymerization assay kit (Cytoskeleton, Inc.). Microtubule polymerization was monitored by recording the DAPI fluorescence enhancement due to the incorporation of a fluorescent reporter into microtubules as polymerization occurs in presence or absence of compound. The reactions were measured in 96-well Costar black polystyrene flat-bottom plates (Corning, Inc.). Each well contained porcine tubulin at 2 mg/mL and GTP at 1 mM in 80 mM PIPES buffer (pH 6.9) with 2 mM MgCl₂ and 0.5 mM EGTA. Tau was added to the wells at a concentration of 1 μM, and the test compounds diluted in DMSO were added at a final concentration of 200 μM. An equal amount of DMSO was added to each of the wells. Another well containing 1 μM paclitaxel (99.1% pure; Cytoskeleton, Inc.) and tubulin served as a positive control for polymerization and as a standard for normalizing results for each of the experiments (not shown). Control reactions containing only buffer without either tau or a compound, and buffer with the individual test compounds but without tau were also performed (not shown). Reaction plates were placed at 37°C and shaken for 5 s in a FlexStation II fluorometer (Molecular Devices Corp.). The fluorescence was measured at a constant interval of 1 min. for 1 h. with an excitation wavelength (λ_{ex}) of 355 nm and an emission wavelength (λ_{em}) of 455 nm. This gave 60 readings for every well sample. The resulting data were normalized to the amount of microtubule polymerization

observed in the presence of tau without a compound and fit to the Gompertz equation²¹⁸.

Experiments were performed in triplicate and averaged.

3.3 Results

3.3.1 Compounds used in this study. We chose 16 compounds obtained from *Aspergillus nidulans* based on their structural similarity to previously identified tau aggregation inhibitors and one of our compounds had a different chemical structure compared to the others. 8 compounds belong to the group of anthraquinones, five are xanthones and four compounds are other types of metabolites. These can be divided as compounds with multiple fused-ring structures of monocyclic aromatic compounds (Figure 1). Emodin, among these compounds has been identified as an inhibitor of tau aggregation in a previous study¹⁶⁶.

3.3.2. Compounds inhibited tau aggregation at 200 μ M. Tau aggregation was initiated *in vitro* using a standard arachidonic acid induction protocol²¹⁸. Each compound was incubated with tau for 20 mins before inducing aggregation using arachidonic acid. The final concentration of each compound in the reactions was 200 μ M. The protein concentration was 2 μ M and that of arachidonic acid was 75 μ M in all the assays. The amount of aggregation was determined using the filtertrap assay and transmission electron microscopy.

Figure 3.1

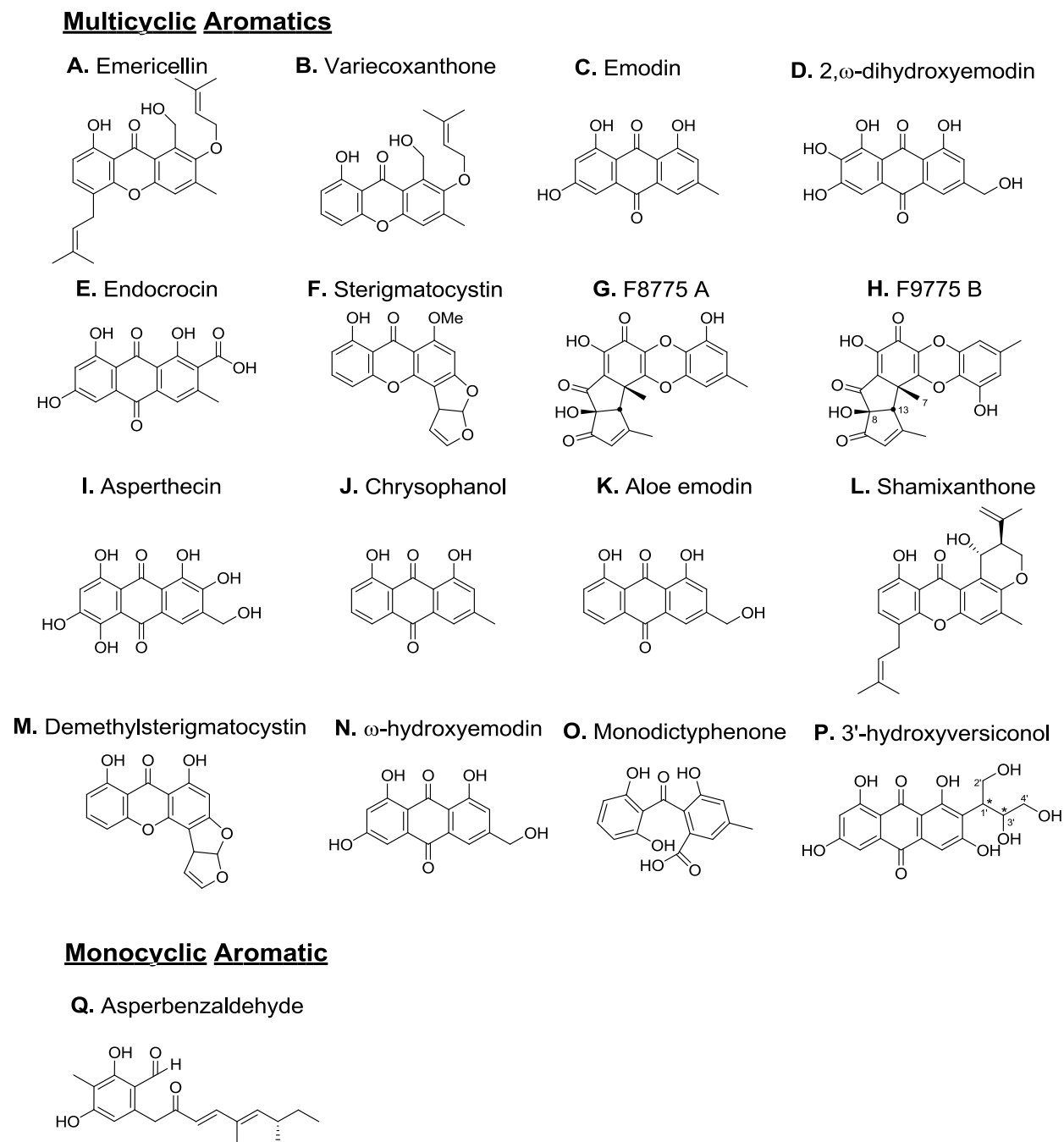


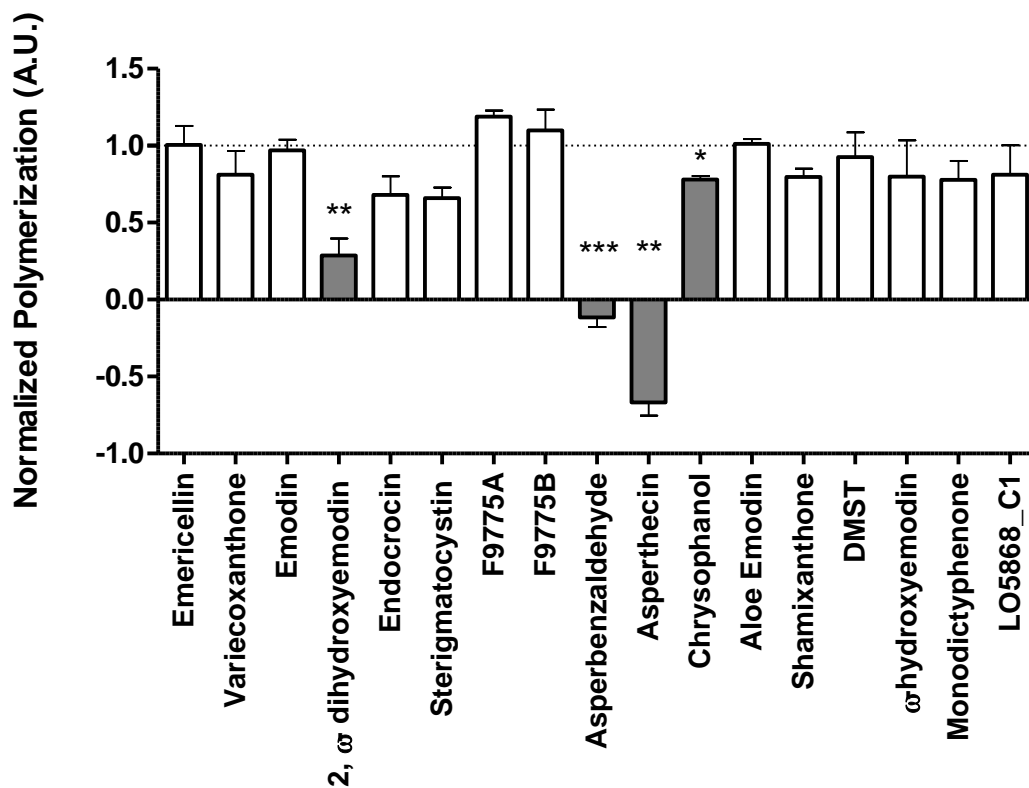
Figure 3.1 Compounds used in this study. Compounds used in this study. (A–Q) Structures of the 17 compounds used in this study: (A) Emericellin, (B) Variecoxanthone, (C) Emodin, (D) 2, ω - dihydroemodin, (E) Endocrocic, (F) Sterigmatocystin, (G) F9775 A, (H) F9775 B, (I) Asperthecin, (J) Chrysophanol, (K) Aloe emodin, (L) Shamixanthone, (M) Demethylsterigmatocystin, (N) ω – hydroxyemodin , (O) Monodictyphenone, (P) 3'- Hydroxyversiconol and (Q) Asperbenzaldehyde.

3.3.2.1. Filter trap assay. There was a decrease in tau aggregation seen in the presence of variacoxanthone, 2, ω -dihydroxyemodin, sterigmatocystin, asperthecin, chrysophanol, endocrocin, asperbenzaldehyde and shamixanthone (Figure 3.2). Among these, 2, ω -dihydroxyemodin, asperthecin, asperbenzaldehyde and chrysophanol showed a significant decrease in aggregation compared to the control reaction with no compound. Emodin, which has previously been shown to inhibit tau aggregation *in vitro*¹⁶⁶, did not show inhibition in our assays. The inducer molecule used in a previous emodin study was the glycosaminoglycan heparin, which is not as potent as arachidonic acid in inducing aggregation²¹⁸. Further, the tau isoform used in the previous study was not the full length tau. These differences could account for the difference in activity seen for emodin. This is discussed in more detail in the discussion section of this chapter.

3.3.2.2 Transmission electron microscopy. The filter trap assay is very informative, but it is an indirect method of quantifying tau aggregation. The results are affected by the ability of nitrocellulose membrane to retain certain types or size of the tau aggregates. Therefore, we viewed the filaments directly by transmission electron microscopy. Asperthecin, asperbenzaldehyde, sterigmatocystin and 2, ω -dihydroxyemodin were the most effective compounds in inhibiting tau filament formation compared to the control reaction where no compound was added (Figure 3.3).

We further analysed the filament lengths in presence and absence of the compounds. We measured the filament lengths and placed them in 50 nm bins ranging from 30 nm to 200nm. The first bin was 30nm-50nm, because anything less than 30 nm is difficult to distinguish from the electron microscope grid background and therefore makes it difficult to measure. We placed all the filaments above 200nm in one group because this cutoff should represent particles retained by the nitrocellulose membrane.

Figure 3.2



Filter trap assay of tau filament formation. The compounds used are listed on the Y-axis. The values for tau polymerization were normalized to the amount in the no compound control (dotted line). Negative values indicate that there was less detectable tau on the filter after treatment with a compound than was observed with monomeric tau in the absence of arachidonic acid. Values are the mean values of three trials \pm SD. * $P \leq 0.05$; ** $P \leq 0.01$; *** $P \leq 0.001$.

Emodin, variecoxanthone, F9775A, endocrocin, F9775B, asperthecin, emericillin, 2, ω -dihydroxyemodin, sterigmatocystin, aloe emodin, monodictyphenone, ω -hydroxyemodin and asperbenzaldehyde had filaments length distributions distinct from those of the no compound control (Figure 3.4). Asperbenzaldehyde had the most effect on the filament lengths with no filaments detected above 100nm in length.

Many of the compounds decreased the amount for tau aggregation which supports our rationale for choosing this set of compounds. Among all the compounds, asperthecin, asperbenzaldehyde and 2, ω -dihydroxyemodin showed reduction in aggregation in both the filter trap assay as well as the in electron microscopy.

3.3.3 Three compounds showed a dose-dependent activity. We sought to determine whether these compounds inhibit tau aggregation in a dose-dependent fashion. Therefore, we did dose-dependent tau aggregation inhibition assays for asperthecin, asperbenzaldehyde, 2, ω -dihydroxyemodin and sterigmatocystin. Sterigmatocystin sometimes showed dose dependent inhibition activity but these data were not reproducible (data not shown), therefore the IC₅₀ value could not be determined. The other three compounds gave reproducible dose dependent inhibition results. The IC₅₀ values for asperthecin, asperbenzaldehyde and 2, ω -dihydroxyemodin were $39 \pm 2 \mu\text{M}$, $177 \pm 103 \mu\text{M}$ and $205 \pm 28 \mu\text{M}$ respectively (Figure 3.5).

Figure 3.3

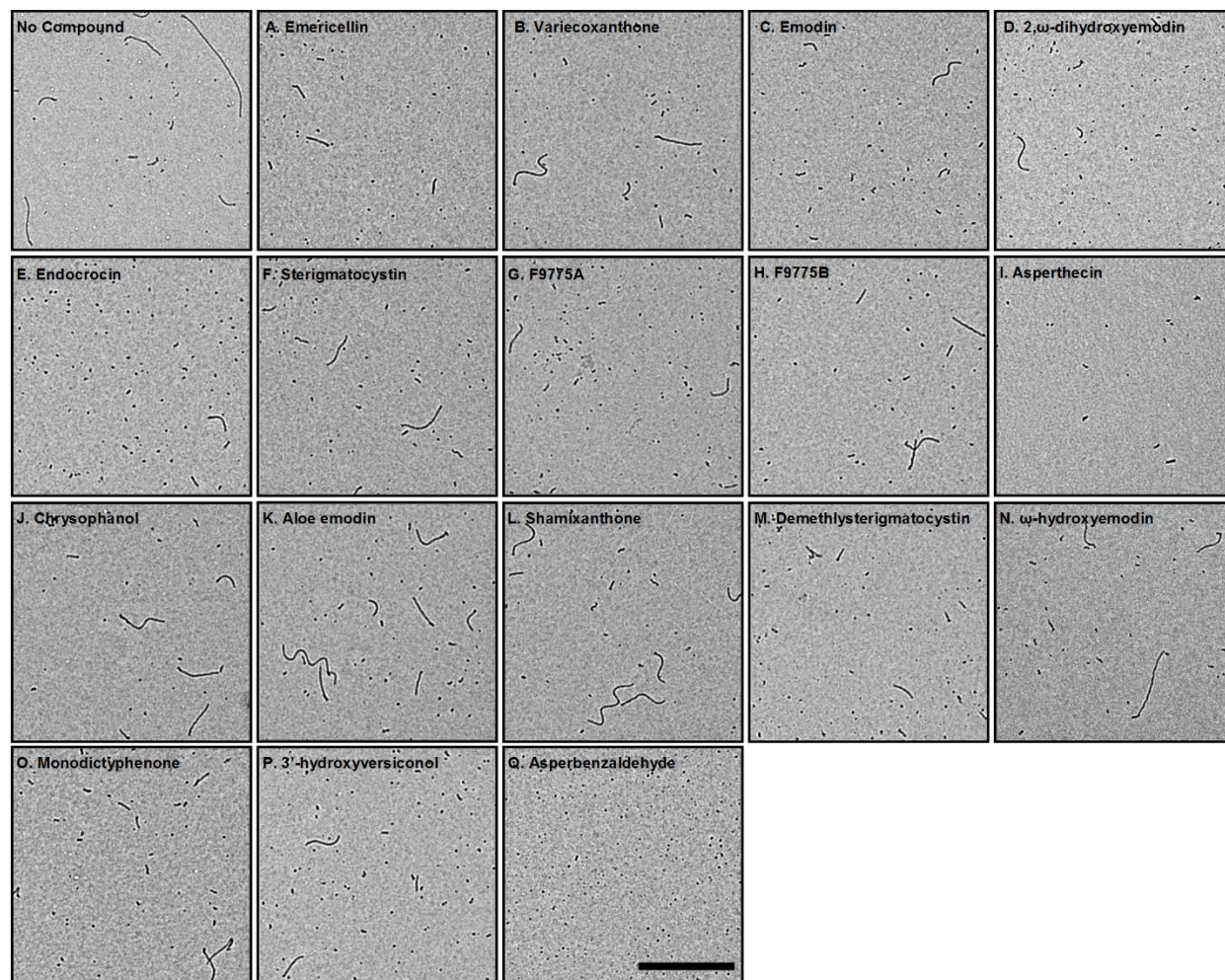


Figure 3.3. Electron microscopy of tau filament formation in the presence of compounds.

Tau polymerization reactions were performed with 2 μM tau and 75 μM arachidonic acid either with or without 200 μM compound. Aliquots of the reactions were prepared for negative stain electron microscopy. Representative images are shown for no compound control and compound treatment reactions (A-Q) (A) emericellin, (B) variecoxanthone, (C) emodin, (D) 2, ω -dihydroxyemodin, (E) endocrocin, (F) sterigmatocystin, (G) F9775A, (H) F9775B, (I) asperthecin, (J) chrysophanol, (K) aloe emodin, (L) shamixanthone, (M) demethylsterigmatocystin, (N) ω -hydroxyemodin, (O) monodictyphenone, (P) 3'-hydroxyversiconol and (Q) asperbenzaldehyde. The scale bar in the lower right panel represents 1 μm and is applicable to all images.

Figure 3.4

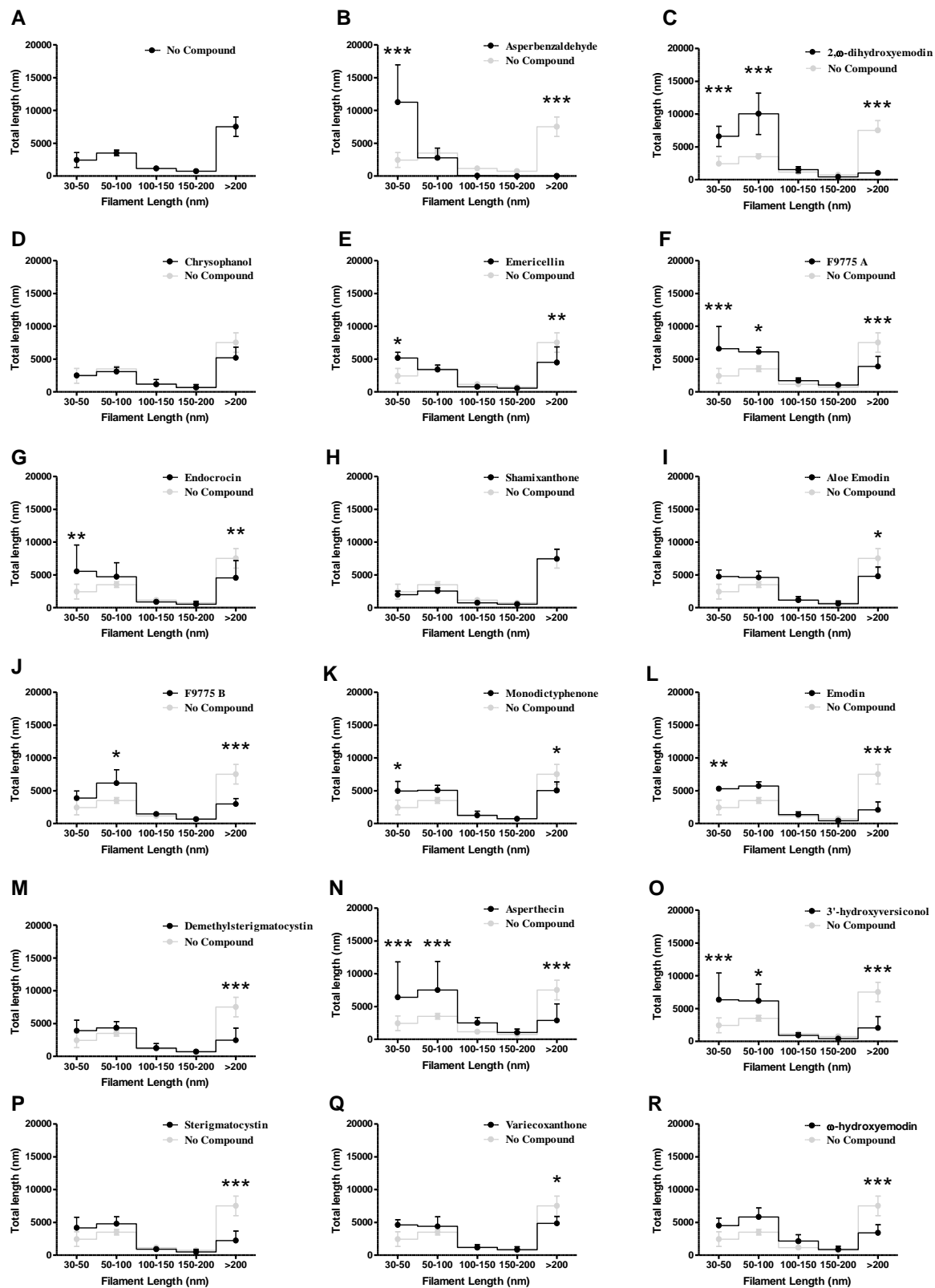
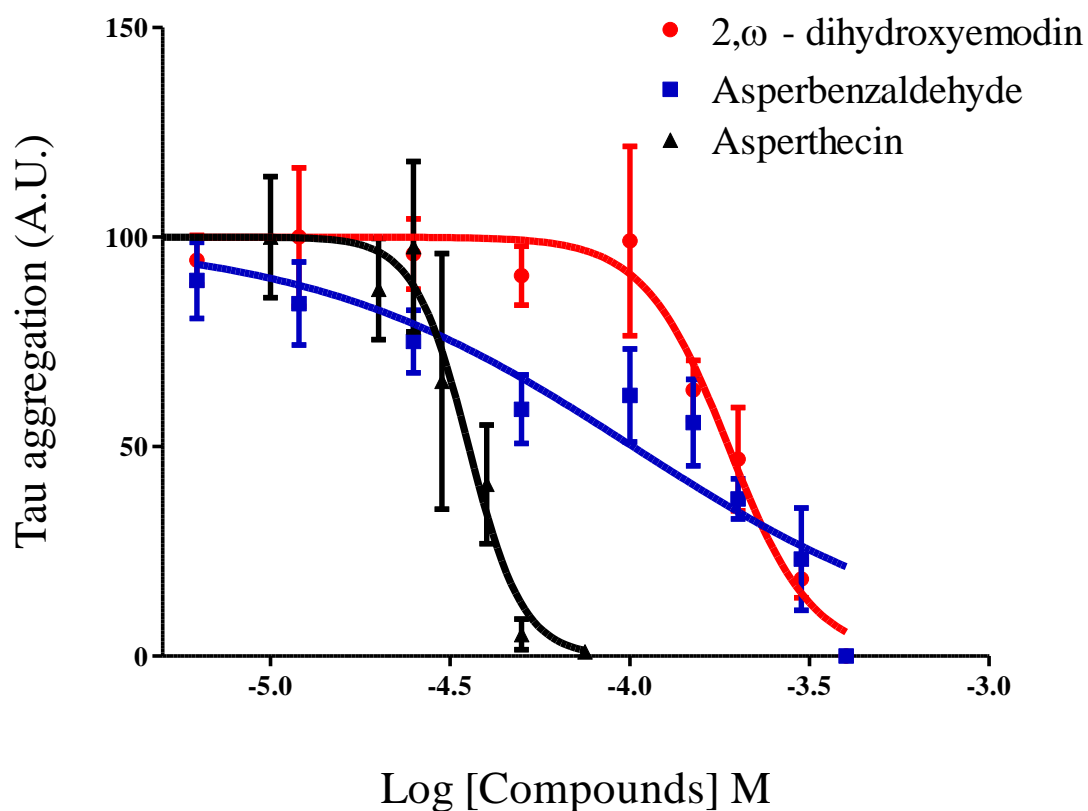


Figure 3.4. Filament length distributions. Filament lengths from electron micrographs of tau polymerization reactions were measured, placed into 50 nm bins (30–50 nm, 50–100 nm, 100–150 nm, 150–200 nm and > 200 nm), and the lengths were summed to determine the total amount of filament length in each bin. The first graph (A) shows the control reaction without a compound, and graphs B-R show the reactions with the different compounds, being labeled with the compound name and number. The filament distribution for the no-compound control is redrawn on each graph as a light gray line for comparison. Each point is the average distribution for images of at least 9 different fields \pm SD. * $P \leq 0.05$; ** $p \leq 0.01$; *** $p \leq 0.001$.

Figure 3.5



IC₅₀ determination tau filament assembly. Polymerization reactions at 2 μM tau and 75 μM arachidonic acid were performed at several different concentrations of the compounds, and the resulting amount of tau filaments in the reaction was determined by a filter trap assay detected by a mixture of antibodies to normal tau (tau 5, tau 7, and tau 12). The amount of polymerization was normalized to controls in the absence of compound (100%). The normalized data was plotted against the log of the inhibition concentration and fit to a dose–response curve to determine the IC₅₀ for asperbenzaldehyde (blue), 2, ω- dihydroxyemodin (red), asperthecin (black). Data points are the average of three trials ± SD.

Figure 3.6

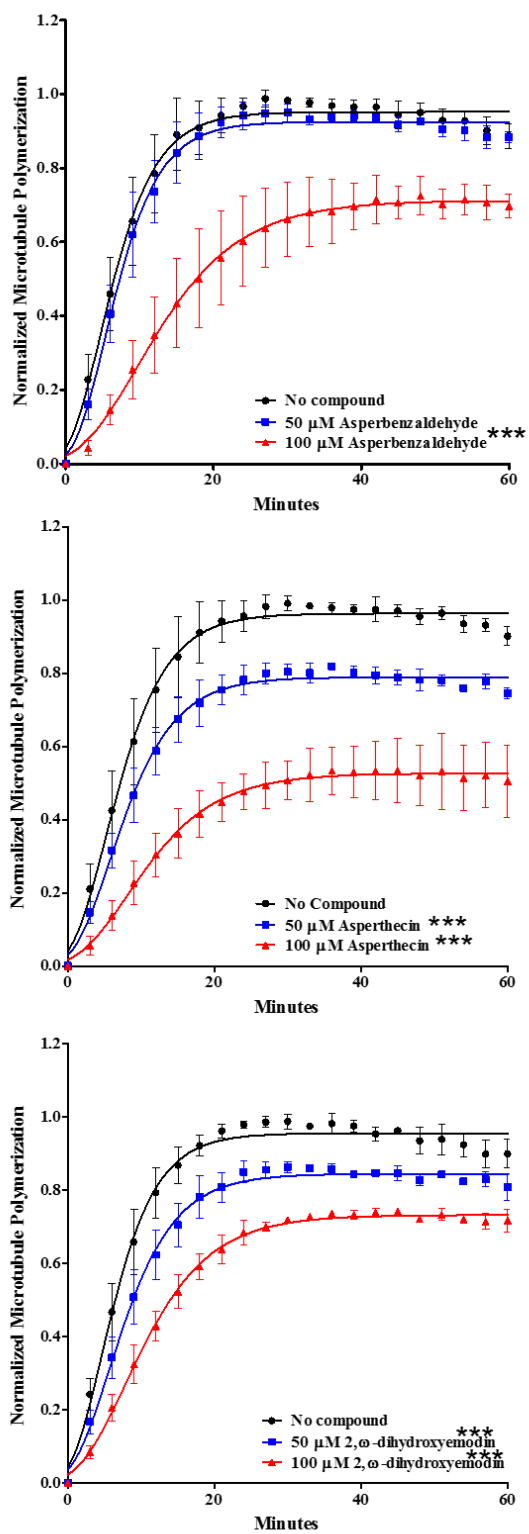


Figure 3.6 Microtubule assembly. Tubulin was incubated with either tau protein alone (black) or tau in the presence of (A) 2, ω -dihydroxyemodin, (B) asperthecin, or (C) asperbenzaldehyde at compound concentrations of 50 μ M (blue) or 100 μ M (red). Microtubule assembly was monitored by DAPI fluorescence (y-axis) over time (x-axis) and normalized to microtubule polymerization in the presence of paclitaxel. Every third time point is shown. Each point is the average of three independent trials \pm SD. The data are fit to a Gompertz growth curve (black, blue, and red lines for no compound, 50 μ M and 100 μ M compound, respectively). * $P \leq 0.05$; ** $p \leq 0.01$; *** $p \leq 0.001$.

Table 3.2 Statistical analysis of the effects of anti-tau aggregation compounds on the stabilization of microtubules.

Asperbenzaldehyde	<i>a</i>	<i>b</i>	<i>ti</i>
No compound	0.96 ± 0.02	4.2 ± 1.2	4.8 ± 1.5
50 μM	0.93 ± 0.01	4.1 ± 1.0	5.4 ± 1.2
100 μM	0.72 ± 0.04***	7.9 ± 2.3	10.2 ± 2.7*

Asperthecin	<i>a</i>	<i>b</i>	<i>ti</i>
No compound	0.97 ± 0.01	4.7 ± 1.3	5.5 ± 1.5
50 μM	0.79 ± 0.02**	5.0 ± 1.3	5.9 ± 0.9
100 μM	0.53 ± 0.08***	6.7 ± 2.6	8.6 ± 3.1

2,ω-dihydroxyemodin	<i>a</i>	<i>b</i>	<i>ti</i>
No compound	0.96 ± 0.02	4.1 ± 0.8	4.7 ± 1.0
50 μM	0.85 ± 0.01***	5.0 ± 0.8	5.8 ± 1.0
100 μM	0.74 ± 0.01***	6.4 ± 0.8*	7.8 ± 1.2*

Table 3.2 Three individual microtubule polymerization curves for each condition were fit to a nonlinear Gompertz growth function:

$$y = ae^{-e^{-(t-t_i)/b}}$$

Where y is the amount of microtubule polymerization measured at time t , a is the maximum amount of microtubule polymerization observed, t_i is the point of inflection of the curve, and b is inversely proportional to the apparent rate of polymerization. The average values for the parameters a , b , and t_i were determined and compared to the no-compound control using a one-way analysis of variance followed by Dunnett's multiple comparison test to determine statistical significance. * $P \leq 0.05$; ** $P \leq 0.01$; *** $P \leq 0.001$

3.4.4 Effect on tau- microtubule interactions. Tau's normal function is to promote microtubule assembly and further stabilise the microtubule structure. We therefore sought to determine whether the most potent compounds, asperthecin, asperbenzaldehyde and 2, ω -dihydroxyemodin, interfered with the normal function of tau. Microtubule polymerization was monitored using DAPI fluorescence in the presence of tau with or without the compound. Although, all three compounds showed a dose-dependent reduction in tau's ability to polymerize microtubules, significant microtubule stabilization was retained at high concentrations of the inhibitors (Figure 3.6). A statistical analysis of the effects of anti-tau aggregation compounds on the stabilization of microtubules is shown in Table 3.2.

3.5 Discussion

Tau aggregation is a common pathological condition seen in AD and other tauopathies. The location and amount of tau aggregation correlates well with the type and severity of the disease progression⁴². There is great interest in finding small molecules which can inhibit tau aggregation. Previous studies have identified several classes of compounds including anthraquinones, polyphenols and phenothiazines that show promise as aggregation inhibitors. These compounds have a common structural motif of ring structures, which are believed to interact with the β -sheet structure found at the core of the tau aggregates, therefore preventing further filament formation. There is a need for identifying additional lead anti-tau aggregation compounds for further development into therapeutics.

Fungi have long been a source for great medicinal products such as antibiotics²²⁰, and recent advances in genetic manipulation of secondary metabolite producing gene clusters have enhanced our capabilities to obtain, purify and characterize fungal natural products. Dr. Berl

Oakley and his colleagues have identified many biosynthetic pathways in *Aspergillus nidulans* that produce of a wide variety of secondary metabolites including anthraquinones, xanthenes and other metabolites in amounts that allow ready purification^{205, 221}. Many of these small compounds have aromatic ring structures similar to those found in tau aggregation inhibitors.

Out of the 17 compounds chosen, three compounds inhibited tau aggregation and gave us reproducible and consistent results. Three compounds out of 17 is a good number of hits for a preliminary screen, therefore supporting our hypothesis for choosing compounds with ring structures. Among the hits, 2, ω -dihydroxyemodin and asperthecin belong to the anthraquinone class of compounds. Other anthraquinones have previously been identified as tau aggregation inhibitors, particularly emodin which we included in our study. Emodin was previously shown to be a strong inhibitor of tau polymerization with an IC_{50} value in the range of 1-5 μM ¹⁶⁶. In our assays, emodin was not a potent inhibitor and at the same time it was surprising to see our potent compounds having high IC_{50} values in the range of 40-200 μM . This difference in activity and IC_{50} values could be due to differences in the assay conditions. Compared to the previous emodin study, our assay conditions strongly drive aggregation and therefore may provide a more rigorous test for inhibition. The previous study was done using the glycosaminoglycan heparin sulfate as an inducer¹⁶⁶ and previous studies have shown that arachidonic acid induces approximately three times the amount of aggregation as heparin sulfate under similar conditions²¹⁸. The tau isoforms used in the previous study were the 0N3R and 0N4R isoforms which have been shown to be less prone to aggregation than the 2N4R isoform used in this study¹⁴. Therefore, these factors could provide an explanation for the higher IC_{50} values seen in our assays compared to those in the previous studies.

We have identified compounds belonging to the class of anthraquinones as tau aggregation inhibitors, while none of the xanthenes were effective. Xanthenes and anthraquinones both possess ring structures but there is a difference in the groups on their central ring.

Anthraquinones contain 2 keto groups on their central ring, while xanthenes have a single keto group and an ether linkage. The keto groups could therefore be playing an important role in inhibiting tau aggregation. The keto groups on the central ring could be better aligned to interact with the β -sheet forming sequences compared to the xanthone ring. It is interesting that arachidonic acid can adopt ring-like conformations when in solution and heparin sulfate also contains ring structures. Therefore, it is possible that the compounds bind to tau in a similar fashion as the inducer molecules but create a conformational change upon binding which blocks further binding to other tau molecules.

Asperbenzaldehyde has a chemical structure that is different from all the previously identified tau aggregation inhibitors. It has a single aromatic ring and is a stable intermediate in the azaphilone biosynthetic pathway. This molecule is particularly interesting because it can be modified in 2 -3 steps to form azaphilones. Azaphilones are a group of compounds which exhibit a great variety of biologically important activities including antioxidant and anti-inflammatory activities, which could be useful for therapeutics against AD²²². Further, asperbenzaldehyde has weak lipoxygenase-1 (LOX-1) inhibitory activity which can be converted into a series of strong LOX-1 inhibitors by simple modifications²¹¹. We know that fatty acid levels are elevated in AD²²³, therefore inhibition of LOX-1 would be useful and derivatives of Asperbenzaldehyde could therefore have dual therapeutic activity against AD.

The most potent compounds partially preserve tau's ability to bind to tubulin and promote microtubule assembly. They do not completely inhibit tau's function of stabilizing the assembly

of tubulin into microtubules. It was not surprising that some diminution occurred in presence of these compounds because the sequences which are likely responsible for tau aggregation ²⁷⁵VQIINK²⁸⁰ and ³⁰⁶VQIVYK³¹¹, reside in the microtubule binding repeats^{44, 202}. Therefore, if the compounds are interacting with these motifs, they would have some impact on the microtubule stabilization as well. It is encouraging that these compounds retain some tau function and therefore are promising future seed compounds which could be used to develop better analogues/ derivatives with greater aggregation inhibiting ability and fewer effects on tau-microtubule interactions.

In this study we have therefore identified a novel aggregation inhibitor molecule, which is also an intermediate in an azaphilone synthesis pathway. It would be interesting to determine whether the azaphilones derived from asperbenzaldehyde retain this ability to inhibit aggregation. We have also shown that selected secondary metabolites from fungi include seed compounds which can possibly be modified for further therapeutic benefit.

Chapter IV Azaphilones as tau aggregation inhibitors: Second generation compounds obtained from *Aspergillus nidulans*

4.1 Introduction

Tau aggregation is one of the hallmarks that define pathology in AD and other tauopathies^{224, 225}. These tau aggregates appear in different forms in tauopathies including neurofibrillary tangles (NFTs) found in cell bodies and cortical deposits of dystrophic neurites and neuropil threads²²⁶. Tau aggregates serve as markers for differential diagnosis and disease staging⁵⁵. Tau aggregates can promote disease propagation²²⁷ and also serve as a direct source of toxicity^{66, 228}. Therefore, tau aggregation is a pathological process which is not related to normal functions of tau, and this makes it a good therapeutic target to apply diverse strategies for inhibiting misfolding and aggregation of tau and eventually halt or reverse disease progression²²⁹.

Previously, we screened seventeen secondary metabolites obtained from *Aspergillus nidulans* which predominantly had fused ring structures and found three compounds that inhibited tau aggregation in a dose dependent fashion *in vitro*²³⁰. Among these compounds asperthecin and 2, ω – dihydroxyemodin belonged to the class of anthraquinones. This was not a surprising result because compounds belonging to this class have been identified as tau aggregation inhibitors (TAIs) *in vitro*¹⁶⁶. A third compound, asperbenzaldehyde was the most interesting compound among these because it was a structurally novel tau aggregation inhibitor and it is a chemical precursor to a class of compounds called azaphilones.

Azaphilones are an interesting class of compounds having a great variety of biologically important activities including antimicrobial activity, enzyme inhibition such as topoisomerase II inhibition, caspase 3 inhibition, and inhibition of gp120-CD4 binding among others (reviewed

in²²²). Several azaphilones are also known to exhibit lipoxygenase inhibitor activity,²¹¹ which could be useful in AD to reduce elevated fatty acid metabolite levels²²³. We therefore sought to determine whether azaphilones derived from asperbenzaldehyde possessed tau aggregation inhibition activity, hoping that they would prove to have two biological targets relevant to treating AD.

Dr. Berl Oakley and his colleagues prepared a small library of azaphilones obtained from asperbenzaldehyde. We used standard biochemical assays to determine the ability of azaphilones to inhibit tau aggregation and its effect on tau's ability to polymerize microtubules. We found that all azaphilones derived from asperbenzaldehyde inhibited tau aggregation assembly, while four compounds showed an additional ability to dissolve pre-formed tau aggregates. The most potent compounds retained the majority of tau's microtubule stabilizing functions.

4.2 Experimental procedures

4.2.1 Compounds. The compounds were made by Dr. Berl Oakley's lab members, Dr. Clay Wang's lab members (University of Southern California) and Andrew Riley, Prizinsano Lab, KU. Asperbenzaldehyde was purified from *A. nidulans* and converted to the compounds aza-7–aza-17 as described previously²¹¹ with the following minor modifications. The Oakley lab constructed a number of strains with various promoter combinations and used a variety of induction conditions to maximize asperbenzaldehyde production. The best yields were obtained with strain LO8355 (*pyrG89*, *pyroA4*, *riboB2*, *nkuA::argB*, *stcJ::AfriboB*, AN1029(p):: *AfpyrG-alcA*(p), AN1033::*AfpyroA*, *alcR*(p)::*ptrA-gpdA*(p)). In this strain, the promoter of the asperfuranone biosynthesis transcription factor AN1029 (using the AspGD nomenclature; <http://aspergillusgenomes.org/>) is replaced with the highly inducible *alcA* promoter, and the *alcR*

promoter is replaced with the strong, constitutive *gpdA* promoter (−1241 to −1). AN1033 is replaced with the *AfpyroA* gene to interrupt the asperfuranone biosynthesis pathway, causing asperbenzaldehyde to accumulate. Growth was in lactose minimal medium (20 g/L lactose, 6 g/L NaNO₃, 0.52 g/L KCl, 0.52 g/L MgSO₄·7H₂O, 1.52 g/L KH₂PO₄, 1 mL/L trace elements solution)²³¹. Spores were inoculated at 10⁶/mL into 500 mL of medium in a 2 L flask. Incubation was at 37 °C on a gyratory shaker, and induction was with 30 mM methyl-ethyl-ketone, added 55 h after inoculation. Cultures were harvested 6 days after inoculation. Yields of purified asperbenzaldehyde were greater than 2 g/L, representing an approximate conversion of 10% of the carbon source to final product.

4.2.2 Protein preparation. Full-length 2N4R tau (441 amino acids) was expressed in *Escherichia coli* and purified as described previously¹⁹⁴.

4.2.3. Inhibition of Tau Aggregation. 75 μM arachidonic acid was used to initiate the aggregation of 2 μM tau in polymerization buffer (PB) (10 mM HEPES (pH 7.64), 5 mM DTT, 100 mM NaCl, 0.1 mM EDTA, and 3.75% ethanol) as previously described²¹⁸. Compounds dissolved in DMSO were added to a final concentration of 200 μM and incubated with tau protein in PB 20 min prior to the addition of arachidonic acid. The reactions were allowed to proceed for 16 h at room temperature before analysis²³⁰. For heparin-induced tau assembly inhibition reactions, 0.6 μM heparin was used to initiate aggregation of 2 μM tau in polymerization buffer for heparin (PBh) (10 mM HEPES (pH 7.64), 5 mM DTT, 17.7 mM NaCl) *in vitro*. Compounds dissolved in DMSO were added to a final concentration of 100 μM and incubated with tau protein in PB 20 min prior to the addition of heparin. The reactions were allowed to proceed for 16 h at 37 °C before analysis.

Figure 4.1

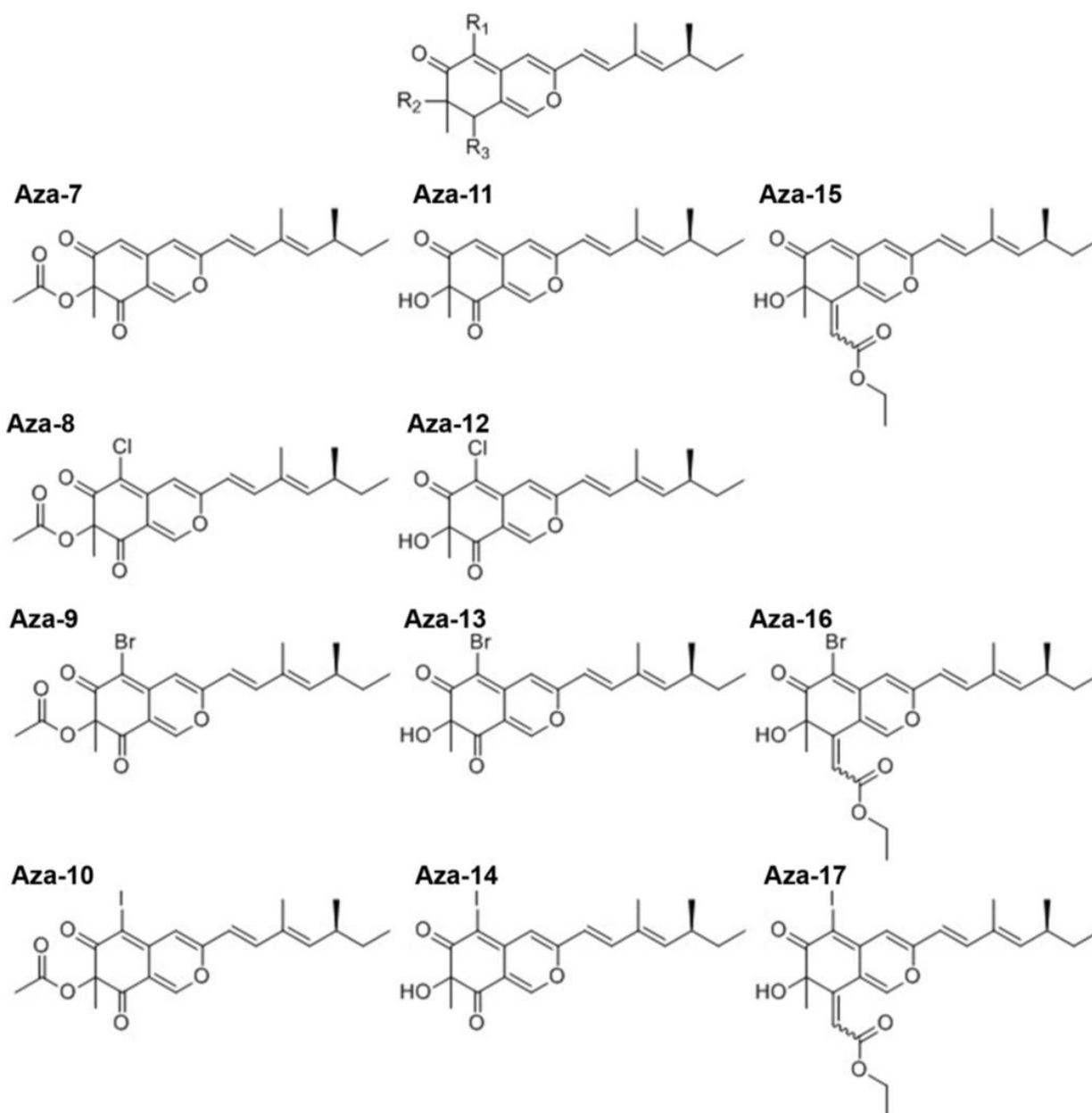


Figure 4.1 Compounds used in this study. The core structure of the azaphilone compounds is shown with the positions of modifications indicated by R₁, R₂, and R₃. Structures of the 11 compounds used in this study: aza-7, aza-8, aza-9, aza-10, aza-11, aza-12, aza-13, aza-14, aza-15, aza-16, and aza-17.

4.2.4. Disassembly of Preformed Filaments. Preformed tau filaments were generated with 2 μM tau and 75 μM ARA in PB as described above for 6 h at room temperature. Compounds dissolved in DMSO were added to the tau solution at final concentrations indicated in the Results section and figure legends. The reactions were allowed to proceed at room temperature for 12 h before analysis. For heparin-induced tau aggregation assays, preformed tau filaments were generated with 2 μM tau and 0.6 μM heparin in PBh as described above for 12 h at 37 °C. Compounds dissolved in DMSO were added to the tau solution at final concentrations indicated in the Results section and figure legends. The reactions were allowed to proceed at 37 °C for 24 h before analysis.

4.2.5. Filter Trap Assay. The amount of tau aggregates following assembly or disassembly reactions was determined by filter trap assay as described previously²³⁰. Reactions were diluted into TBS such that they contained 20 ng of protein in 300 μL . For heparin-induced tau aggregation reactions, the reactions were diluted into TBS such that they contained 60 ng of protein in 300 μL . Solutions were passed through a nitrocellulose membrane using house vacuum in a dot-blot apparatus. The aggregates trapped on the membrane were detected by either general antibodies (a mixture of tau 5 antibody²¹⁹ at 1:50 000 dilution, tau 12 antibody⁹⁶ at 1:250 000 dilution, and tau 7 antibody¹⁹² at 1:250 000 dilution) or antibodies to toxic conformations (TNT1²³² at 1:200 000 or TOC1²³³ at 1:7000). All antibodies were a kind gift from Drs. Nick Kanaan and Lester I. Binder. HRP-linked goat anti-mouse IgG (general antibodies and TNT1) or HRP-linked goat anti-mouse IgM (TOC1) (Thermo Scientific, Rockford, IL) were used as the secondary antibodies, and blots were developed using ECL (enhanced chemiluminescence) western blotting analysis system (GE Healthcare, Buckinghamshire, UK). Images were captured with a Kodak Image Station 4000R or ChemiDoc-

It2 imager and were quantified using the histogram function of Adobe Photoshop 7.0. Statistical analyses were performed using unpaired t-tests to compare the triplicate values to control values.

4.2.6 Transmission Electron Microscopy. Polymerization reaction samples were diluted 1:10 in PB and fixed with 2% glutaraldehyde for 5 min. Fixed samples were placed on Formvar carbon-coated grids and stained with uranyl acetate as previously described²³⁰. Images were captured with a Technai F20 XT field emission transmission electron microscope (FEI Co., Hillsboro, OR) and Gatan Digital Micrograph imaging system (Gatan, Inc., Pleasanton, CA). The filaments were quantified using Image-Pro Plus 6.0 software (Media Cybernetics, Inc., Rockville, MD) as previously described²³⁰. For quantitative analysis, filament lengths were placed into bins as described in Results. Statistical analyses were performed using unpaired t-tests to compare four or five replicates for each bin size with the no-compound data serving as reference values.

4.2.7 Tubulin Polymerization Assay. Polymerization of tubulin was measured using a tubulin polymerization assay kit (BK006P, Cytoskeleton, Inc., Denver, CO) following the manufacturer's protocol. Briefly, 2 mg/mL porcine tubulin was incubated with 1.5 μ M tau and 90 μ M aza-8, aza-9, aza-12, or aza-13 compound. Tubulin polymerization was monitored by turbidity at 340 nm in a Varian 50 MPR microplate reader at 37 °C for 1 h. Experiments were performed in triplicate, averaged, and fit to a Gompertz growth equation as previously described¹⁴ using the equation

$$y = ae^{-e^{-(t-t_i)/b}}$$

where y is the amount of microtubule polymerization measured at time t, a is the maximum amount of microtubule polymerization observed at an absorbance of 340 nm (max), t_i is the point

of inflection of the curve at the time of maximum growth rate in minutes, and b is inversely proportional to the apparent rate of polymerization (k_{app} , min^{-1}). The average values for parameters a , b , and t_i were determined and compared to the no-compound control using a paired t -test to determine statistical significance. *, $P \leq 0.05$; **, $P \leq 0.01$; ***, $P \leq 0.001$.

4.3 Results

4.3.1. Tau aggregation inhibition assay

Eleven compounds with the same azaphilone backbone differing at three points of diversity (R1, R2, and R3) were used in this study (Figure 4.1). Tau polymerization was initiated *in vitro* using a standard arachidonic acid induction assay²¹⁸. The degree of tau aggregation inhibition for each compound was determined using a membrane filter assay²³⁴. This assay has been used previously to screen *A. nidulans* secondary metabolites including anthraquinones, xanthenes, polyketides, a benzophenone, and the asperbenzaldehyde compound that was the parent compound for the synthesis of the azaphilones used in this study²³⁰. A mixture of antibodies to the amino terminal, central, and carboxy terminal regions of tau (tau 12, tau 5, and tau 7, respectively) was used to detect tau aggregates. In this assay, only compound aza-11 significantly reduced the amount of tau aggregation detected. Compounds aza-13 and aza-15 significantly increased the amount of tau aggregation, and the remaining compounds had no significant effect (Figure 4.2).

4.3.2. The aggregates formed in the presence of the compounds were not toxic.

Upon use of antibodies against toxic species of tau for detection, we observed that all azaphilones completely abolished recognition by the TOC1 antibody, which recognizes toxic oligomers *in vitro* and in Alzheimer's disease tissue as compared to that for controls without compound (Figure 4.3 B). Similarly, significant reductions in recognition by TNT1, an antibody

that recognizes the phosphatase-activating domain of tau and is exposed in pathological forms of tau, were observed for all aza compounds as compared to that for controls without compound (Figure 4.3 A).

4.3.3 All Azaphilones inhibited filament formation

When the resulting tau aggregates from the inhibition reactions were visualized by electron microscopy, there were abundant numbers of long filaments in the absence of added compound (Figure 4.4). Surprisingly, all of the azaphilones inhibited the formation of long tau filaments that were observed in the absence of compounds. Instead, amorphous small aggregates were observed after treatment with the compounds (Figure 4.4). This degree of tau aggregation inhibition was similar to what was observed by electron microscopy for asperbenzaldehyde and asperthecin and was stronger than what was observed for 2, ω -dihydroxyemodin in Chapter III²³⁰. Because tau aggregation inhibitors that inhibit filament formation have previously been shown to stabilize off-pathway soluble oligomers that are large enough to be trapped in the membrane filter assay²³⁵, we believe that the mixture of tau antibodies to normal tau was detecting these aggregates in the filter trap assay (Figure 4.2). These aggregates do not seem to be toxic because of their lack of reactivity to TOC1 (Figure 4.3A) and TNT1 (Figure 4.3B). We did assays to detect whether the azaphilones block adherence of tau filaments to the EM grids (Figure 4.5). The azaphilones did not affect the adherence of filaments to the grid.

Figure 4.2

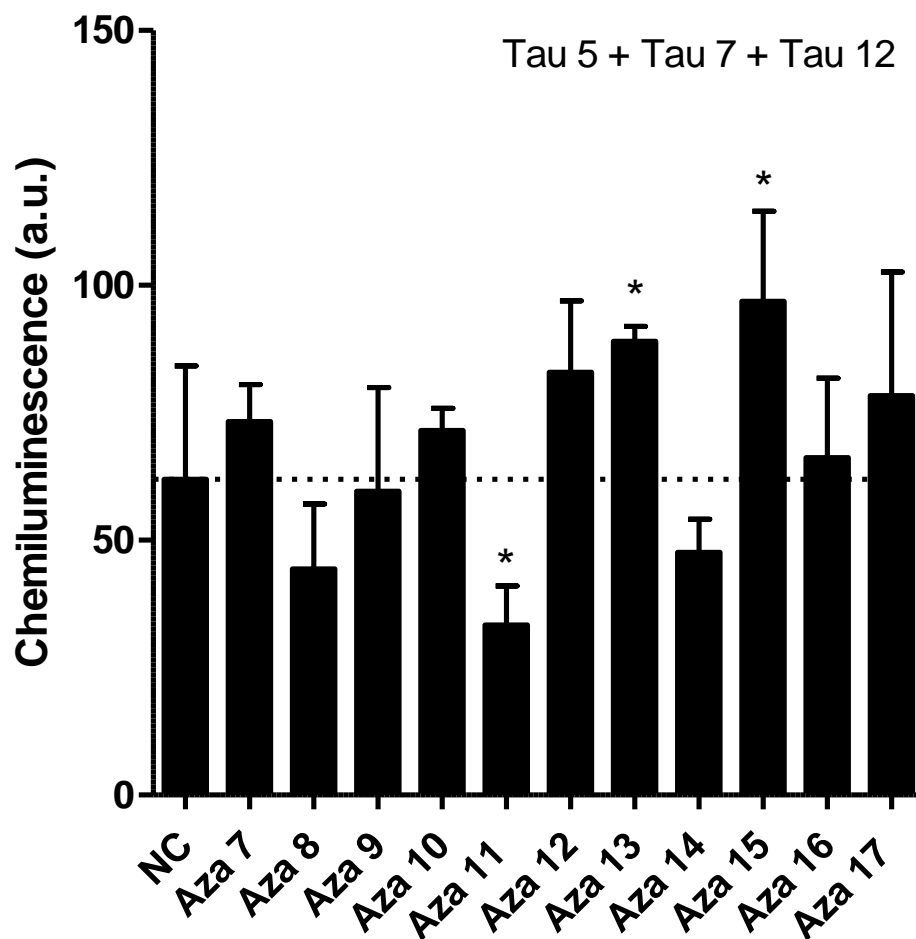


Figure 4.2 Filter trap assay of tau filament formation. Tau polymerization reactions were performed with 2 μM tau and 75 μM arachidonic acid either with or without 200 μM compound. The compounds used are listed on the x axis. The resulting amount of tau filament formation was determined using a filter trap assay. The values for tau filament formation were normalized to the amount of aggregation in the absence of compound (dashed line). The amount of tau on the filter was detected using a mixture of antibodies tau 5, tau 7, and tau 12. Values are the average of three trials \pm SD. *, $P \leq 0.05$; **, $P \leq 0.01$; ***, $P \leq 0.001$

Figure 4.3

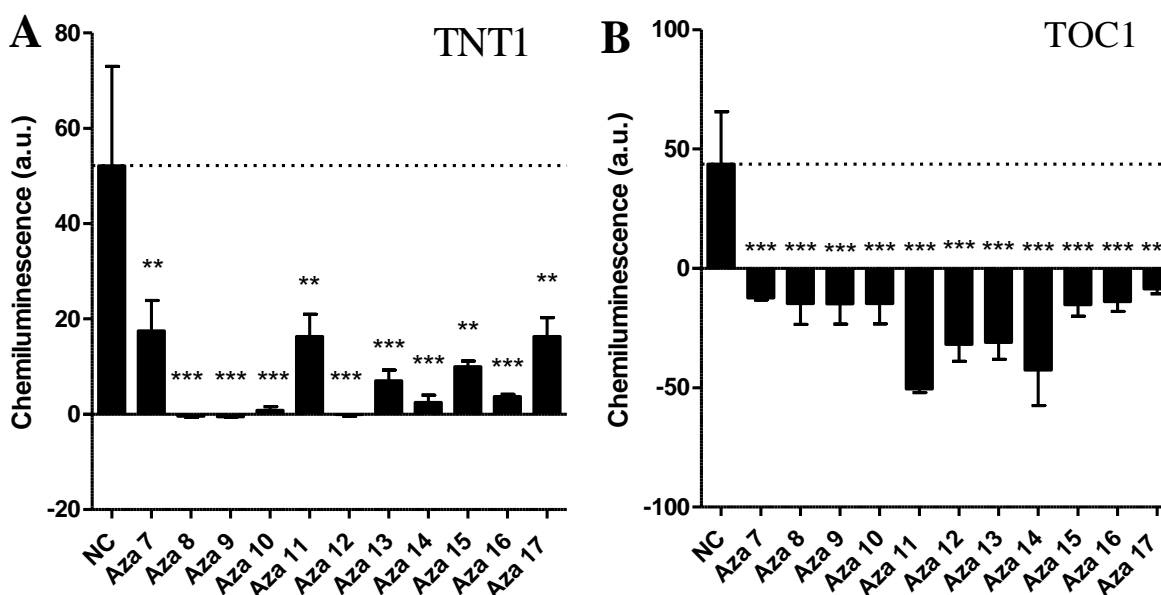


Figure 4.3 Filter trap assay of tau filament formation. Tau polymerization reactions in (A and B) were performed with 2 μ M tau and 75 μ M arachidonic acid either with or without 200 μ M compound. The compounds used are listed on the x axis. The resulting amount of tau filament formation was determined using a filter trap assay. The values for tau filament formation were normalized to the amount of aggregation in the absence of compound (dashed line). Negative values indicate that there was less detectable tau on the filter after treatment with a compound than was observed with monomeric tau in the absence of arachidonic acid. The amount of tau on the filter was detected using (A) antibody TOC1 and (B) antibody TNT1. The observation suggests that the tau aggregates that are retained on the filters are not in the toxic oligomeric form recognized by the TOC1 antibody and that the phosphatase domain recognized by TNT1 antibody is not exposed. Values are the average of three trials \pm SD. *, $P \leq 0.05$; **, $P \leq 0.01$; ***, $P \leq 0.001$

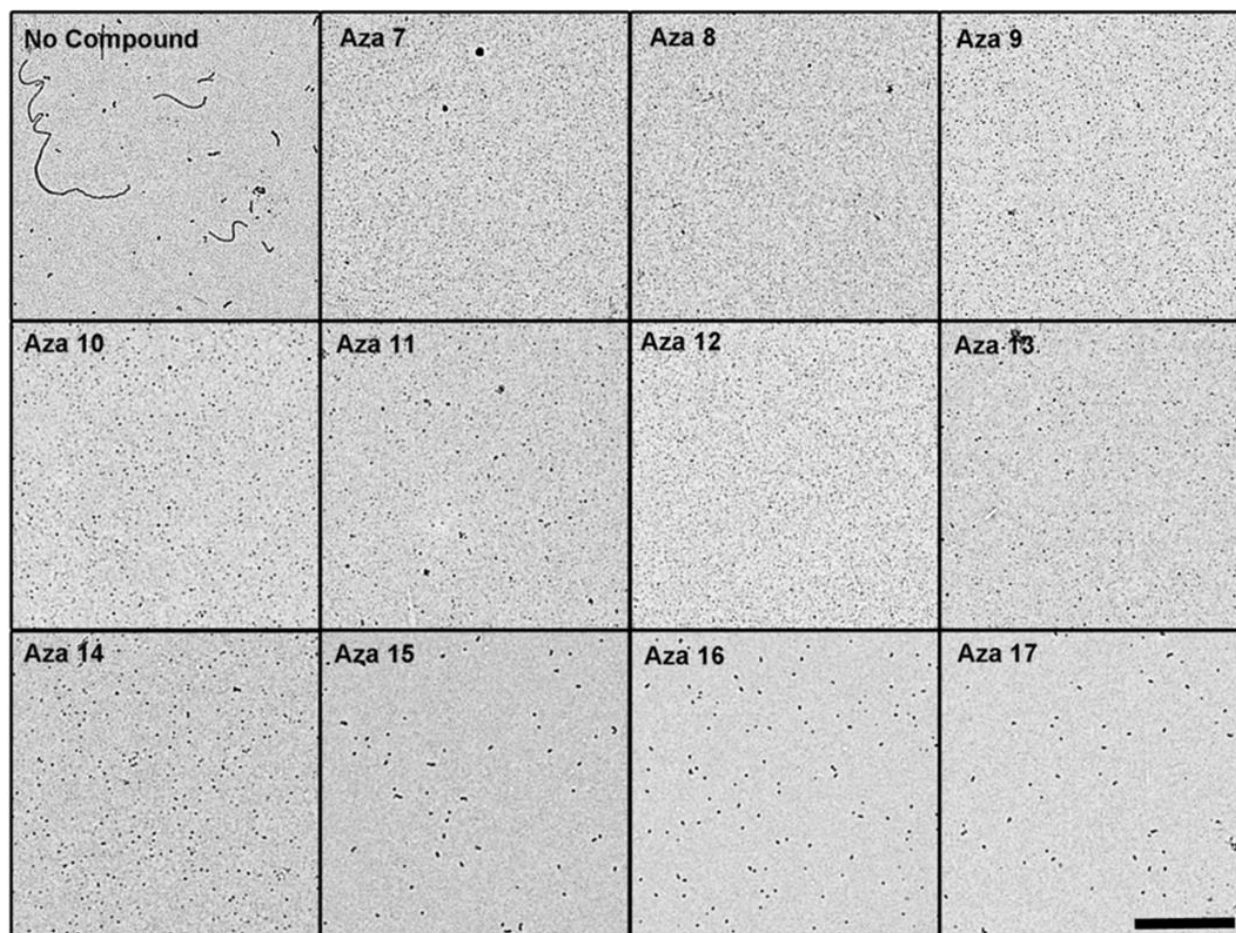
Figure 4.4

Figure 4.4 Electron microscopy of tau filament formation in the presence of azaphilone derivatives. Tau polymerization reactions were performed with 2 μM tau and 75 μM arachidonic acid either with or without 200 μM compound. Aliquots of the reactions were prepared for negative stain electron microscopy. Representative images are shown for no compound control, aza-7, aza-8, aza-9, aza-10, aza-11, aza-12, aza-13, aza-14, aza-15, aza-16, and aza-17. The scale bar in the lower right panel represents 1 μm and is applicable to all images.

4.3.4 Aza-8, aza-9, aza-12 and aza-13 completely disassembled pre-formed tau filaments.

To determine whether these compounds can disassemble preformed tau aggregates, tau aggregation was allowed to proceed for 6 h before the addition of compounds to a final concentration of 200 μ M. After 12 h, the effect of compounds on the tau aggregation was examined by a filter trap assay using the mixture of antibodies against normal tau (Figure 4.5). All compounds reduced the amount of preformed tau filaments, with compounds aza-8, aza-9, aza-11, aza-12, and aza-13 having the greatest activity. Electron microscopy was used to validate and extend the results from the filter trap assay. Compounds aza-8, aza-9, aza-12, and aza-13 substantially reduced the pre-existing filament mass, whereas the other compounds had less effect (Figure 4.6). To test whether compounds aza-8, aza-9, aza-12, and aza-13 were not simply blocking the adherence of tau filaments to the electron microscopy grids, compounds were added to preformed tau filaments and were immediately prepared for electron microscopy without allowing time for disassembly to occur. Under these conditions, none of the compounds blocked the binding of the filaments to the grid (figure 4.8). Quantitative analysis of the filament lengths in the presence and absence of compounds confirmed that compounds aza-8, aza-9, aza-12, and aza-13 had fewer aggregates overall compared to that in reactions without compound and virtually no filaments remaining that were greater than 200 nm in length (Figure 4.7).

Figure 4.5

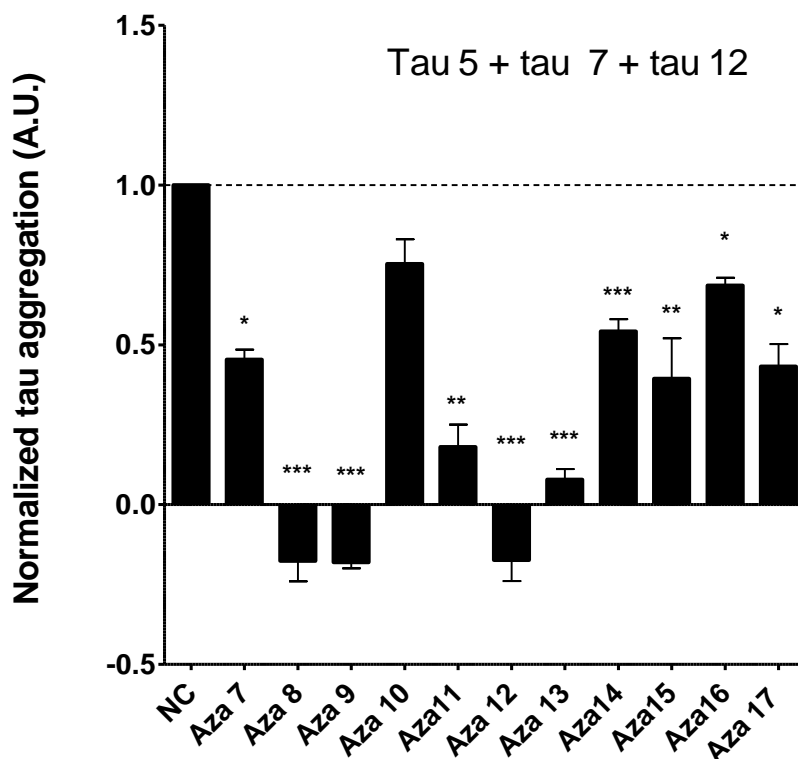


Figure 4.5 Filter trap assay of tau filament disassembly. Tau polymerization reactions were performed with 2 μ M tau and 75 μ M arachidonic acid at room temperature. After 6 h, 200 μ M compound or an equal volume of DMSO was added to the reactions. The compounds used are listed on the x axis. The resulting amount of tau filament formation was determined using a filter trap assay. The values for tau filament formation were normalized to the amount of aggregates detected in the absence of compound (dashed line). Negative values indicate that there was less detectable tau on the filter after treatment with a compound than was observed with monomeric tau in the absence of arachidonic acid. The amount of tau on the filter was detected using a mixture of antibodies tau 5, tau 7, and tau 12. Values are the average of three trials \pm SD. *, $P \leq 0.05$; **, $P \leq 0.01$; ***, $P \leq 0.001$.

Figure 4.6

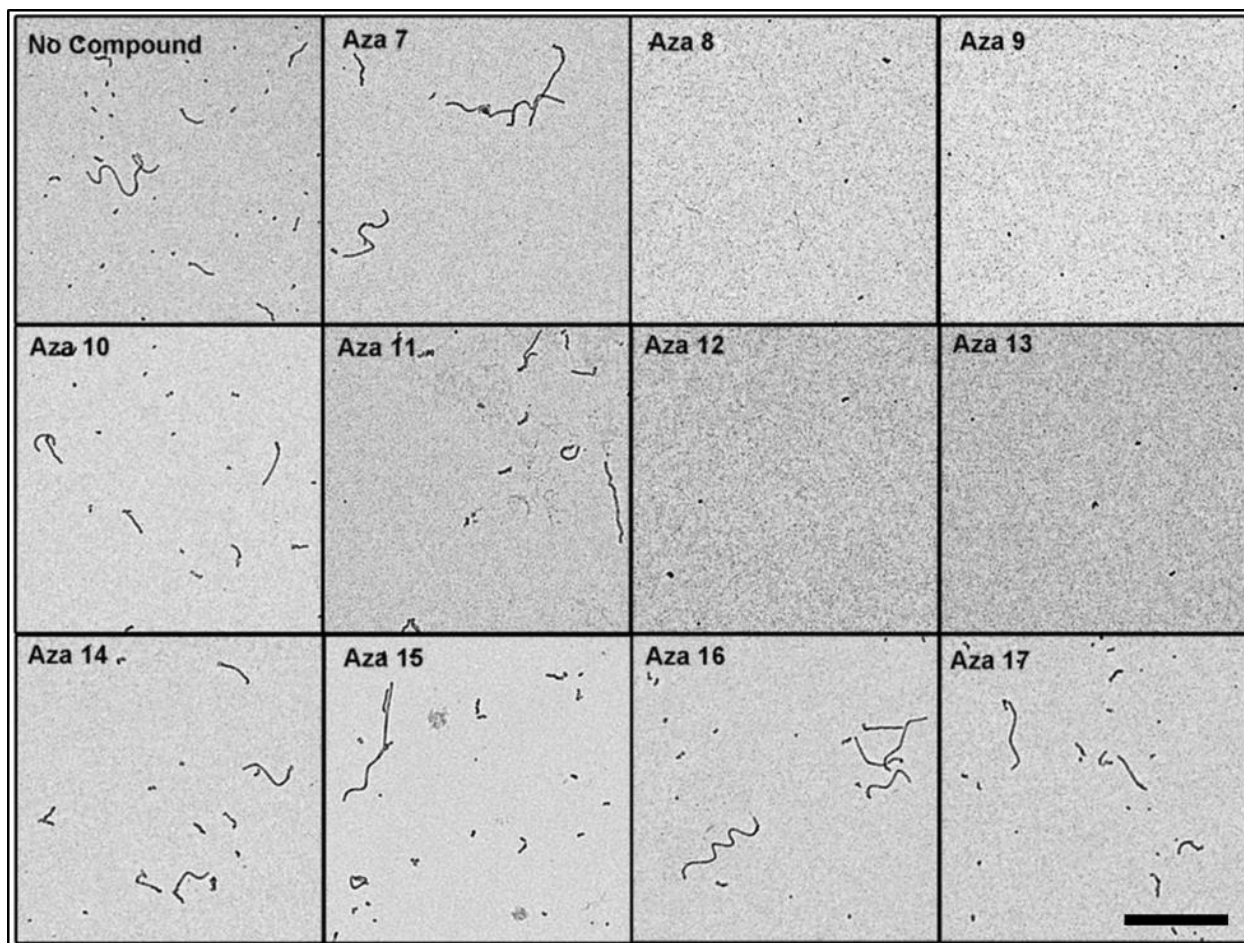


Figure 4.6 Electron microscopy of tau filament disassembly in the presence of azaphilone derivatives. Tau polymerization reactions were performed with 2 μM tau and 75 μM arachidonic acid at room temperature. After 6 h, 200 μM compound or equal volume of DMSO was added to the reactions. Aliquots of the reactions were prepared for negative stain electron microscopy. Representative images are shown for no compound control, aza-7, aza-8, aza-9, aza-10, aza-11, aza-12, aza-13, aza-14, aza-15, aza-16, and aza-17. The scale bar in the lower right panel represents 1 μM and is applicable to all images.

Figure 4.7

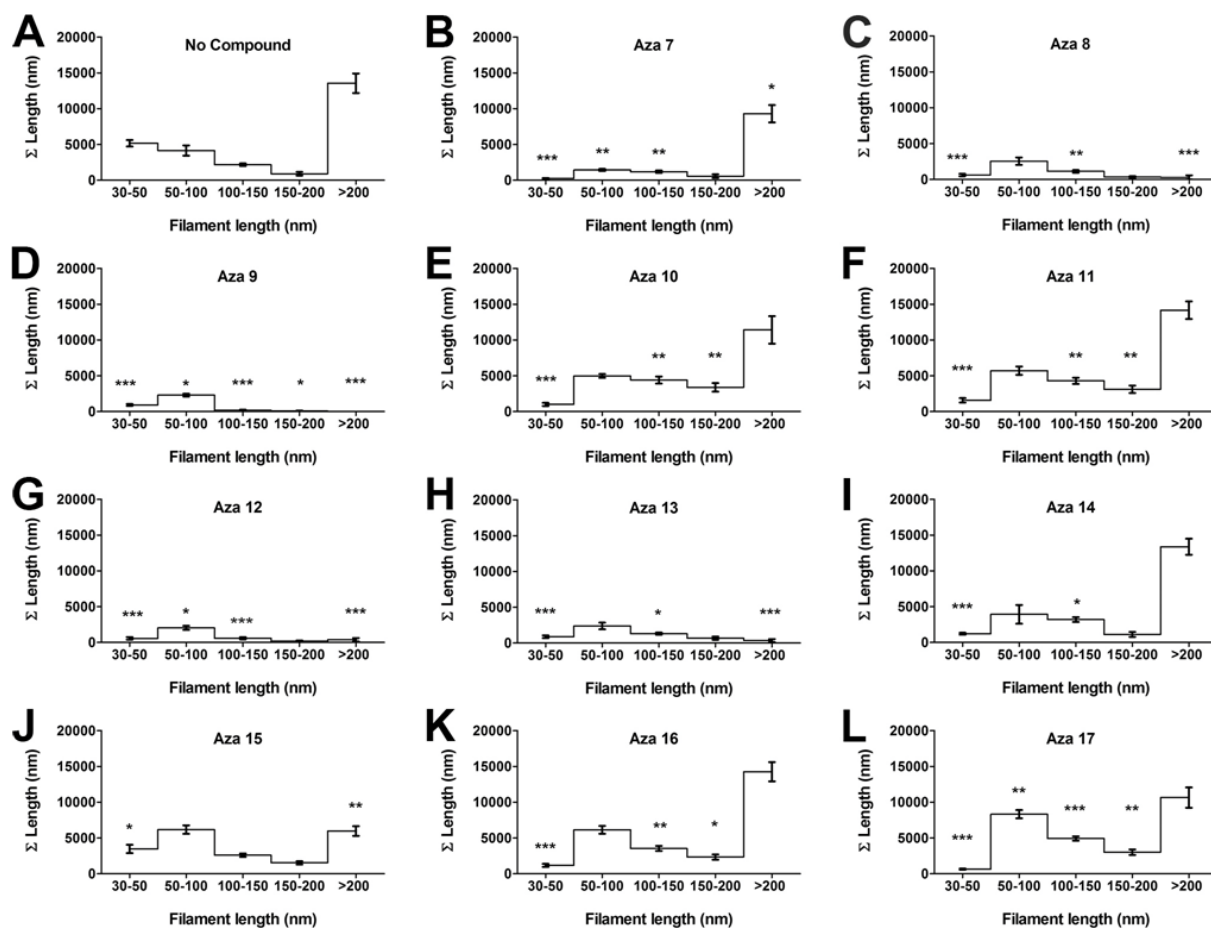


Figure 4.7 Filament length distributions. Tau disassembly reactions were performed and viewed by electron microscopy. The filaments remaining following incubation with or without compound were measured and placed into bins according to their length (30–50, 50–100, 100–150, 150–200, and >200 nm). The lengths within a bin were summed to determine the total amount of filament length in each bin. (A) Length distributions for filaments in the control reaction without compound. The length distributions are also shown for filaments remaining following incubation in the presence of (B) aza-7, (C) aza-8, (D) aza-9, (E) aza-10, (F) aza-11, (G) aza-12, (H) aza-13, (I) aza-14, (J) aza-15, (K) aza-16, and (L) aza-17. Each point is the average distribution for images of five different fields \pm SD. *, $P \leq 0.05$; **, $P \leq 0.01$; ***, $P \leq 0.001$.

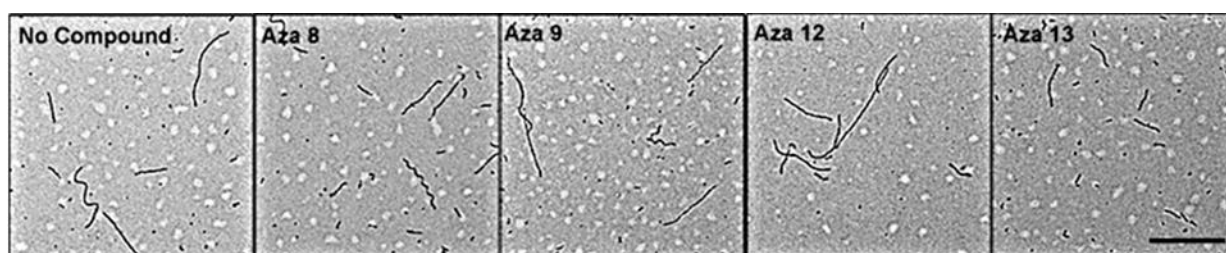
Figure 4.8

Figure 4.8 Pre-formed tau filaments binding to electron microscopy grids in the presence of azaphilone compounds. To test whether azaphilone compounds may block adherence of tau filaments to EM grids, preformed tau filaments were mixed with compounds aza-8, aza-9, aza-12, and aza-13 and immediately prepared for electron microscopy without allowing time for disassembly. As seen in the micrographs, similar amounts of filaments were observed with or without the added azaphilone compounds, indicating that the compounds do not block adherence of tau filaments to EM grids. The scale bar represents 1 μM and is applicable to all images.

4.3.5 Aza-8, aza-9, aza-12 and aza-13 disassembled filaments in a dose-dependent fashion.

The IC₅₀ of the four most potent compounds was determined using the filter trap assay. The amount of preformed filaments remaining following treatment with compounds for 12 h was reduced in a concentration-dependent manner for all four compounds tested (Figure 4.9).

Compound aza-9 had an IC₅₀ of $56 \pm 14 \mu\text{M}$, compared to 118 ± 19 , 98 ± 16 , and $216 \pm 18 \mu\text{M}$ for compounds aza-8, aza-12, and aza-13 respectively, indicating that aza-9 has the most activity for dissolving preformed tau filaments *in vitro* (Figure 4.9).

4.3.6 Aza-9 disassembled heparin-induced tau filaments. In a number of studies, heparin has been used to induce tau aggregation. Because heparin-induced tau filaments might be different from arachidonic acid induced filaments, we wished to determine if aza-9 inhibited heparin-induced tau aggregation or disassembled heparin-assembled tau aggregates. We chose aza-9 because it was the most potent compound among the 11 azaphilones. Filter trap assays were performed using the mixture of antibodies against normal tau, the TOC1 antibody, and the TNT1 antibody. Aza-9 significantly reduced the assembly of TOC1- and TNT1-positive aggregates (Figure 4.10A). The addition of aza-9 also resulted in the significant disassembly of preformed filaments recognized by the TOC1 and TNT1 antibodies (Figure 4.10B).

Figure 4.9

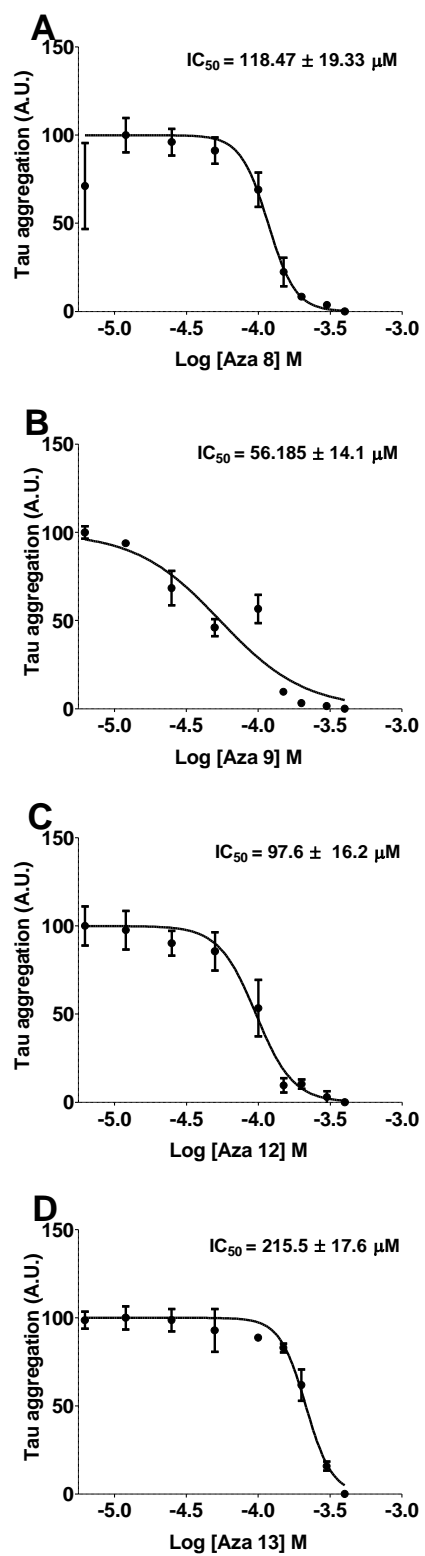
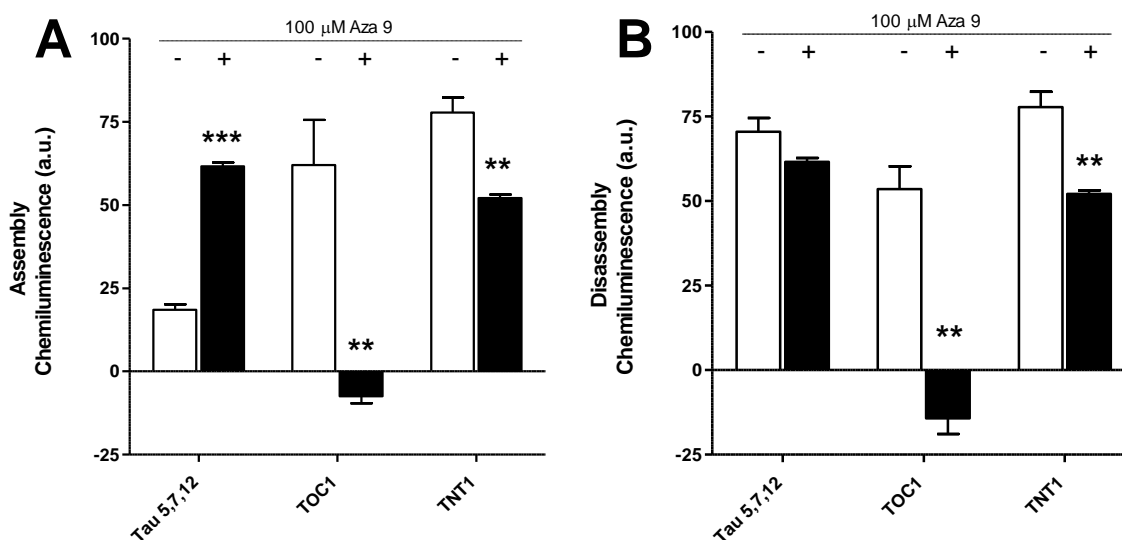


Figure 4.9 IC₅₀ determination tau filament disassembly. Polymerization reactions at 2 μ M tau and 75 μ M arachidonic acid were performed at room temperature. After 6 h, compounds were added to these reactions at several different concentrations, and the mixtures were incubated for an additional 12 h. The resulting amount of tau filaments in the reaction was determined by a filter trap assay detected by a mixture of antibodies to normal tau (tau 5, tau 7, and tau 12). The amount of polymerization was normalized to controls in the absence of compound (100%). The normalized data was plotted against the log of the inhibition concentration and fit to a dose–response curve to determine the IC₅₀ for (A) Aza-8, (B) Aza-9, (C) Aza-12 and (D) Aza-13. Data points are the average of three trials \pm SD.

Figure 4.10



Filter trap assay for filament assembly and disassembly of heparin-induced tau filaments.

(A) For assembly inhibition, 100 μM aza-9 was incubated with 2 μM tau for 20 min before the addition 0.6 μM heparin. Sixteen hours after induction, the degree of aggregation was determined using the filter trap assay detected by a mixture of antibodies to normal tau (tau 5, tau 7, and tau 12), an antibody to oligomeric tau (TOC1), and an antibody to a toxic conformation of tau (TNT1). The average of three independent trials \pm SD is shown for no compound controls (white bars) and 100 μM aza-9 (black bars). (B) 2 μM tau and 0.6 μM heparin were incubated together for 12 h prior to the addition of 100 μM aza-9 or an equal volume of DMSO. Disassembly reactions proceeded for an additional 24 h, and the degree of aggregation was determined using the filter trap assay detected by a mixture of antibodies (tau 5, tau 7, and tau 12), TOC1, and TNT1. The average of three independent trials \pm SD is shown for no compound controls (white bars) and 100 μM aza-9 (black bars). *, $P \leq 0.05$; **, $P \leq 0.01$; ***, $P \leq 0.001$.

4.3.7 Aza-8, aza-9, aza-12 and aza-13 did not completely inhibit tau's ability to polymerize microtubules. We chose the most potent azaphilone derivatives, aza-8, aza-9, aza-12, and aza-13, to determine their effects on the normal function of tau to stabilize microtubules. Tubulin was mixed with tau in the presence or absence of 90 μM compound, and the resulting microtubule formation was monitored by turbidity. All polymerization curves were fit using a Gompertz growth equation (Figure 4.11). While all four compounds affected the apparent rate and maximum amount of microtubule formation at the concentration tested (Table 4.1), tau still retained a significant ability to stabilize microtubule formation.

4.4 Discussion

Tau-based therapeutic strategies have recently been gaining additional attention largely due to the major role that tau pathology plays in many neurological disorders including Alzheimer's disease. Several tau-directed therapeutic strategies with disease-modifying potential have been identified, including modulating tau phosphorylation, microtubule stabilization, tau aggregation inhibitors, and tau clearance using antibodies²³⁶⁻²⁴¹. Conversion of soluble monomeric tau into insoluble tau aggregates could, potentially, result in both loss-of-function and gain-of-function toxicities⁴⁰. Therefore, inhibiting aggregation of tau might prevent formation of the toxic oligomers or tangles. Inhibiting aggregation could also increase the levels of monomeric tau, thereby increasing the chances for its clearance through chaperone-mediated processes. Previous studies have identified several tau aggregation inhibitor (TAI) molecules, including those belonging to the class of anthraquinones, phenothiazines, and a benzothiazolidine derivative, among others^{166, 242, 243}. One TAI, a stable, reduced form of methylthioninium chloride, is currently in Phase III clinical trials¹⁶⁰, indicating that this approach has promise and that it is, consequently, worthwhile to identify additional structural backbones with this activity.

Figure 4.11

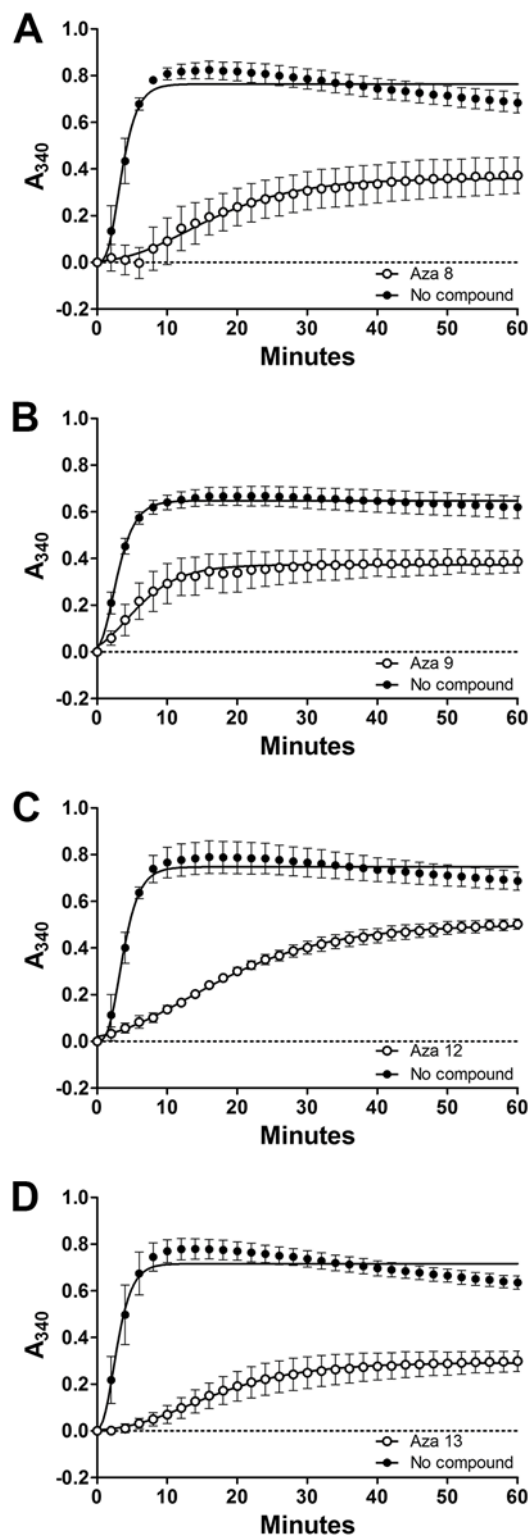


Figure 4.11 Microtubule assembly in the presence of the most potent azaphilone tau aggregation inhibitors. Tubulin was incubated with either tau protein alone or tau in the presence of (A) aza-8, (B) aza-9, (C) aza-12, or (D) aza-13 at a concentration of 90 μM . Microtubule assembly was monitored by absorbance at 340 nm (y axis) over time (x axis). Each point is the average of three independent trails \pm SD. All data were fit to Gompertz growth curve (dashed and solid lines for no compound and 90 μM azaphilones, respectively). For clarity, only every other time point is shown on the graph. *, $P \leq 0.05$; **, $P \leq 0.01$; ***, $P \leq 0.001$

Table 4.1. Statistical analysis of the effects of compounds aza-8, aza-9, aza-12, and aza-13 on the stabilization of microtubules.

		t_i (min)	k_{app} (min^{-1})	Max (A_{340})
Aza-8	-	3.08 \pm 1.28	0.87 \pm 0.14	0.76 \pm 0.36
	+	13.42 \pm 6.59	0.12 \pm 0.02***	0.36 \pm 0.14*
Aza-9	-	2.26 \pm 0.65	0.62 \pm 0.08	0.65 \pm 0.38
	+	5.03 \pm 1.93	0.26 \pm 0.19*	0.38 \pm 0.10*
Aza-12	-	3.11 \pm 1.22	0.78 \pm 0.09	0.75 \pm 0.10
	+	12.83 \pm 1.35***	0.09 \pm 0.02***	0.50 \pm 0.04*
Aza-13	-	2.58 \pm 1.29	0.86 \pm 0.17	0.72 \pm 0.06
	+	15.65 \pm 7.72*	0.12 \pm 0.05**	0.30 \pm 0.07**

Table 4.1. Statistical analysis of the effects of compounds aza-8, aza-9, aza-12, and aza-13 on the stabilization of microtubules. Max (A_{340}) is the maximum amount of microtubule polymerization, t_i is the point of inflection of the curve at the time of maximum growth rate in minutes, and b is inversely proportional to the apparent rate of polymerization (k_{app} , min^{-1}), as determined from the fit of three individual microtubule polymerization curves for each condition to a nonlinear Gompertz growth function (see Methods). *, $P \leq 0.05$; **, $P \leq 0.01$; ***, $P \leq 0.001$.

Many of the previously identified TAIs are composed of fused ring structures believed to be capable of interacting with the β -sheet structures formed in tau aggregates, thereby inhibiting formation of tau filaments^{230, 235}

Fungal extracts are known to include pharmaceutically important secondary metabolites²²⁰. We therefore previously screened 17 secondary metabolites obtained from the fungus *A. nidulans* for TAIs due to their structural similarity to previously identified TAIs²³⁰. From this screen, we identified three compounds that inhibited tau aggregation at micromolar concentrations. Two of these compounds belong to the anthraquinone class of compounds, and one was structurally unique from all previously identified TAIs. We were particularly interested in this compound, asperbenzaldehyde. Asperbenzaldehyde is a precursor to an important class of natural products called azaphilones. Azaphilones are a structurally diverse group of polyketides that share a highly oxygenated bicyclic core and chiral quaternary center²²². The azaphilones used in this study were obtained by semisynthetic diversification of asperbenzaldehyde.

All 11 azaphilones inhibited the formation of tau filaments, but some of them produced small amorphous tau aggregates, which can be seen in the electron micrographs in Figure 4.4. These aggregates were not recognized by TOC1²³² and TNT1²³³ antibodies, which bind to toxic forms of tau; therefore, we believe that these compounds promote the formation of small off-pathway aggregates of tau that are not toxic and do not act as seeds for further tau filament assembly. The induction of these aggregates could be similar to soluble aggregates of tau induced by porphyrin phthalocyanine tetrasulfonate that have a different conformation from that of insoluble toxic tau oligomers²³⁵.

From a therapeutic point of view, TAIs would be more useful if they could also dissolve preformed tau filaments because they could theoretically be beneficial to patients that already demonstrate cognitive impairments. We found that a subset of the compounds, aza-8, aza-9, aza-12, and aza-13, showed this property. These four compounds have Br or Cl at position R1, whereas the other compounds have either I or H at R1 (Figure 4.1). Therefore, halogenation at position R1 may not necessarily be important for inhibition of tau filament formation, but electron-withdrawing groups at R1 specifically seem to enhance disassembly of tau filaments. Cl and Br are more electronegative (3.0 and 2.8, respectively) than I (2.5) and H (2.1), indicating that increased electronegativity at position R1 could have a significant impact on the activity of tau aggregation inhibitors with this scaffold. The four disassembly causing compounds have a ketone at position R3, whereas the presence of the CHCO_2Et moiety at the same position seems to virtually eliminate disassembly, even with halogenation. The impact of the chemical groups at the R2 position seems to be dependent upon the substitution at R1. Compounds aza-8 and aza-12 both have Cl at R1, but they possess acetate and hydroxyl groups at R2, respectively. Despite this structural difference, there is no significant difference in their activity levels. However, compounds aza-9 and aza-13, both containing Br at R1 and acetate and hydroxyl groups at R2, respectively, differ in their levels of activity. Aza-9 is more potent than aza-13; therefore, positioning of the acetate group at R2 in the presence of a Br at R1 might be important for compound activity.

Additionally, all four disassembly causing compounds have lipoxygenase-1 inhibitory activity in the low micromolar range (IC_{50} of 2–8 μm)²¹¹. Inhibition of LOX-1 may help to reduce fatty acid metabolites of arachidonic acid and docosahexaenoic acid that are elevated in Alzheimer's disease²²³. These compounds could therefore have two positive therapeutic activities in tau

dementias. The relatively high IC₅₀ values of our compounds indicate that they are unlikely to be of therapeutic value, and we do not know if they have suitable bioavailability or pharmacokinetic properties. It is important, however, to identify new scaffolds with the appropriate biological activity for further development. We believe that these compounds provide a novel TAI scaffold with the added features that they inhibit LOX-1 and some of them disassemble preformed tau aggregates.

The core of tau aggregates is made up of highly ordered β -sheet structures²⁰². The tau protein has two hexapeptide motifs ²⁷⁵VQIINK²⁸⁰ and ³⁰⁶VQIVYK³¹¹ that are absolutely essential for the formation of tau aggregates⁴⁴. Compounds that inhibit tau aggregation could, therefore, be interacting with these hexapeptide motifs. Azaphilones can react with primary amines to form vinylogous γ -pyridines²²². It is therefore possible that these azaphilones could covalently bind to the primary amine of lysine in the hexapeptide motifs. The hexapeptide motifs lie within the microtubule-binding repeat (MTBR) region of tau protein, raising the possibility that compounds that inhibit tau aggregation would inhibit tau's ability to bind to tubulin and promote its assembly into microtubules. Even at relatively high concentrations of the group of compounds that disassemble preformed aggregates, tau's natural function was not completely inhibited. However there are two obvious explanations 1) azaphilones are not binding to the hexapeptide repeats, and are exerting their activities in some other way or 2) azaphilones bind to the repeats but only partially inhibit the tau-tubulin interaction. In this regard we note that ²⁷⁵VQIINK²⁸⁰ and ³⁰⁶VQIVYK³¹¹ are located in the inter-repeat region and not directly within the 18-amino acid imperfect repeat regions of the MTBR

In conclusion, this study shows that these compounds inhibit assembly of tau aggregates, disassemble preformed tau aggregates, and partially preserve tau's ability to bind to tubulin and

promote microtubule assembly. These compounds provide a promising novel scaffold for TAI molecules. The structure–activity relationship studies give us several leads for the probable important chemical groups required in this scaffold structure required for the anti-tau aggregation activity of the compounds. Further studies on the interaction between the compounds and tau will help to determine the precise mechanism of action of these compounds.

Chapter V: Using NMR to determine interaction between Aza-9 and tau protein.

5.1 Introduction

Alzheimer's disease is characterized by presence of intracellular abnormal tau aggregates and extracellular amyloid plaques. Tau aggregation occurs in many other diseases such as Frontotemporal dementia, Pick's disease and other tauopathies. The primary initiation factor for the process of tau aggregation is not known as yet, though it is now agreed upon that tau aggregation plays a major role in disease pathogenesis. Therefore, inhibition of tau aggregation is a good therapeutic strategy which could potentially stop or reverse disease progression. There is a strong interest in identifying small molecules which could inhibit tau aggregation. Similar searches are also being done to find inhibitors for other aggregating proteins in other diseases such as α -synuclein in Parkinson's disease, prion protein in Creutzfeldt- Jacob disease and transthyretin in systemic amyloidosis^{244, 245}.

In the search of tau aggregation inhibitors, we tested secondary metabolites obtained from *Aspergillus nidulans* for their ability to inhibit tau aggregation. In this screen, we identified a novel class of compounds, azaphilones as molecules which could inhibit tau aggregation *in vitro* as well as dissolve pre-formed tau aggregates without inhibiting the tau-microtubule interactions completely²⁴⁶. Among these, Aza-9 was the most potent compound. Aza-9 inhibited tau aggregation assembly and disassembled pre-formed tau aggregates with an IC₅₀ value of 56 μ M.

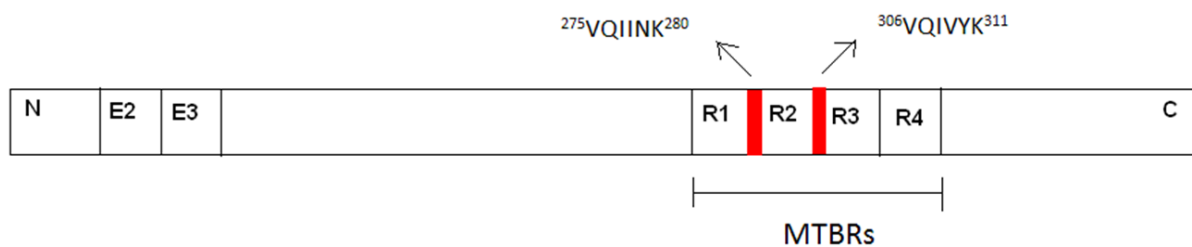
Figure 5.1

Figure 5.1 Hexapeptide motifs on full length tau protein. This cartoon depicts the protein structure of full length tau. Two exons E2 and E3 are seen at the N-terminal. There are four microtubule binding repeats (MTBR) at the C-terminal marked as R1 through R4. Exon E10 codes for R2. The two hexapeptide motifs are located within the MTBR region shown in red blocks before the R2 and R3 regions. The first hexapeptide motif called PHF6 is $^{275}\text{VQIINK}^{280}$ and the second hexapeptide PHF* motif is $^{306}\text{VQIVYK}^{311}$.

Tau protein has two hexapeptide motifs which are found in the MTBR region near the C-terminal of tau protein that are essential for tau aggregation. The tau molecules bind to each other via these hexapeptide motif regions to form β -sheet structures⁴⁵. Aza-9 could therefore be interacting with residues in and around these motifs. The hexapeptide motif regions are ²⁷⁵VQIINK²⁸⁰ which is referred to as PHF6 motif, and the ³⁰⁶VQIVYK³¹¹ which is referred to as PHF6* motif (**Figure 5.1**). Aza-9 affects the MT polymerization in the presence of tau. That further supports the hypothesis that tau could be interacting with the region in and around the hexapeptide motifs, because the motifs are located within the MTBR region.

The aim of this study was to determine whether aza-9 interacts with tau and, to identify the potential residues in tau which could be involved in the interaction. We therefore did titration NMR experiments with tau and aza-9 and found that aza-9 interacts with specific residues in tau. We used different labeling techniques to obtain more information regarding the interaction.

5.2 Experimental procedures

5.2.1 Mutagenesis and Protein purification. Wild type tau and I308L mutant tau were cloned into PT7c vectors with an N-terminal polyhistidine tag as previously described²⁴⁷. The mutagenesis for I308L was done using the Quikchange site-directed mutagenesis kit from Stratagene (La Jolla, CA). The vector containing cells were grown in Minimal Media (Na₂HPO₄, KH₂PO₄ and NaCl). The minimal media was supplemented with 0.1M CaCl₂, 1M MgSO₄, 40% Glucose, Vitamin mix, Trace metal mix and Kanamycin. For obtaining ¹⁵N labelled tau, we added ¹⁵N NH₄Cl to the minimal media. For obtaining ILV labeled tau, we supplemented the minimal media with Ile, Val and Leu during the log phase of growth of the culture, which is when the OD reaches 0.5 (before the IPTG induction step). The proteins were isolated by

affinity chromatography through a Ni NTA Agarose (Qiagen, Valencia, CA) column followed by gel filtration through a Superdex 200 column on AKTA fast protein liquid chromatography (FPLC) (Amersham Biosciences, Piscataway, NJ) as described previously¹⁹⁴.

5.2.2. Preparing samples for NMR. The proteins were dialyzed into phosphate buffer (10mM Na₂HPO₄) using dialysis cassettes (Pierce, Rockford, IL) having a molecular weight cut-off of 10KDa. The protein concentration used in all the experiments was 0.1 mM. Aza-9 was used in final concentrations of 0.1 mM, 0.2mM and 0.4 mM for titration studies against wild type tau and I308L mutant tau. The compounds were dissolved in DMSO. The total amount of DMSO in every NMR tube sample was less than 2%.

5.2.3 Obtaining NMR spectra. We obtained 2-D ¹H-¹⁵N HSQC NMR spectra for obtaining the full length tau spectrum and the titration experiments with wild type tau and aza-9. We also obtained 2-D NMR ¹H-¹³C HSQC spectrum for ILV labelled tau and for titration studies with ILV labelled tau and Aza-9. These experiments were carried out under the guidance of Dr, Asokan at the KU NMR core facility. Kawaljit Kaur from the De Guzman lab helped in analyzing the data.

5.3 Results:

5.3.1 Obtained 2D spectrum of full length tau protein.

We labelled full length WT tau protein amide backbone with ^{15}N and obtained a ^1H - ^{15}N HSQC spectrum for the same. Tau is a natively unfolded protein and therefore the individual residue peaks were of overlapping nature rather than being very spread out as would be the case with structured proteins. There were certain residues which could be identified as individual peaks (Figure 5.2).

5.3.2 Titration studies with Tau and Aza 9

We sought to determine whether aza-9 interacted with tau residues. We therefore did titration studies with increasing concentrations of aza-9 against tau. The protein concentration used was 0.1mM throughout. Aza-9 was added in increasing ratios with WT tau in three separate experiments (WT: aza-9 in 1:0, 1:1, 1:2 and 1:4). With an increase in compound concentration 11 specific residues of tau were affected as seen in figure 5.3. Out of the 11 residues, 7 peaks showed a reduction in peak intensity with an increase in Aza-9 concentration. These have been marked as circles in figure 5.4. 3 peaks showed subtle chemical deviations marked in squares in figure 5.4. These changes in the peaks are indicative of an intermediate exchange regime. This means that the compound interacts with the residues in micro molar range. This correlates with the IC_{50} value we obtained for disassembly which was around 56 μM . None of the other peaks showed any change in position or intensity in the presence of the compound. This means that aza-9 interacts with specific residues in the tau (Figure 5.4).

Figure 5.2

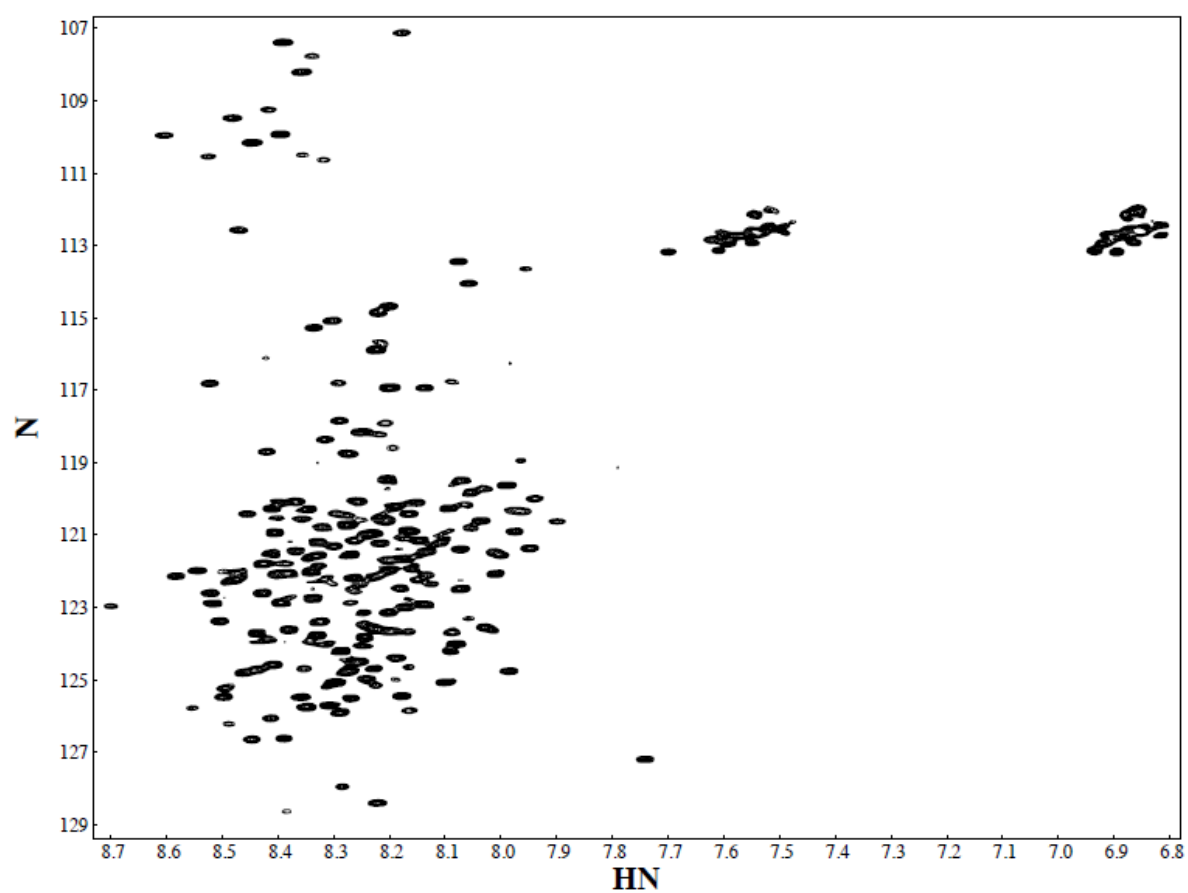


Figure 5.2 2D ^1H - ^{15}N HSQC NMR spectrum for full length ^{15}N labelled tau protein. The X-axis shows the labelled proton while the Y-axis shows the labelled nitrogen

Figure 5.3

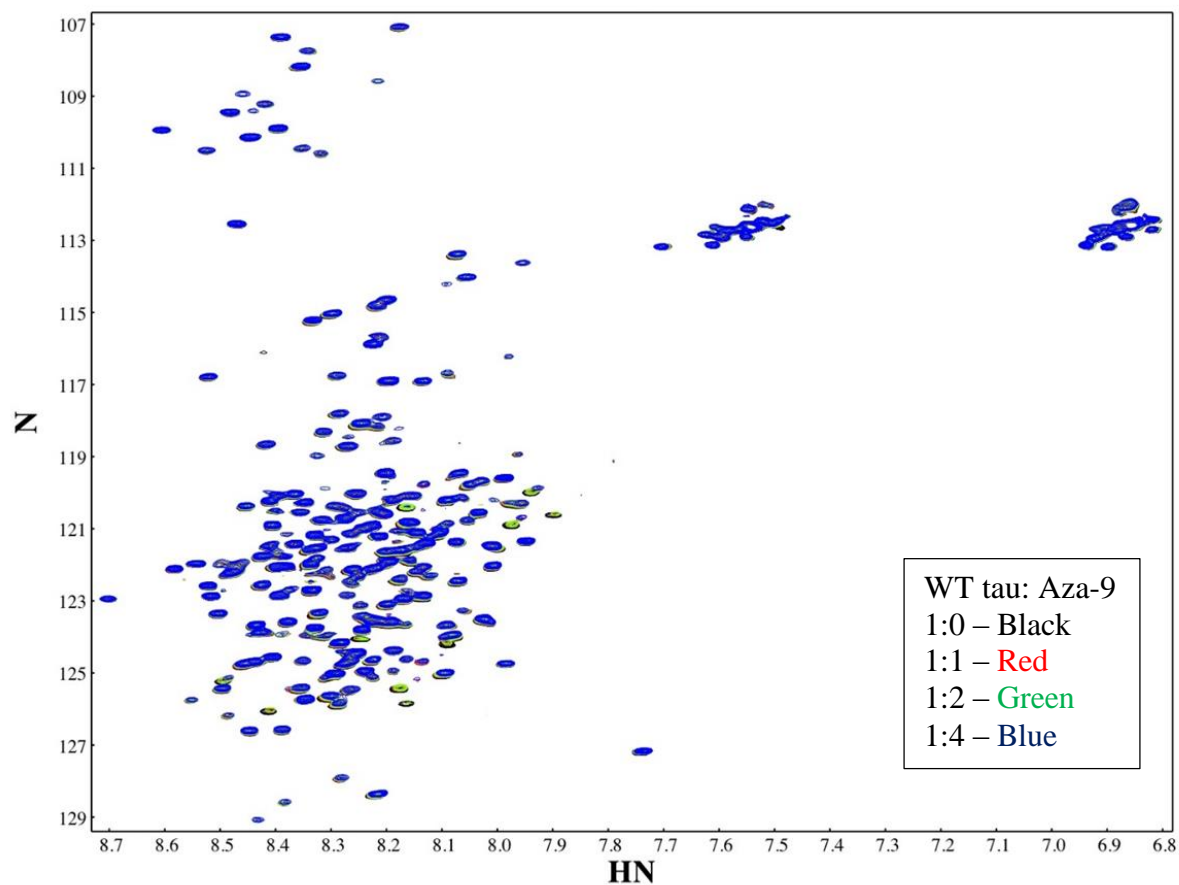


Figure 5.3 2D ^1H - ^{15}N HSQC NMR spectrum for titration studies with ^{15}N labelled Tau and Aza-9. The figure shows four overlaid 2D ^1H - ^{15}N HSQC NMR spectra with increasing amounts of aza-9. The ratio of WT tau: aza-9 is denoted next to every spectrum description. The X-axis shows the labelled proton while the Y-axis shows the labelled Nitrogen.

Figure 5.4

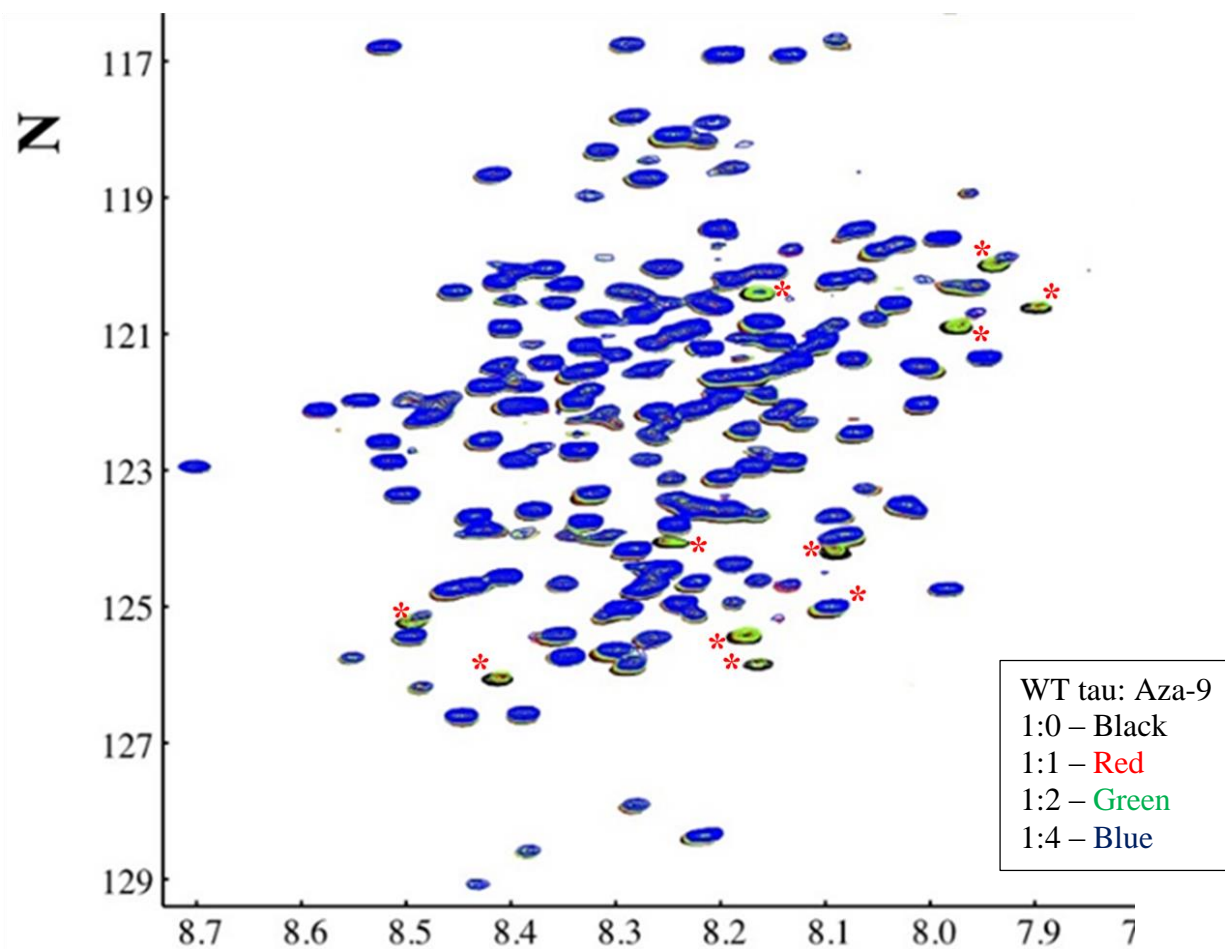
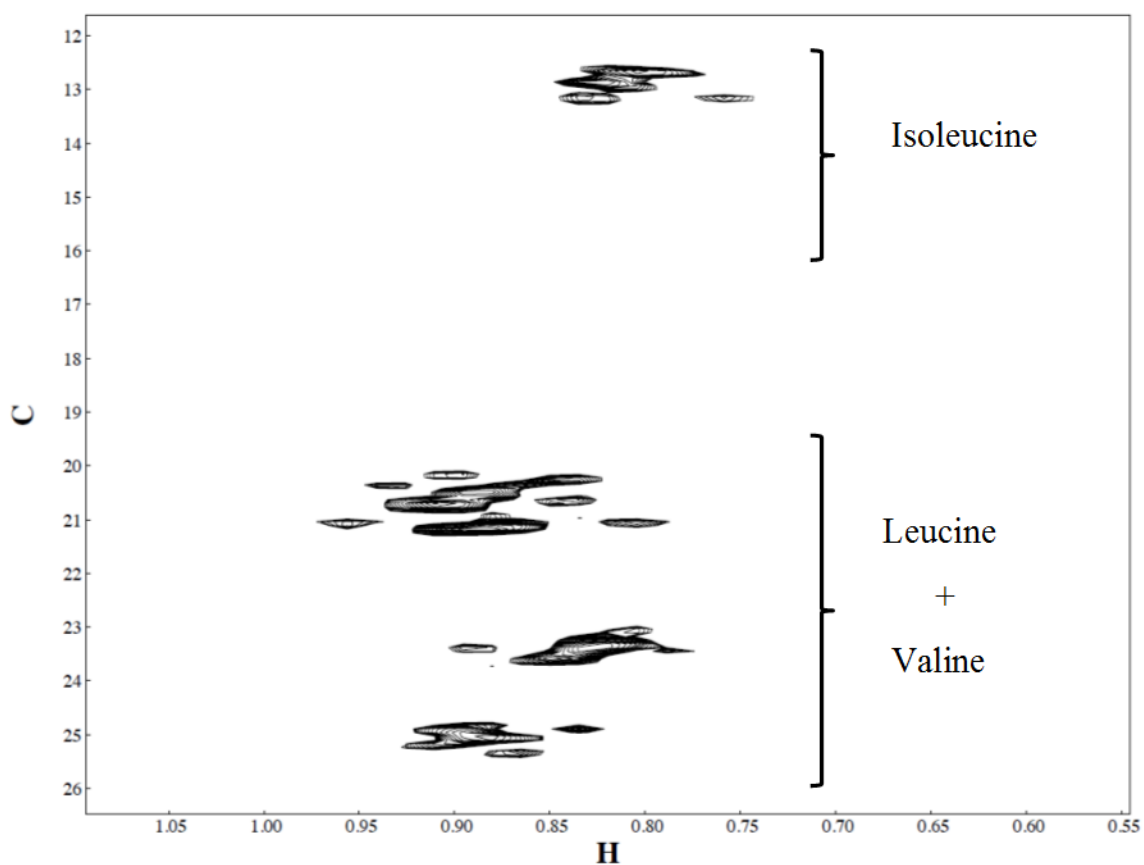


Figure 5.4 2D ^1H - ^{15}N HSQC NMR spectrum for titration studies with ^{15}N labelled Tau and Aza 9. This figure is a zoomed in image of the spectrum in figure 5.3. The peaks marked with a red asterisk are the peaks showing a decrease in peak intensity with subtle chemical deviation with an increase in aza-9. The changes in peaks indicate an intermediate exchange regime in micro molar range.

5.3.3 Titration studies with ILV labelled tau and aza-9

As mentioned in the introduction, we believe that aza-9 could be interacting with residues in/or around the hexapeptide motifs in the MTBR region. These motifs have lot of hydrophobic residues specifically Ile, Leu and Val. We therefore labelled these three amino acids specifically to determine whether aza-9 interacts with these residues. This would provide us more information regarding the residues involved in the interaction. We first obtained ILV-labelled tau ^1H - ^{13}C HSQC spectrum shown in figure 5.5. We further did titration studies with increasing concentrations of aza-9 against tau protein. The protein concentration used was 0.1mM throughout. Aza-9 was added in increasing ratios with ILV WT tau in three separate experiments (tau:aza9 in 1:0, 1:1, 1:2 and 1:4). As can be seen in the NMR spectrum for ILV labelled tau, the residues have overlapping peaks and therefore it was difficult to identify specific peaks affected after titration studies. One isolated Isoleucine peak showed a decrease in intensity with increase in aza-9 concentration (encircled in figure 5.6). Other affected peaks were buried among other closely located peaks and therefore were difficult to interpret. From this experiment, we understood that a one specific isoleucine is definitely affected by aza-9. But because of the overlapping nature of the other isoleucine peaks, it is difficult to interpret whether any other isoleucine residues being affected by aza-9.

Figure 5.5**Figure 5.5 2D NMR ^1H - ^{13}C HSQC spectrum for full length ILV-labelled tau protein**

In this spectrum the positions of the isoleucine residues are labeled, while the valine and leucine residues are non-distinguishable from each other and have been labeled accordingly.

Figure 5.6

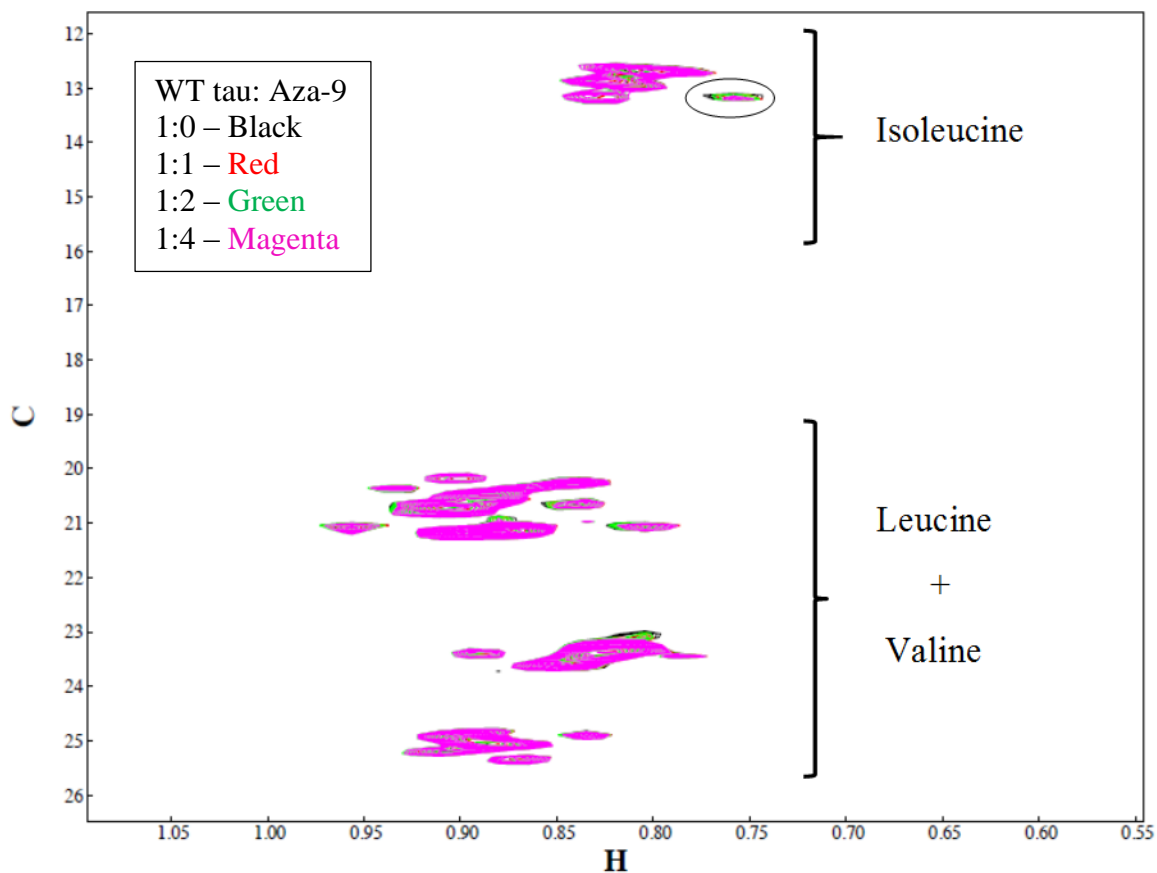


Figure 5.6: 2-D NMR ^1H - ^{13}C HSQC spectrum for titration studies with ILV labelled tau and Aza 9

The figure shows four overlaid 2D ^1H - ^{13}C HSQC NMR spectra with increasing amounts of aza-9.

5.4.4 Hexapeptide PHF6* is involved in interaction with aza-9

We sought to determine whether the isoleucine interacting with aza-9 is within the hexapeptide motif. We therefore created a tau construct with mutated PH6* motif I308L mutant. We chose the isoleucine from ³⁰⁶VQIVYK³¹¹ to mutate because it was more prone to making the β -sheet structure due to its alternating pattern of polar and nonpolar residues compared to that of ²⁷⁵VQIINK²⁸⁰. We made a double labelled protein with ¹⁵N as well as Ile-labelled- ¹⁵N Ile I308L. We first obtained 2D Ile ¹H-¹³C HSQC NMR Spectrum for ¹⁵N Ile I308L. Upon overlapping the Ile-spectra of WT tau with that of I308L, there was no change observed in the isolated isoleucine peak (Figure 5.7). Therefore, the affected isoleucine residue is not at 308 position. We would need to do more such single a.a. substitutions to assign the peaks in the future.

We further obtained a 2D NMR spectrum of ¹⁵N I308L (figure 5.8). The single a.a. substitution affected specific residues. Three individual peaks disappeared (encircled in figure 5.9) from the I308L protein spectrum while several others showed minor changes. The three peaks seen (figures 5.3 and 5.4) clearly in WT tau were also involved in interaction with aza-9 as seen in the titration experiment. Therefore, based on this experiment we could say that aza-9 might be interacting with the residues in and around the hexapeptide motifs in tau.

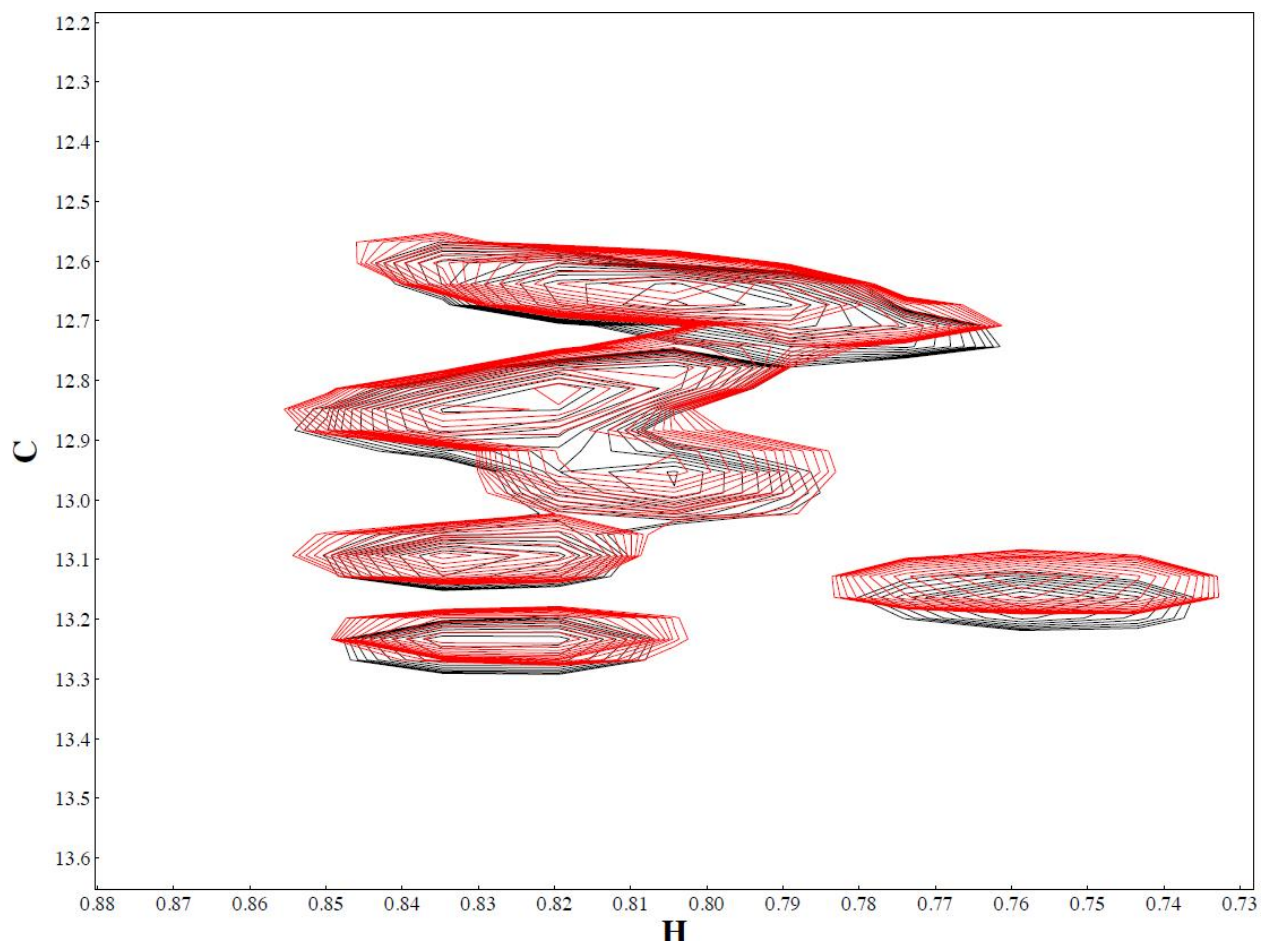
Figure 5.7

Figure 5.7: 2-D NMR ^1H - ^{13}C HSQC spectrum of isoleucine-labelled I308L protein. The NMR spectrum of wild type tau is in black. The NMR spectrum of I308L is in red and has been overlaid on the wild type tau spectrum.

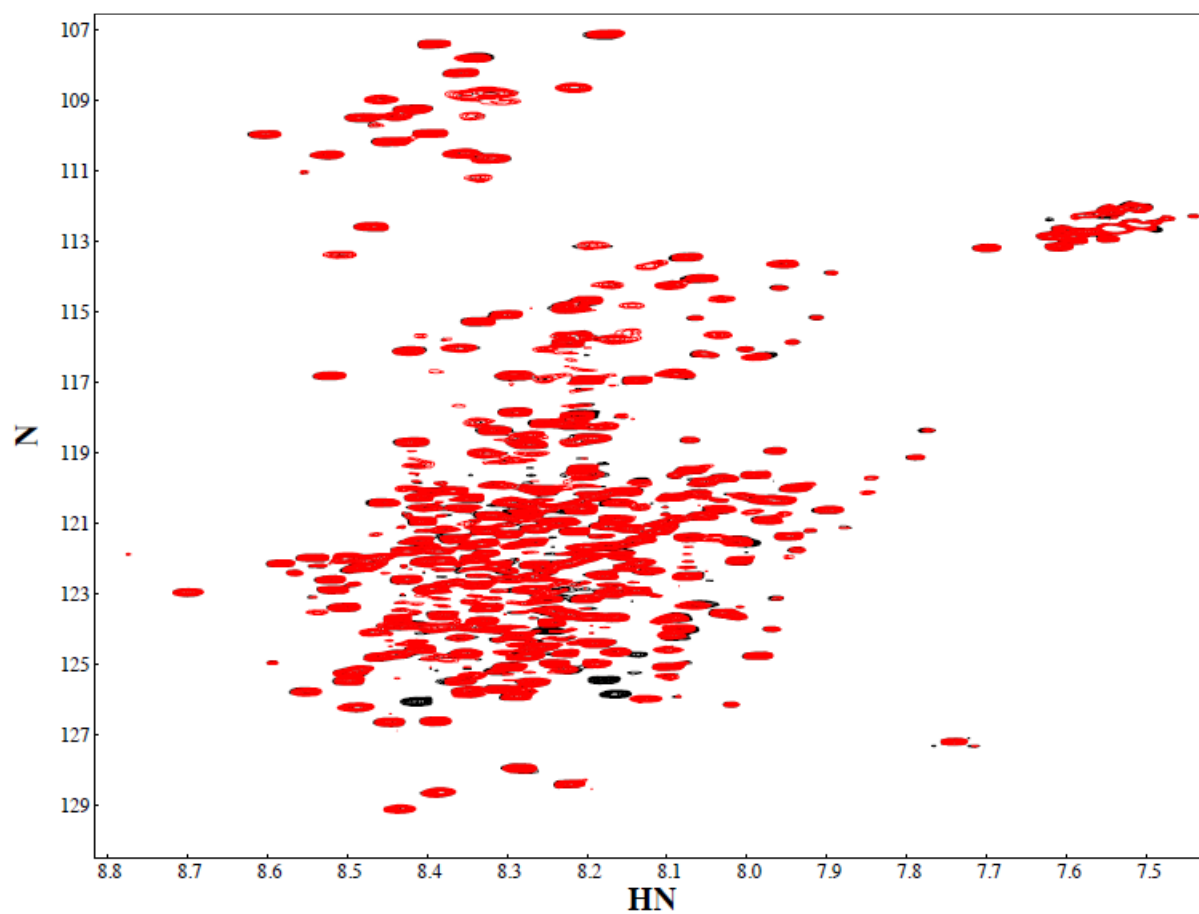
Figure 5.8:

Figure 5.8: 2-D NMR ^1H - ^{13}C HSQC spectrum of ^{15}N -labelled I308L protein overlaid on the NMR spectrum of full length wild-type ^{15}N -labelled tau protein. The NMR spectrum of wild type tau is in black. The NMR spectrum of I308L is in red and has been overlaid on the wild type tau spectrum.

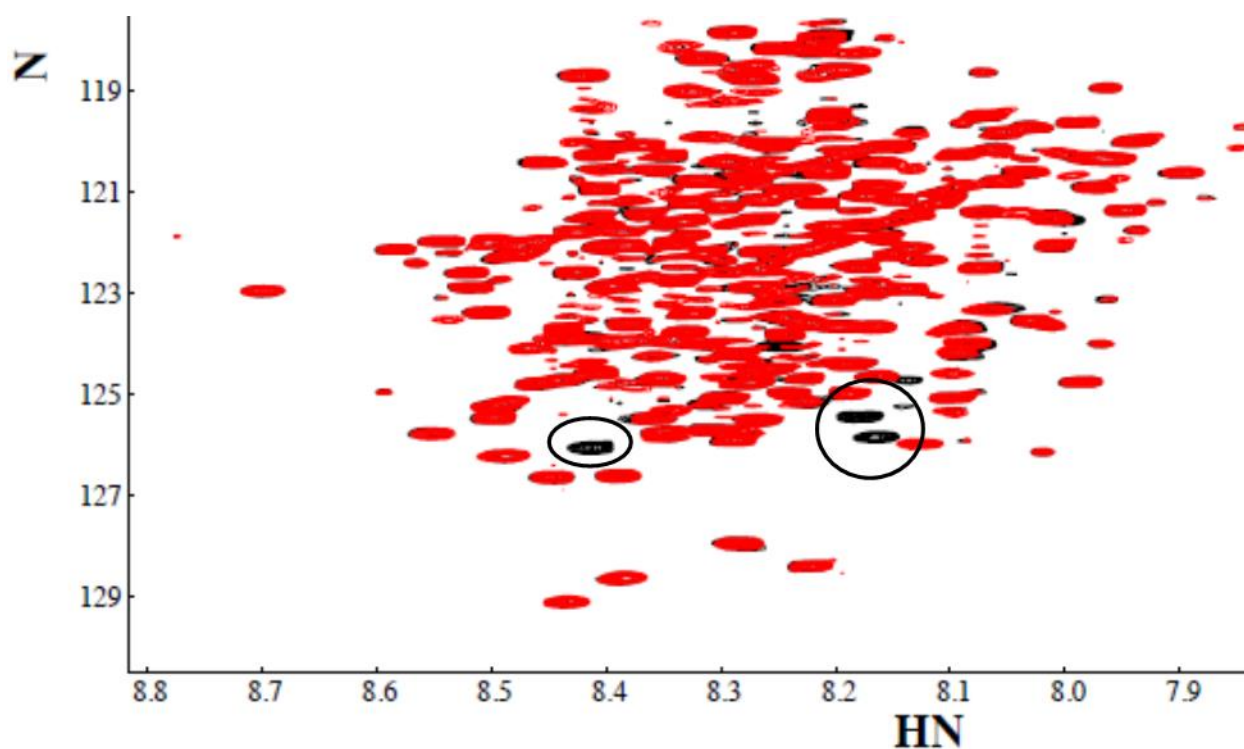
Figure 5.9:

Figure 5.9: Zoomed in 2-D NMR ^{15}N -labelled I308L protein overlaid on 2-D NMR of full length wild-type ^{15}N -labelled TAU protein. This image is a zoomed in image of the spectrum in figure 5.8. The NMR spectrum of wild type tau is in black. The NMR spectrum of I308L is in red and has been overlaid on the wild type tau spectrum. The encircled peaks denote peaks which are missing in the I308L tau mutant.

5.4 Discussion

This study gave us the following information regarding the mode of action of Aza 9 – 1) there is specific dose- dependent interaction between aza 9 and eleven tau residues. The nature of the interaction is that of intermediate exchange (micro molar range). 2) The hexapeptide motif residues are involved in this interaction. We do not eliminate the possibility of additional residues being affected that may not be visible in the 2D spectrum due to the overlapping nature of the peaks.

The ^{15}N labelling technique of tau gave us a 2D spectrum with closely placed peaks compared to that of ILV-specific labelling. The affected residues in the ^{15}N labelled spectrum were easily distinguishable because they were relatively isolated peaks compared to the ILV spectrum we obtained for tau. The ILV-labeled 2D NMR spectra for tau had many overlapping peaks and made it difficult to identify individual residues. For example, tau has a total of 15 isoleucine residues in its a.a. sequence. In the spectrum, only one isoleucine peak was isolated while all the other 14 isoleucine residues had overlapping peaks making it difficult to identify the 14 residues. Titration studies with aza-9 and ILV-labelled tau showed reduction in peak intensity in that isolated isoleucine residue. There may be other isoleucine, valine or leucine residues affected but it we could not detect those because of the overlapping nature of the peaks. Upon replacing I308 with leucine, we did not see a change in the isoleucine labelled tau spectrum. We now know that the affected isoleucine peak is not in the VQIVYK sequence. To identify this peak, we would have to replace other possible isoleucine residues and look for changes in this spectrum. There are two more isoleucine residues within the hexapeptide motifs. We would like to create more mutants with single isoleucine residues being replaced by leucine starting with I277L and I278L. This would help in identifying the affected isoleucine residue. The other strategy to assign the

peaks is by a special labelling technique, ^{15}N amino acid specific labelling. Using this technique, we can label the amide backbone of specific amino acids, for example we can obtain a ^{15}N Isoleucine spectrum. We would then get a spectrum showing 15 specific isoleucine peaks. These would be more spread out like in the ^{15}N 2D spectrum, and therefore we can conduct titration experiments with aza-9 and potentially identify the number of specific isoleucine residues being affected. Further we can do specific mutations such as I308L, I277L and I278L to identify the peaks on the spectrum. We can this way obtain ^{15}N Valine spectrum as well.

Further studies need to be done to obtain more information about aza-9 – tau interaction. Firstly, we need to assign peaks for the MTBR region of tau protein. This will help us in identifying the residues affected. Aza-9 belongs to the class of azaphilones, which can react with primary amines to form vinylogous γ -pyridines²²². It is therefore possible that these aza-9 could covalently bind to the primary amine of lysine in the hexapeptide motifs. It would be interesting to carry out more binding experiments and obtain a K_d value for the drug-protein interaction.

Chapter VI Aza 9 is effective against aggregation enhancing truncation mutant 1-391

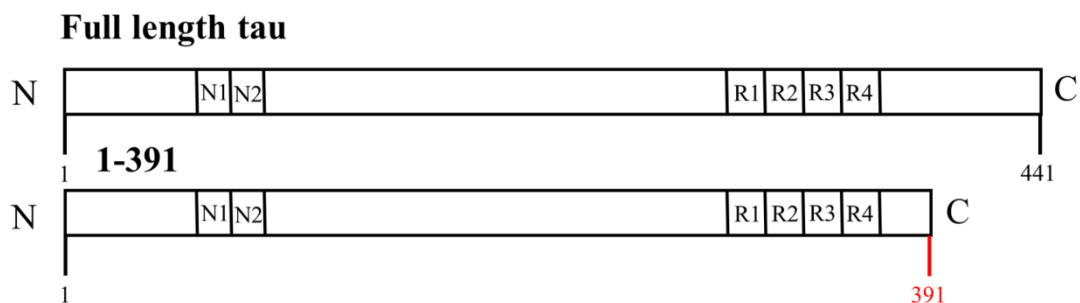
6.1 Introduction

Tau plays a prominent role in microtubule polymerization in neurons, axonal transport via microtubules and in neurite outgrowth among other functions. Tau is soluble, highly dynamic and is known to adopt a global hairpin folding structure when in solution^{5,248}. Based on experiments done using electron microscopy, X-ray diffraction, FTIR, CD, fluorescence microscopy and NMR spectroscopy, tau behaves as a random coil in solution^{23, 44, 107}. In spite of its hydrophilic character, tau aggregates to form insoluble tau filaments in Alzheimer's disease and other tauopathies^{25, 201}. In a diseased state, tau assumes specific conformations such as Alz50 and Tau 66, which stabilize the tau structure and make it more prone to aggregation compared to normal tau⁹². Tau aggregation is known to play a major role in tau pathogenesis. The amount and location of tau tangles in the brain correlates well with disease progression⁴² and tau aggregates are known to induce toxicity in cell culture and animal models⁴³.

Tau undergoes many post-translational modifications such as phosphorylation, ubiquitination, acetylation and truncations which could be responsible for the conversion of soluble tau into insoluble tau aggregates. Truncation of tau protein occurs in AD and tau is known to be truncated at both its termini during disease progression. We have shown in our previous studies (unpublished, chapter II), that tau truncations have differential effects on tau aggregation mechanisms. We found that truncating tau at E391 at the C-terminal increases the amount and rate of tau aggregation *in vitro*. Truncation at E391 is known to occur fairly late in AD.

Figure 6.1

A) Tau truncation mutant



B) Aza-9 compound structure

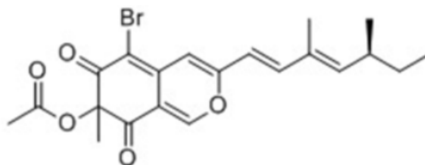


Figure 6.1 Structure of the tau truncation mutant and the aza-9 compounds structure. A) The structures of the full length tau and that of the 1-391 truncation are shown. The N and the C termini have been labelled accordingly. N1 and N2 are the exons at the N –terminal of tau and the R1-R4 are the microtubule binding repeats shown near the C-terminal end. B) The structure of Aza-9 has been shown.

Inhibiting tau aggregation is a good target for therapeutics against AD and other tauopathies, as they could help stop or reverse disease progression. There is a great deal of interest in finding compounds which can inhibit tau aggregation and/or disassemble tau aggregates. Compounds belonging to different classes including phenothiazines¹⁶², anthraquinones¹⁶⁶, benzothioles¹⁷⁵ and rhodanine-based compounds¹⁶⁸ have been identified as tau aggregation inhibitors. We recently identified a novel class of compound, azaphilones as tau aggregation inhibitors²⁴⁶. In our study, we found that four azaphilones could inhibit tau filament assembly and could disassemble preformed tau filaments. Aza-9 among these was the most potent compound with an IC₅₀ value of around 56 μ M for disassembly against tau aggregates containing full length tau.

Tau aggregates obtained from an AD brain are known to be reactive against antibodies such as MN423 and DC11, identify truncated tau⁹⁵. Therefore from a therapeutic point of view, it would be useful to have tau aggregation inhibitors which can disassemble aggregates composed of truncated tau as well. In this study, we sought to determine whether our most potent azaphilone, aza-9 was effective against aggregates composed of 1-391. We did experiments to determine whether aza-9 can inhibit 1-391 filament assembly process and also disassemble pre-formed 1-391 tau aggregates. Aza-9 inhibited 1-391 assembly and further disassembled 1-391 aggregates in a dose- dependent manner.

6.2 Experimental procedures

6.2.1 Protein expression and purification. All wild-type (WT) and truncation constructs were expressed and purified as described previously¹⁹⁴. The mutagenesis was done using the Quikchange site-directed mutagenesis kit from Stratagene (La Jolla, CA). The 1-391 truncation mutant was generated in a full-length 2N4R tau background contained in a pT7C vector.

6.2.2. Inhibition of Tau Aggregation. 75 μM arachidonic acid was used to initiate the aggregation of 2 μM tau in polymerization buffer (PB, 10 mM HEPES (pH 7.64), 5 mM DTT, 100 mM NaCl, 0.1 mM EDTA, and 3.75% ethanol) *in vitro* as previously described²¹⁸.

Compounds dissolved in DMSO were added to a final concentration of 200 μM and incubated with tau protein in PB 20 min prior to the addition of arachidonic acid. The reactions were allowed to proceed for 16 h at room temperature before analysis.

6.2.3 Disassembly of Preformed Filaments. Preformed tau filaments were generated with 2 μM tau and 75 μM ARA in PB as described above for 6 h at room temperature. Compounds dissolved in DMSO were added to the tau solution at final concentrations indicated in the Results section and figure legends. The reactions were allowed to proceed at room temperature for 12 h before analysis.

6.2.4. Filter Trap Assay. The amount of tau aggregates following assembly or disassembly reactions was determined by filter trap assay as described previously²³⁰. Reactions were diluted into TBS such that they contained 20 ng of protein in 300 μL . Solutions were passed through a nitrocellulose membrane using house vacuum in a dot-blot apparatus. The aggregates trapped on the membrane were detected by general antibodies (a mixture of tau 5²¹⁹ at 1:50 000 dilution, tau 12⁹⁶ at 1:250 000 dilution, and tau 7¹⁹² at 1:250 000 dilution). All antibodies were a kind gift from Drs. Nick Kanaan and Lester I. Binder. HRP-linked goat anti-mouse IgG (Thermo Scientific, Rockford, IL) was used as the secondary antibody, and blots were developed using ECL (enhanced chemiluminescence) western blotting analysis system (GE Healthcare, Buckinghamshire, UK). Images were captured with a Kodak Image Station 4000R or ChemiDoc-It2 imager and were quantified using the histogram function of Adobe Photoshop 7.0. Statistical analyses were performed using unpaired t-tests to compare the triplicate values to control values.

6.2.5. Transmission Electron Microscopy. Polymerization reaction samples were diluted 1:10 in PB and fixed with 2% glutaraldehyde for 5 min. Fixed samples were placed on Formvar carbon-coated grids and stained with uranyl acetate as previously described²³⁰. Images were captured with a Technai F20 XT field emission transmission electron microscope (FEI Co., Hillsboro, OR) and Gatan Digital Micrograph imaging system (Gatan, Inc., Pleasanton, CA). The filaments were quantified using Image-Pro Plus 6.0 software (Media Cybernetics, Inc., Rockville, MD) as previously described²³⁰. Statistical analyses were performed using unpaired t-tests to compare four or five replicates for each bin size with the no-compound data serving as reference values.

6.3 Results

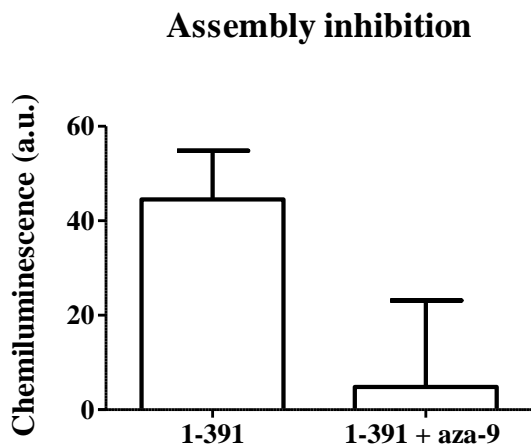
6.3.1. Tau aggregation inhibition assay

1-391 polymerization was initiated *in vitro* using a standard arachidonic acid induction assay²¹⁸. To determine whether aza-9 could inhibit assembly of tau filaments, it was added at a final concentration of 200 μ M, was preincubated with 2 μ M tau for 20 min before the addition of 75 μ M arachidonic acid. The degree of tau aggregation inhibition was determined using a membrane filter assay²³⁴. A mixture of antibodies to the amino terminal, central, and carboxy terminal regions of tau (tau 12, tau 5, and tau 7, respectively) was used to detect tau aggregates. In this assay, aza-9 significantly reduced the amount of tau aggregation detected (Figure 6.2 A). Further, the resulting tau aggregates from the inhibition reaction were visualized by electron microscopy- there were long filaments in the absence of aza-9. Upon treatment with aza-9, there were no filaments seen on the grid. There were small aggregates seen on the grids instead. Our

observations from the electron microscopy correlate well with the results obtained from the filter trap assay (Figure 6.2 B).

Figure 6.2.

A) Filter trap assay



B) Electron microscopy images

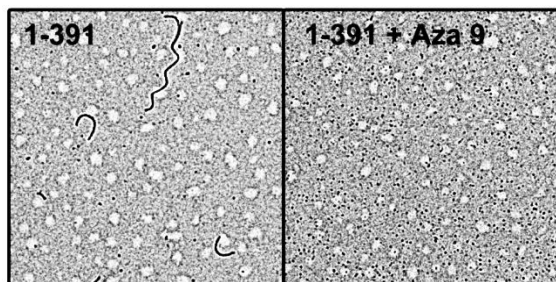


Figure 6.2. Inhibition of filament assembly at 200 μ M aza-9. 1-391 polymerization reactions were performed with 2 μ M tau and 75 μ M arachidonic acid either with or without 200 μ M aza-9. The resulting amount of tau filament formation was determined using a filter trap assay (A). The amount of tau on the filter was detected using a mixture of antibodies tau 5, tau 7, and tau 12. (B) Aliquots of the reactions were prepared for negative stain electron microscopy. Representative images are shown for no compound control and aza-9.

6.3.2 Aza-9 completely disassembled pre-formed 1-391 filaments

To determine whether aza-9 can disassemble preformed 1-391 aggregates, tau aggregation was allowed to proceed for 6 h before the addition of aza-9 to a final concentration of 200 μM . After 12 h, the effect of aza-9 on the 1-391 aggregation was examined by a filter trap assay using the mixture of antibodies against normal tau (Figure 6.3 A). Aza-9 reduced the amount of preformed tau filaments. Electron microscopy was used to validate and extend the results from the filter trap assay. Aza-9 substantially reduced the pre-existing filament mass (Figure 6.3 B).

6.3.3. Aza-9 disassembled 1-391 filaments in a dose-dependent fashion.

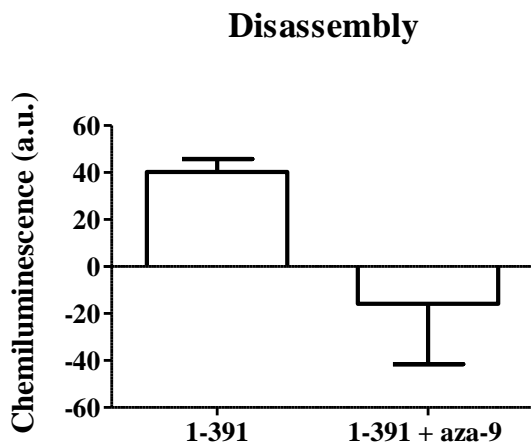
The IC_{50} of aza-9 was determined using the filter trap assay. The amount of preformed filaments remaining following treatment with compounds for 12 h was reduced in a concentration-dependent manner (Figure 6.3). Aza-9 had an IC_{50} of $212.25 \pm 105.65 \mu\text{M}$.

6.4 Discussion

Tau is altered in the diseased condition by post translational modifications such as hyperphosphorylation, acetylation, oxidation, ubiquitination and truncation. The modified tau further leads to formation of tau aggregates. Tau aggregates are composed of 3-repeat as well as 4-repeat tau isoforms. It is therefore necessary to find tau aggregation inhibitors which are effective against all the different tau isoforms and on disease modified tau molecules. We identified azaphilones as a novel class of tau aggregation inhibitors which also have the ability to disassemble pre-formed tau filaments. In our study, we tested the effectiveness of azaphilones against full length tau. We therefore sought to determine whether the compounds are effective against aggregation enhancing tau mutants as well.

Figure 6.3.

A) Filter trap assay



B) Electron microscopy images

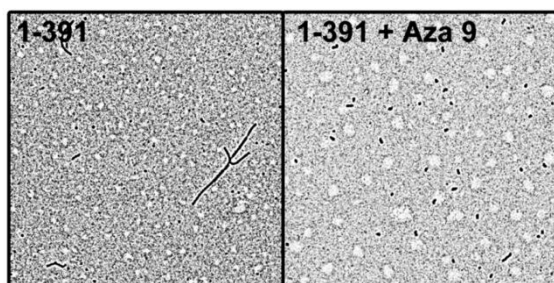


Figure 6.2. Disassembly at 200 μ M aza-9. 1-391 polymerization reactions were performed with 2 μ M tau and 75 μ M arachidonic acid either with or without 200 μ M aza-9. The resulting amount of tau filament was determined using a filter trap assay (A). Negative values indicate that there was less detectable tau on the filter after treatment with a compound than was observed with monomeric tau in the absence of arachidonic acid. The amount of tau on the filter was detected using a mixture of antibodies tau 5, tau 7, and tau 12. (B) Aliquots of the reactions were prepared for negative stain electron microscopy. Representative images are shown for no compound control and aza-9.

Figure 6.3.

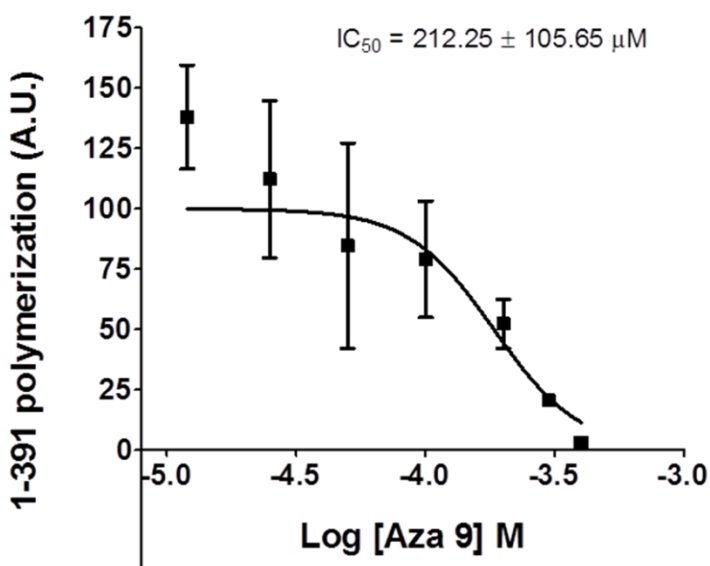


Figure 6.3. IC₅₀ determination tau filament disassembly. Polymerization reactions at 2 μM tau and 75 μM arachidonic acid were performed at room temperature. After 6 h, compounds were added to these reactions at several different concentrations, and the mixtures were incubated for an additional 12 h. The resulting amount of tau filaments in the reaction was determined by a filter trap assay detected by a mixture of antibodies to normal tau (tau 5, tau 7, and tau 12). The amount of polymerization was normalized to controls in the absence of compound (100%). The normalized data was plotted against the log of the inhibition concentration and fit to a dose–response curve to determine the IC₅₀ for Aza-9.

At a concentration of 200 μM , aza-9 inhibited filament formation by 1-391 and also disassembled pre-formed 1-391 tau aggregates. The results observed in the filter trap assays correlated well with those of the transmission electron microscopy. Aza-9 therefore is effective against tau aggregation enhancing truncation mutant 1-391. We further obtained an IC_{50} value of 212 μM for disassembly of 1-391 aggregates. This value is higher than the IC_{50} value obtained for disassembly of full length wild type tau by aza-9 and the experiments were done under similar experimental conditions. The aggregation rate of 1-391 truncation is higher than WT tau and therefore the aggregates could be differently packed or more compactly arranged than the WT tau aggregates. This may be one reason for the higher IC_{50} values.

It would be interesting to test the effectiveness of aza-9 against other tau modifications such as hyperphosphorylated tau, FTDP-17 mutants and also on other isoforms of tau. This would provide us more knowledge about the mode of action of the compound. From a therapeutic point of view, tau aggregates found in patients suffering from AD and other tauopathies and will be composed of different variations of tau and a tau aggregation inhibitor would be useful only if it effective against all types of tau aggregates.

Chapter VII Conclusions and Future Directions

7.1 Introduction

Alzheimer's disease (AD) is the most common form of dementia and it mainly causes problems with thinking, memory and behavior²⁴⁹. The symptoms for AD develop slowly; patients develop cognitive dysfunction, the condition gets worse over time and eventually reaches a point when the symptoms are severe enough to interfere with everyday tasks such as moving, speaking, swallowing and breathing. The incidence of AD is currently on the rise due to lengthening life spans and changing lifestyles. The currently available knowledge in the field supports the idea that accumulation of misfolded or mutant proteins inside and/or outside neurons plays a major role in development of AD and other neurodegenerative disorders including tauopathies and Parkinson's disease^{250, 251}. Misfolding and aggregation of proteins are thought to cause synaptic loss and neuronal death. Tauopathies are a group of neurological disorders that are characterized by prominent intracellular aggregates composed of the microtubule-associated protein tau as a common mechanism for disease pathogenesis. Tau protein undergoes post-translational modifications that are believed to alter the protein structure and conformations such it is more prone to aggregate. The reasons for, and the process of, tau aggregation are not completely understood. Inhibiting tau aggregation is a potentially good target for therapeutics towards these diseases. Currently a tau aggregation inhibitor, a stable, reduced form of methylthioninium chloride, has reached Phase III clinical trials. But there remains a need to identify more compounds that can be developed further for therapeutic use.

7.2 Tau truncations

Truncations are known to occur in tauopathies. Prior studies have shown that they can influence tau aggregation and are known to cause conformational changes that induce a misfolding cascade in Alzheimer's disease (AD) and other tauopathies. Although the N and C terminal regions of tau protein play different roles in the process of tau aggregation, both termini are involved in generating pathological conformations of tau in the diseased state. They maintain the global hairpin conformation of tau and also make conformations identified by alz50 and tau66 antibodies which identify tau in diseased form. It is known that removal of the amino-terminal greatly inhibits the polymerization process by reducing the rate and extent of tau aggregation. The C-terminus on the other hand inhibits tau filament formation. Therefore, removal of the C-terminal greatly enhances the polymerization process. We hypothesized that the site of truncation on the N-terminal and C-terminal will alter the structure of tau, thereby changing its global conformation and tendency for aggregation. Our studies described in chapter II, show that there are differences in the effects of N-terminal and C-terminal truncations on tau aggregation depending on the site of truncation. Upon using ARA as an inducer for tau aggregation, formation of either the Alz 50 or Tau 66 conformation may be required for tau filament assembly. This needs to be verified in the future using alz50 and tau 66 antibodies against all the truncation mutant aggregates. It would be interesting to test whether this holds true for heparin induced tau aggregation. Truncations at the N-terminal did not increase the total amount of tau aggregation compared to that of WT tau. But, there was an increase in the rate of tau aggregation upon elimination of the N-terminal amino acids required for Alz 50 conformation (a.a. 2-18). Upon further eliminating the proline rich region in tau (a.a 197-244), the tau 66 conformation

cannot be formed and there was no tau filament formation observed under electron microscopy. We therefore believe truncation after alz50 N –terminal epitope and before the proline rich region, alters the tau structure such that it favors tau 66 conformation and therefore leads to increase in the rate of tau aggregation. The C-terminal truncations lead to an increase in tau aggregation. Truncation at N and C-terminal in 4-repeat isoforms further leads to inhibition of tau’s ability to aggregate, unlike that of the K19 construct (explained in chapter II discussion in detail). This may be because the intramolecular cross-linking of 4R-tau into compact monomers inhibits aggregation. Further studies are required to identify critical truncation sites on the N and C- termini which alter tau aggregation and function. Based on our results, we may infer that N-terminal truncation events are unlikely to trigger tau aggregation process and may be playing a role in the disease progression after formation of NFTs. These results need to be tested under different experimental conditions – using different tau inducer molecules, truncations in different isoforms of tau and eventually test the effect of the truncation mutants on tau aggregation in cell culture and animal models.

In my dissertation specifically, the study also contributed to finding aggregation enhancing tau truncations made under similar experimental conditions as WT tau (ARA induced reactions) to be tested against the tau aggregation inhibitor molecules. This is because it is important that tau aggregation inhibitors should be effective against disease modified tau aggregates. We chose 1-391 truncation mutant for this study because in our experiments it increased the rate of tau aggregation and also the total amount of tau aggregation compared to WT tau. Aza-9 was seen to inhibit assembly of 1-391 and also disassemble 1-391 aggregates in a dose dependent manner.

7.3 Azaphilones obtained from *Aspergillus nidulans* as tau aggregation inhibitors

Tau aggregation is a common underlying molecular mechanism in pathogenesis of AD and other tauopathies. Inhibiting tau aggregation is therefore a potentially good therapeutic strategy for treating AD because it might help stop or reverse the disease progression. Fungi have been a great source of biologically important compounds. Dr. Berl Oakley's lab was the first to identify and elucidate an azaphilone biosynthesis pathway. The azaphilones have a wide array of activities and therefore it may not be surprising that we saw useful activities among the compounds we tested. One possible reason that fungi secrete anti-aggregation compounds may be due to the amyloid nature of bacterial biofilms²⁵². We have identified compounds obtained from *Aspergillus nidulans* that have the ability to inhibit tau aggregation. The compounds have IC₅₀ values in the micro molar range. We have identified a novel inhibitor, belonging to the azaphilone class of compounds, that inhibit tau aggregation and disassemble pre-formed tau filaments. We carried out structure activity relationship studies and have identified important sites on the compound that affect the ability of the compound to dissolve pre-formed tau aggregates (Figure 7.1). Aza-9 was the most potent compound with an IC₅₀ value of 56 μM for disassembly. Aza-9 had an acetate group at R₂ and a Br at R₁. This specific arrangement of groups seems to be important for compound activity. The presence of Br seemed more potent than the presence of Cl. Therefore, increased electronegativity at R₂ position seems to have an impact on the ability of the compounds to disassemble tau aggregates. Azaphilones can react with primary amines to form vinylogous γ-pyridines. We therefore hypothesized that aza-9 could covalently bind to the primary amine of lysine in the hexapeptide motifs (VQIVYK), and that way would break the tau aggregates apart. It would be possible to identify the covalent bond formation if any using mass spectrometry analysis and also we could identify the exact lysine

that could be being modified. Azaphilones provide a novel scaffold for tau aggregation inhibitors with great potential to create a variety of analogues, which could have better activity compared to the compounds we have identified currently.

Based on preliminary data from NMR experiments we have identified the potential residues that interact with aza-9. The residues in and around the hexapeptide motif region of tau seem to be affected in a dose-dependent fashion. The NMR peak shifts suggested that the interaction between the compound and tau is in the micromolar range as were our IC₅₀ values. Aza-9 was also potent against filaments formed from the aggregation-enhancing C-truncation mutant 1-391. It inhibited assembly of 1-391 filaments and also disassembled pre-formed 1-391 tau aggregates. This further adds potential value to the compound's ability to inhibit aggregation. The azaphilone structural backbone is therefore a very promising new scaffold for effective tau aggregation inhibitors.

7.4 Future directions

In our work using tau truncation mutants, we developed insight into the effects of truncations on tau aggregation and function. It would be interesting to make other truncations apart from the ones used in our study to further narrow down the sites that are critical for polymerization. For example, 14-441 and 43-441 do not affect tau aggregation, whereas, 81-441 reduces the overall amount of tau aggregation. Truncations 201-441 and 256-441 completely inhibit formation of tau filaments. Therefore, it would be interesting to make truncations on sites between a.a. 43 and 81 and sites before a.a. 201. Further, we could use conformation specific antibodies to determine whether the truncated tau can form the alz50 or tau 66 conformations. This will provide us more information about the relation between the tau conformations and their influence on tau aggregation.

Figure 7.1

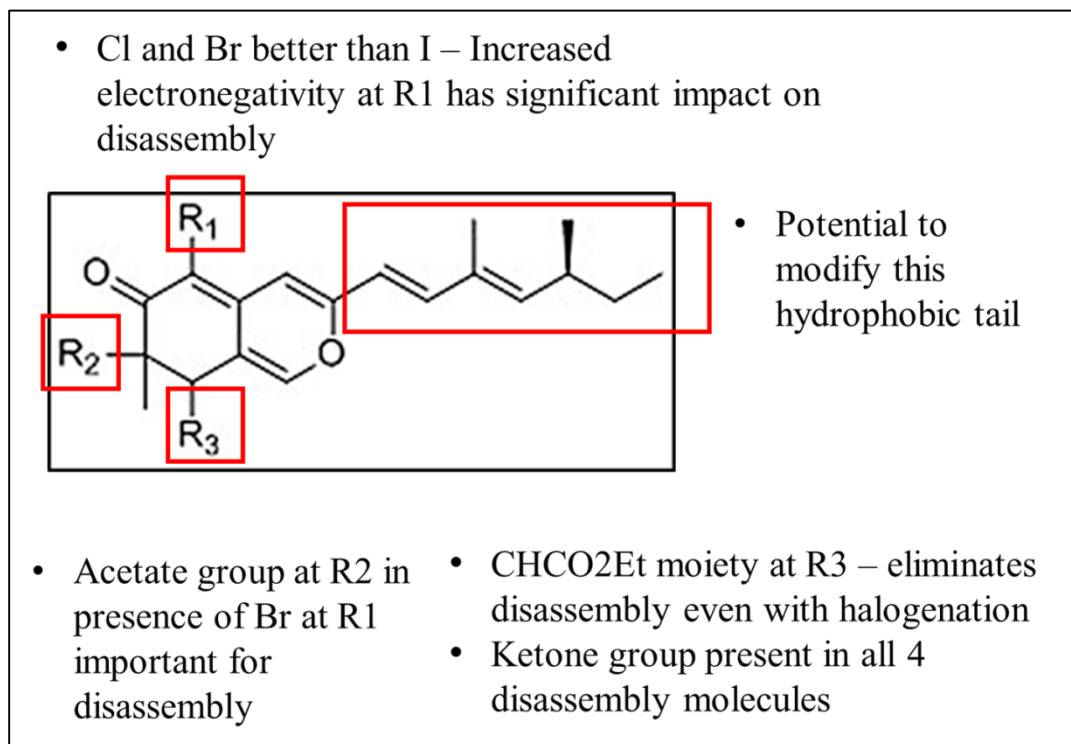


Figure 7.1 Structure-activity relationship (SAR) studies. The potential sites which could or have been modified have been marked in red squares.

In the case of truncation mutants 201-441, 256-441 and 256-391, in the electron microscope images there are no tau filaments observed but we see tiny amorphous aggregates on the grids. We do not know whether these aggregates are toxic in nature. The truncation mutants 1-391, 81-441 and 1-421 led to formation of tau filaments with smaller filament lengths and also increased number of oligomeric tau aggregates on the grids. We could use TOC1 and TNT1 antibodies to determine whether the tau aggregates formed by the truncation mutants are toxic in nature. In our study we have produced all the truncation mutants from the full-length tau protein. It would be interesting to study the effects of the same truncations in different isoforms of tau protein. The tau protein is present in all the six isoforms in the human brain and therefore it is important to see the effects of the truncation in every isoform to get a collective idea about their effects. Therefore, further characterization of the truncation mutants will likely help in explaining their role in aggregation. Eventually it would be useful to study their effects *in vivo*. This would help in understanding the role played by tau truncations in tauopathies and how these mechanisms are affecting the progression of sporadic tauopathies.

We have identified a novel scaffold for tau aggregation inhibitors. The SAR studies give us several leads for the probable important chemical groups required in this scaffold structure for the anti-tau aggregation activity of the compounds (Figure 7.1). (The hydrophobic tail region of the scaffold hasn't been explored in this study.) Therefore, in the future we could develop better analogues of the compounds that have increased activity and reduced effect on the tau-microtubule interaction. Further studies on the interaction between the compounds and tau will help to determine the precise mechanism of action of these compounds. We could perform biochemical binding assays such as surface plasmon resonance to obtain a dissociation constant for the tau-compound interaction. Further studies with NMR such as peak assignment for full

length tau will help us in identifying the specific residues involved in the interaction. These compounds are in their initial stages of discovery and therefore it is not known whether they would be effective *in vivo* or whether they have the required pharmacokinetic properties and can cross the blood brain barrier. By knowing the mode of action of these compounds and the kind of interaction between the compound and tau, we would be able to better predict parameters important for drug development, which include the possible side effects of the drug, the mode of drug delivery, its chances of crossing the blood brain barrier and the drug dosage.

Lastly, from a therapeutic point of view the tau aggregation inhibitors need to be effective against post translationally modified tau protein because the tau aggregates are known to be composed of hyper phosphorylated and truncated tau protein. Aza-9 inhibits aggregation enhancing 1-391 tau aggregates. We would like to test the effect of the compounds against FTDP-17 tau mutants, hyper phosphorylation mutants, as well as the truncation mutants. It would be interesting to see whether the treatment of the tau aggregates composed of post-translationally modified tau would show a reduction in toxicity with the help of TOC1 and TNT1 antibodies. These studies described here show that use of *in vitro* assays are useful in determining the effects of modifications of tau that could be altering key factors associated with tauopathies, and also for testing potential lead compounds for their ability to inhibit tau aggregation which can then be used to further analyze their effect in an *in vivo* setting. It is a good system to compare and analyze results because it would be challenging and time consuming to directly compare results from animal models that utilize varying methods to induce tau aggregation. Through the continuation of these studies we can begin to gain a clearer understanding of the role of tau truncations in tau toxicity and progression of Alzheimer's disease and other tauopathies. Azaphilones are promising new class tau aggregation inhibitor

and further development of these compounds could hopefully help in advancing in the search for treatments for Alzheimer's disease and other tauopathies.

Bibliography

1. Weingarten, M. D., Lockwood, A. H., Hwo, S. Y., and Kirschner, M. W. (1975) A protein factor essential for microtubule assembly, *Proceedings of the National Academy of Sciences of the United States of America* 72, 1858-1862.
2. Murphy, D. B., and Borisy, G. G. (1975) Association of high-molecular-weight proteins with microtubules and their role in microtubule assembly in vitro, *Proceedings of the National Academy of Sciences of the United States of America* 72, 2696-2700.
3. Sloboda, R. D., Rudolph, S. A., Rosenbaum, J. L., and Greengard, P. (1975) Cyclic AMP-dependent endogenous phosphorylation of a microtubule-associated protein, *Proceedings of the National Academy of Sciences of the United States of America* 72, 177-181.
4. Takemura, R., Okabe, S., Umeyama, T., Kanai, Y., Cowan, N. J., and Hirokawa, N. (1992) Increased microtubule stability and alpha tubulin acetylation in cells transfected with microtubule-associated proteins MAP1B, MAP2 or tau, *Journal of cell science* 103 (Pt 4), 953-964.
5. Cleveland, D. W., Hwo, S. Y., and Kirschner, M. W. (1977) Physical and chemical properties of purified tau factor and the role of tau in microtubule assembly, *Journal of molecular biology* 116, 227-247.
6. Witman, G. B., Cleveland, D. W., Weingarten, M. D., and Kirschner, M. W. (1976) Tubulin requires tau for growth onto microtubule initiating sites, *Proceedings of the National Academy of Sciences of the United States of America* 73, 4070-4074.
7. Nukina, N., and Ihara, Y. (1986) One of the antigenic determinants of paired helical filaments is related to tau protein, *Journal of biochemistry* 99, 1541-1544.
8. Kosik, K. S., Joachim, C. L., and Selkoe, D. J. (1986) Microtubule-associated protein tau (tau) is a major antigenic component of paired helical filaments in Alzheimer disease, *Proceedings of the National Academy of Sciences of the United States of America* 83, 4044-4048.
9. Grundke-Iqbal, I., Iqbal, K., Quinlan, M., Tung, Y. C., Zaidi, M. S., and Wisniewski, H. M. (1986) Microtubule-associated protein tau. A component of Alzheimer paired helical filaments, *The Journal of biological chemistry* 261, 6084-6089.
10. Ihara, Y., Nukina, N., Miura, R., and Ogawara, M. (1986) Phosphorylated tau protein is integrated into paired helical filaments in Alzheimer's disease, *Journal of biochemistry* 99, 1807-1810.
11. Yancopoulos, D., and Spillantini, M. G. (2003) Tau protein in familial and sporadic diseases, *Neuromolecular medicine* 4, 37-48.
12. Dickson, D. W. (2009) Neuropathology of non-Alzheimer degenerative disorders, *International journal of clinical and experimental pathology* 3, 1-23.
13. Goedert, M. (2004) Tau protein and neurodegeneration, *Seminars in cell & developmental biology* 15, 45-49.
14. Combs, B., Voss, K., and Gamblin, T. C. (2011) Pseudohyperphosphorylation has differential effects on polymerization and function of tau isoforms, *Biochemistry* 50, 9446-9456.
15. Novak, M. (1994) Truncated tau protein as a new marker for Alzheimer's disease, *Acta virologica* 38, 173-189.
16. Morishima-Kawashima, M., Hasegawa, M., Takio, K., Suzuki, M., Titani, K., and Ihara, Y. (1993) Ubiquitin is conjugated with amino-terminally processed tau in paired helical filaments, *Neuron* 10, 1151-1160.
17. Cohen, T. J., Guo, J. L., Hurtado, D. E., Kwong, L. K., Mills, I. P., Trojanowski, J. Q., and Lee, V. M. (2011) The acetylation of tau inhibits its function and promotes pathological tau aggregation, *Nature communications* 2, 252.

18. Wang, J. Z., Grundke-Iqbal, I., and Iqbal, K. (1996) Glycosylation of microtubule-associated protein tau: an abnormal posttranslational modification in Alzheimer's disease, *Nature medicine* 2, 871-875.
19. Schweers, O., Mandelkow, E. M., Biernat, J., and Mandelkow, E. (1995) Oxidation of cysteine-322 in the repeat domain of microtubule-associated protein tau controls the in vitro assembly of paired helical filaments, *Proceedings of the National Academy of Sciences of the United States of America* 92, 8463-8467.
20. Neve, R. L., Harris, P., Kosik, K. S., Kurnit, D. M., and Donlon, T. A. (1986) Identification of cDNA clones for the human microtubule-associated protein tau and chromosomal localization of the genes for tau and microtubule-associated protein 2, *Brain research* 387, 271-280.
21. Goedert, M., and Jakes, R. (1990) Expression of separate isoforms of human tau protein: correlation with the tau pattern in brain and effects on tubulin polymerization, *The EMBO journal* 9, 4225-4230.
22. Niblock, M., and Gallo, J. M. (2012) Tau alternative splicing in familial and sporadic tauopathies, *Biochemical Society transactions* 40, 677-680.
23. Schweers, O., Schonbrunn-Hanebeck, E., Marx, A., and Mandelkow, E. (1994) Structural studies of tau protein and Alzheimer paired helical filaments show no evidence for beta-structure, *The Journal of biological chemistry* 269, 24290-24297.
24. Mukrasch, M. D., Bibow, S., Korukottu, J., Jeganathan, S., Biernat, J., Griesinger, C., Mandelkow, E., and Zweckstetter, M. (2009) Structural polymorphism of 441-residue tau at single residue resolution, *PLoS biology* 7, e34.
25. Gamblin, T. C., Berry, R. W., and Binder, L. I. (2003) Modeling tau polymerization in vitro: a review and synthesis, *Biochemistry* 42, 15009-15017.
26. Brandt, R., and Lee, G. (1994) Orientation, assembly, and stability of microtubule bundles induced by a fragment of tau protein, *Cell motility and the cytoskeleton* 28, 143-154.
27. Drubin, D. G., and Kirschner, M. W. (1986) Tau protein function in living cells, *The Journal of cell biology* 103, 2739-2746.
28. Kadavath, H., Hofele, R. V., Biernat, J., Kumar, S., Tepper, K., Urlaub, H., Mandelkow, E., and Zweckstetter, M. (2015) Tau stabilizes microtubules by binding at the interface between tubulin heterodimers, *Proceedings of the National Academy of Sciences of the United States of America* 112, 7501-7506.
29. Nangaku, M., Sato-Yoshitake, R., Okada, Y., Noda, Y., Takemura, R., Yamazaki, H., and Hirokawa, N. (1994) KIF1B, a novel microtubule plus end-directed monomeric motor protein for transport of mitochondria, *Cell* 79, 1209-1220.
30. Hollenbeck, P. J., and Swanson, J. A. (1990) Radial extension of macrophage tubular lysosomes supported by kinesin, *Nature* 346, 864-866.
31. Wiemer, E. A., Wenzel, T., Deerinck, T. J., Ellisman, M. H., and Subramani, S. (1997) Visualization of the peroxisomal compartment in living mammalian cells: dynamic behavior and association with microtubules, *The Journal of cell biology* 136, 71-80.
32. Stamer, K., Vogel, R., Thies, E., Mandelkow, E., and Mandelkow, E. M. (2002) Tau blocks traffic of organelles, neurofilaments, and APP vesicles in neurons and enhances oxidative stress, *The Journal of cell biology* 156, 1051-1063.
33. Trinczek, B., Ebnet, A., Mandelkow, E. M., and Mandelkow, E. (1999) Tau regulates the attachment/detachment but not the speed of motors in microtubule-dependent transport of single vesicles and organelles, *Journal of cell science* 112 (Pt 14), 2355-2367.
34. Ebnet, A., Godemann, R., Stamer, K., Illenberger, S., Trinczek, B., and Mandelkow, E. (1998) Overexpression of tau protein inhibits kinesin-dependent trafficking of vesicles, mitochondria,

- and endoplasmic reticulum: implications for Alzheimer's disease, *The Journal of cell biology* 143, 777-794.
35. Brandt, R., Leger, J., and Lee, G. (1995) Interaction of tau with the neural plasma membrane mediated by tau's amino-terminal projection domain, *The Journal of cell biology* 131, 1327-1340.
 36. Liao, H., Li, Y., Brautigan, D. L., and Gundersen, G. G. (1998) Protein phosphatase 1 is targeted to microtubules by the microtubule-associated protein Tau, *The Journal of biological chemistry* 273, 21901-21908.
 37. Sontag, E., Nunbhakdi-Craig, V., Lee, G., Brandt, R., Kamibayashi, C., Kuret, J., White, C. L., 3rd, Mumby, M. C., and Bloom, G. S. (1999) Molecular interactions among protein phosphatase 2A, tau, and microtubules. Implications for the regulation of tau phosphorylation and the development of tauopathies, *The Journal of biological chemistry* 274, 25490-25498.
 38. Frappier, T. F., Georgieff, I. S., Brown, K., and Shelanski, M. L. (1994) tau Regulation of microtubule-microtubule spacing and bundling, *Journal of neurochemistry* 63, 2288-2294.
 39. Dou, F., Netzer, W. J., Tanemura, K., Li, F., Hartl, F. U., Takashima, A., Gouras, G. K., Greengard, P., and Xu, H. (2003) Chaperones increase association of tau protein with microtubules, *Proceedings of the National Academy of Sciences of the United States of America* 100, 721-726.
 40. Sahara, N., Maeda, S., and Takashima, A. (2008) Tau oligomerization: a role for tau aggregation intermediates linked to neurodegeneration, *Current Alzheimer research* 5, 591-598.
 41. Garcia-Sierra, F., Ghoshal, N., Quinn, B., Berry, R. W., and Binder, L. I. (2003) Conformational changes and truncation of tau protein during tangle evolution in Alzheimer's disease, *Journal of Alzheimer's disease : JAD* 5, 65-77.
 42. Arriagada, P. V., Growdon, J. H., Hedley-Whyte, E. T., and Hyman, B. T. (1992) Neurofibrillary tangles but not senile plaques parallel duration and severity of Alzheimer's disease, *Neurology* 42, 631-639.
 43. Ko, L. W., DeTure, M., Sahara, N., Chihab, R., Vega, I. E., and Yen, S. H. (2005) Recent advances in experimental modeling of the assembly of tau filaments, *Biochimica et biophysica acta* 1739, 125-139.
 44. von Bergen, M., Friedhoff, P., Biernat, J., Heberle, J., Mandelkow, E. M., and Mandelkow, E. (2000) Assembly of tau protein into Alzheimer paired helical filaments depends on a local sequence motif ((306)VQIVYK(311)) forming beta structure, *Proceedings of the National Academy of Sciences of the United States of America* 97, 5129-5134.
 45. von Bergen, M., Barghorn, S., Li, L., Marx, A., Biernat, J., Mandelkow, E. M., and Mandelkow, E. (2001) Mutations of tau protein in frontotemporal dementia promote aggregation of paired helical filaments by enhancing local beta-structure, *The Journal of biological chemistry* 276, 48165-48174.
 46. Lasagna-Reeves, C. A., Castillo-Carranza, D. L., Sengupta, U., Sarmiento, J., Troncoso, J., Jackson, G. R., and Kaye, R. (2012) Identification of oligomers at early stages of tau aggregation in Alzheimer's disease, *FASEB journal : official publication of the Federation of American Societies for Experimental Biology* 26, 1946-1959.
 47. Wischik, C. M., Novak, M., Edwards, P. C., Klug, A., Tichelaar, W., and Crowther, R. A. (1988) Structural characterization of the core of the paired helical filament of Alzheimer disease, *Proceedings of the National Academy of Sciences of the United States of America* 85, 4884-4888.
 48. Takauchi, S., Hosomi, M., Marasigan, S., Sato, M., Hayashi, S., and Miyoshi, K. (1984) An ultrastructural study of Pick bodies, *Acta neuropathologica* 64, 344-348.
 49. Steele, J. C., Richardson, J. C., and Olszewski, J. (1964) Progressive Supranuclear Palsy. A Heterogeneous Degeneration Involving the Brain Stem, Basal Ganglia and Cerebellum with

- Vertical Gaze and Pseudobulbar Palsy, Nuchal Dystonia and Dementia, *Archives of neurology* 10, 333-359.
50. Patterson, K. R., Remmers, C., Fu, Y., Brooker, S., Kanaan, N. M., Vana, L., Ward, S., Reyes, J. F., Philibert, K., Glucksman, M. J., and Binder, L. I. (2011) Characterization of prefibrillar Tau oligomers in vitro and in Alzheimer disease, *The Journal of biological chemistry* 286, 23063-23076.
 51. Lee, G., and Leugers, C. J. (2012) Tau and tauopathies, *Progress in molecular biology and translational science* 107, 263-293.
 52. Braak, H., and Braak, E. (1995) Staging of Alzheimer's disease-related neurofibrillary changes, *Neurobiology of aging* 16, 271-278; discussion 278-284.
 53. Schonheit, B., Zarski, R., and Ohm, T. G. (2004) Spatial and temporal relationships between plaques and tangles in Alzheimer-pathology, *Neurobiology of aging* 25, 697-711.
 54. Goedert, M., Spillantini, M. G., Cairns, N. J., and Crowther, R. A. (1992) Tau proteins of Alzheimer paired helical filaments: abnormal phosphorylation of all six brain isoforms, *Neuron* 8, 159-168.
 55. Braak, H., Thal, D. R., Ghebremedhin, E., and Del Tredici, K. (2011) Stages of the pathologic process in Alzheimer disease: age categories from 1 to 100 years, *Journal of neuropathology and experimental neurology* 70, 960-969.
 56. Markesbery, W. R., Schmitt, F. A., Kryscio, R. J., Davis, D. G., Smith, C. D., and Wekstein, D. R. (2006) Neuropathologic substrate of mild cognitive impairment, *Archives of neurology* 63, 38-46.
 57. Braak, H., Alafuzoff, I., Arzberger, T., Kretschmar, H., and Del Tredici, K. (2006) Staging of Alzheimer disease-associated neurofibrillary pathology using paraffin sections and immunocytochemistry, *Acta neuropathologica* 112, 389-404.
 58. Goedert, M., Jakes, R., and Vanmechelen, E. (1995) Monoclonal antibody AT8 recognises tau protein phosphorylated at both serine 202 and threonine 205, *Neuroscience letters* 189, 167-169.
 59. Braak, H., and Del Tredici, K. (2011) Alzheimer's pathogenesis: is there neuron-to-neuron propagation?, *Acta neuropathologica* 121, 589-595.
 60. Ness, S., Rafii, M., Aisen, P., Krams, M., Silverman, W., and Manji, H. (2012) Down's syndrome and Alzheimer's disease: towards secondary prevention, *Nature reviews. Drug discovery* 11, 655-656.
 61. Waring, S. C., and Rosenberg, R. N. (2008) Genome-wide association studies in Alzheimer disease, *Archives of neurology* 65, 329-334.
 62. Lewis, J., Dickson, D. W., Lin, W. L., Chisholm, L., Corral, A., Jones, G., Yen, S. H., Sahara, N., Skipper, L., Yager, D., Eckman, C., Hardy, J., Hutton, M., and McGowan, E. (2001) Enhanced neurofibrillary degeneration in transgenic mice expressing mutant tau and APP, *Science* 293, 1487-1491.
 63. Samuel, W., Terry, R. D., DeTeresa, R., Butters, N., and Masliah, E. (1994) Clinical correlates of cortical and nucleus basalis pathology in Alzheimer dementia, *Archives of neurology* 51, 772-778.
 64. Poorkaj, P., Bird, T. D., Wijsman, E., Nemens, E., Garruto, R. M., Anderson, L., Andreadis, A., Wiederholt, W. C., Raskind, M., and Schellenberg, G. D. (1998) Tau is a candidate gene for chromosome 17 frontotemporal dementia, *Annals of neurology* 43, 815-825.
 65. Spillantini, M. G., Murrell, J. R., Goedert, M., Farlow, M. R., Klug, A., and Ghetti, B. (1998) Mutation in the tau gene in familial multiple system tauopathy with presenile dementia, *Proceedings of the National Academy of Sciences of the United States of America* 95, 7737-7741.
 66. Bandyopadhyay, B., Li, G., Yin, H., and Kuret, J. (2007) Tau aggregation and toxicity in a cell culture model of tauopathy, *The Journal of biological chemistry* 282, 16454-16464.

67. Rapoport, M., Dawson, H. N., Binder, L. I., Vitek, M. P., and Ferreira, A. (2002) Tau is essential to beta -amyloid-induced neurotoxicity, *Proceedings of the National Academy of Sciences of the United States of America* 99, 6364-6369.
68. Roberson, E. D., Searce-Levie, K., Palop, J. J., Yan, F., Cheng, I. H., Wu, T., Gerstein, H., Yu, G. Q., and Mucke, L. (2007) Reducing endogenous tau ameliorates amyloid beta-induced deficits in an Alzheimer's disease mouse model, *Science* 316, 750-754.
69. Hutton, M., Lendon, C. L., Rizzu, P., Baker, M., Froelich, S., Houlden, H., Pickering-Brown, S., Chakraverty, S., Isaacs, A., Grover, A., Hackett, J., Adamson, J., Lincoln, S., Dickson, D., Davies, P., Petersen, R. C., Stevens, M., de Graaff, E., Wauters, E., van Baren, J., Hillebrand, M., Joosse, M., Kwon, J. M., Nowotny, P., Che, L. K., Norton, J., Morris, J. C., Reed, L. A., Trojanowski, J., Basun, H., Lannfelt, L., Neystat, M., Fahn, S., Dark, F., Tannenberg, T., Dodd, P. R., Hayward, N., Kwok, J. B., Schofield, P. R., Andreadis, A., Snowden, J., Craufurd, D., Neary, D., Owen, F., Oostra, B. A., Hardy, J., Goate, A., van Swieten, J., Mann, D., Lynch, T., and Heutink, P. (1998) Association of missense and 5'-splice-site mutations in tau with the inherited dementia FTDP-17, *Nature* 393, 702-705.
70. Frederick, J. (2006) Pick disease: a brief overview, *Archives of pathology & laboratory medicine* 130, 1063-1066.
71. Delacourte, A., Robitaille, Y., Sergeant, N., Buee, L., Hof, P. R., Wattez, A., Laroche-Cholette, A., Mathieu, J., Chagnon, P., and Gauvreau, D. (1996) Specific pathological Tau protein variants characterize Pick's disease, *Journal of neuropathology and experimental neurology* 55, 159-168.
72. Hauw, J. J., Daniel, S. E., Dickson, D., Horoupian, D. S., Jellinger, K., Lantos, P. L., McKee, A., Tabaton, M., and Litvan, I. (1994) Preliminary NINDS neuropathologic criteria for Steele-Richardson-Olszewski syndrome (progressive supranuclear palsy), *Neurology* 44, 2015-2019.
73. Sergeant, N., David, J. P., Lefranc, D., Vermersch, P., Wattez, A., and Delacourte, A. (1997) Different distribution of phosphorylated tau protein isoforms in Alzheimer's and Pick's diseases, *FEBS letters* 412, 578-582.
74. Probst, A., Tolnay, M., Langui, D., Goedert, M., and Spillantini, M. G. (1996) Pick's disease: hyperphosphorylated tau protein segregates to the somatoaxonal compartment, *Acta neuropathologica* 92, 588-596.
75. Cervos-Navarro, J., and Schumacher, K. (1994) Neurofibrillary pathology in progressive supranuclear palsy (PSP), *Journal of neural transmission. Supplementum* 42, 153-164.
76. Chambers, C. B., Lee, J. M., Troncoso, J. C., Reich, S., and Muma, N. A. (1999) Overexpression of four-repeat tau mRNA isoforms in progressive supranuclear palsy but not in Alzheimer's disease, *Annals of neurology* 46, 325-332.
77. Feany, M. B., and Dickson, D. W. (1995) Widespread cytoskeletal pathology characterizes corticobasal degeneration, *The American journal of pathology* 146, 1388-1396.
78. Ksiazak-Reding, H., Morgan, K., Mattiace, L. A., Davies, P., Liu, W. K., Yen, S. H., Weidenheim, K., and Dickson, D. W. (1994) Ultrastructure and biochemical composition of paired helical filaments in corticobasal degeneration, *The American journal of pathology* 145, 1496-1508.
79. Wakabayashi, K., and Takahashi, H. (2004) Pathological heterogeneity in progressive supranuclear palsy and corticobasal degeneration, *Neuropathology : official journal of the Japanese Society of Neuropathology* 24, 79-86.
80. Rabano, A., Rodal, I., Cuadros, R., Calero, M., Hernandez, F., and Avila, J. (2014) Argyrophilic grain pathology as a natural model of tau propagation, *Journal of Alzheimer's disease : JAD* 40 Suppl 1, S123-133.
81. Probst, A., and Tolnay, M. (2002) [Argyrophilic grain disease (AgD), a frequent and largely underestimated cause of dementia in old patients], *Revue neurologique* 158, 155-165.

82. Kopke, E., Tung, Y. C., Shaikh, S., Alonso, A. C., Iqbal, K., and Grundke-Iqbal, I. (1993) Microtubule-associated protein tau. Abnormal phosphorylation of a non-paired helical filament pool in Alzheimer disease, *The Journal of biological chemistry* 268, 24374-24384.
83. Alonso, A. C., Grundke-Iqbal, I., and Iqbal, K. (1996) Alzheimer's disease hyperphosphorylated tau sequesters normal tau into tangles of filaments and disassembles microtubules, *Nature medicine* 2, 783-787.
84. Alonso, A. C., Zaidi, T., Grundke-Iqbal, I., and Iqbal, K. (1994) Role of abnormally phosphorylated tau in the breakdown of microtubules in Alzheimer disease, *Proceedings of the National Academy of Sciences of the United States of America* 91, 5562-5566.
85. Necula, M., and Kuret, J. (2004) Pseudophosphorylation and glycation of tau protein enhance but do not trigger fibrillization in vitro, *The Journal of biological chemistry* 279, 49694-49703.
86. Sun, Q., and Gamblin, T. C. (2009) Pseudohyperphosphorylation causing AD-like changes in tau has significant effects on its polymerization, *Biochemistry* 48, 6002-6011.
87. Pei, J. J., Braak, E., Braak, H., Grundke-Iqbal, I., Iqbal, K., Winblad, B., and Cowburn, R. F. (1999) Distribution of active glycogen synthase kinase 3beta (GSK-3beta) in brains staged for Alzheimer disease neurofibrillary changes, *Journal of neuropathology and experimental neurology* 58, 1010-1019.
88. Pei, J. J., Gong, C. X., Iqbal, K., Grundke-Iqbal, I., Wu, Q. L., Winblad, B., and Cowburn, R. F. (1998) Subcellular distribution of protein phosphatases and abnormally phosphorylated tau in the temporal cortex from Alzheimer's disease and control brains, *Journal of neural transmission* 105, 69-83.
89. Liu, F., Zaidi, T., Iqbal, K., Grundke-Iqbal, I., Merkle, R. K., and Gong, C. X. (2002) Role of glycosylation in hyperphosphorylation of tau in Alzheimer's disease, *FEBS letters* 512, 101-106.
90. Min, S. W., Cho, S. H., Zhou, Y., Schroeder, S., Haroutunian, V., Seeley, W. W., Huang, E. J., Shen, Y., Masliah, E., Mukherjee, C., Meyers, D., Cole, P. A., Ott, M., and Gan, L. (2010) Acetylation of tau inhibits its degradation and contributes to tauopathy, *Neuron* 67, 953-966.
91. Ciechanover, A., and Kwon, Y. T. (2015) Degradation of misfolded proteins in neurodegenerative diseases: therapeutic targets and strategies, *Experimental & molecular medicine* 47, e147.
92. Binder, L. I., Guillozet-Bongaarts, A. L., Garcia-Sierra, F., and Berry, R. W. (2005) Tau, tangles, and Alzheimer's disease, *Biochimica et biophysica acta* 1739, 216-223.
93. Novak, M., Kabat, J., and Wischik, C. M. (1993) Molecular characterization of the minimal protease resistant tau unit of the Alzheimer's disease paired helical filament, *The EMBO journal* 12, 365-370.
94. Bondareff, W., Wischik, C. M., Novak, M., Amos, W. B., Klug, A., and Roth, M. (1990) Molecular analysis of neurofibrillary degeneration in Alzheimer's disease. An immunohistochemical study, *The American journal of pathology* 137, 711-723.
95. Basurto-Islas, G., Luna-Munoz, J., Guillozet-Bongaarts, A. L., Binder, L. I., Mena, R., and Garcia-Sierra, F. (2008) Accumulation of aspartic acid421- and glutamic acid391-cleaved tau in neurofibrillary tangles correlates with progression in Alzheimer disease, *Journal of neuropathology and experimental neurology* 67, 470-483.
96. Horowitz, P. M., Patterson, K. R., Guillozet-Bongaarts, A. L., Reynolds, M. R., Carroll, C. A., Weintraub, S. T., Bennett, D. A., Cryns, V. L., Berry, R. W., and Binder, L. I. (2004) Early N-terminal changes and caspase-6 cleavage of tau in Alzheimer's disease, *The Journal of neuroscience : the official journal of the Society for Neuroscience* 24, 7895-7902.
97. Gamblin, T. C., Chen, F., Zambrano, A., Abraha, A., Lagalwar, S., Guillozet, A. L., Lu, M., Fu, Y., Garcia-Sierra, F., LaPointe, N., Miller, R., Berry, R. W., Binder, L. I., and Cryns, V. L. (2003) Caspase cleavage of tau: linking amyloid and neurofibrillary tangles in Alzheimer's disease,

- Proceedings of the National Academy of Sciences of the United States of America* 100, 10032-10037.
98. Rissman, R. A., Poon, W. W., Blurton-Jones, M., Oddo, S., Torp, R., Vitek, M. P., LaFerla, F. M., Rohn, T. T., and Cotman, C. W. (2004) Caspase-cleavage of tau is an early event in Alzheimer disease tangle pathology, *The Journal of clinical investigation* 114, 121-130.
 99. Gamblin, T. C., Berry, R. W., and Binder, L. I. (2003) Tau polymerization: role of the amino terminus, *Biochemistry* 42, 2252-2257.
 100. Abraha, A., Ghoshal, N., Gamblin, T. C., Cryns, V., Berry, R. W., Kuret, J., and Binder, L. I. (2000) C-terminal inhibition of tau assembly in vitro and in Alzheimer's disease, *Journal of cell science* 113 Pt 21, 3737-3745.
 101. Perez, M., Valpuesta, J. M., Medina, M., Montejo de Garcini, E., and Avila, J. (1996) Polymerization of tau into filaments in the presence of heparin: the minimal sequence required for tau-tau interaction, *Journal of neurochemistry* 67, 1183-1190.
 102. Friedhoff, P., Schneider, A., Mandelkow, E. M., and Mandelkow, E. (1998) Rapid assembly of Alzheimer-like paired helical filaments from microtubule-associated protein tau monitored by fluorescence in solution, *Biochemistry* 37, 10223-10230.
 103. Kampers, T., Friedhoff, P., Biernat, J., Mandelkow, E. M., and Mandelkow, E. (1996) RNA stimulates aggregation of microtubule-associated protein tau into Alzheimer-like paired helical filaments, *FEBS letters* 399, 344-349.
 104. Wilson, D. M., and Binder, L. I. (1997) Free fatty acids stimulate the polymerization of tau and amyloid beta peptides. In vitro evidence for a common effector of pathogenesis in Alzheimer's disease, *The American journal of pathology* 150, 2181-2195.
 105. Gamblin, T. C., King, M. E., Kuret, J., Berry, R. W., and Binder, L. I. (2000) Oxidative regulation of fatty acid-induced tau polymerization, *Biochemistry* 39, 14203-14210.
 106. Chirita, C. N., Necula, M., and Kuret, J. (2003) Anionic micelles and vesicles induce tau fibrillization in vitro, *The Journal of biological chemistry* 278, 25644-25650.
 107. Barghorn, S., and Mandelkow, E. (2002) Toward a unified scheme for the aggregation of tau into Alzheimer paired helical filaments, *Biochemistry* 41, 14885-14896.
 108. King, M. E., Ahuja, V., Binder, L. I., and Kuret, J. (1999) Ligand-dependent tau filament formation: implications for Alzheimer's disease progression, *Biochemistry* 38, 14851-14859.
 109. Auld, D. S., Kornecook, T. J., Bastianetto, S., and Quirion, R. (2002) Alzheimer's disease and the basal forebrain cholinergic system: relations to beta-amyloid peptides, cognition, and treatment strategies, *Progress in neurobiology* 68, 209-245.
 110. Schneider, L. S., Mangialasche, F., Andreasen, N., Feldman, H., Giacobini, E., Jones, R., Mantua, V., Mecocci, P., Pani, L., Winblad, B., and Kivipelto, M. (2014) Clinical trials and late-stage drug development for Alzheimer's disease: an appraisal from 1984 to 2014, *Journal of internal medicine* 275, 251-283.
 111. Francis, P. T., Palmer, A. M., Snape, M., and Wilcock, G. K. (1999) The cholinergic hypothesis of Alzheimer's disease: a review of progress, *Journal of neurology, neurosurgery, and psychiatry* 66, 137-147.
 112. Arundine, M., and Tymianski, M. (2003) Molecular mechanisms of calcium-dependent neurodegeneration in excitotoxicity, *Cell calcium* 34, 325-337.
 113. Danysz, W., Parsons, C. G., Mobius, H. J., Stoffler, A., and Quack, G. (2000) Neuroprotective and symptomatological action of memantine relevant for Alzheimer's disease--a unified glutamatergic hypothesis on the mechanism of action, *Neurotoxicity research* 2, 85-97.

114. Farlow, M. R., Miller, M. L., and Pejovic, V. (2008) Treatment options in Alzheimer's disease: maximizing benefit, managing expectations, *Dementia and geriatric cognitive disorders* 25, 408-422.
115. Hogan, D. B. (2014) Long-term efficacy and toxicity of cholinesterase inhibitors in the treatment of Alzheimer disease, *Canadian journal of psychiatry. Revue canadienne de psychiatrie* 59, 618-623.
116. Hardy, J. A., and Higgins, G. A. (1992) Alzheimer's disease: the amyloid cascade hypothesis, *Science* 256, 184-185.
117. Haass, C., and De Strooper, B. (1999) The presenilins in Alzheimer's disease--proteolysis holds the key, *Science* 286, 916-919.
118. Fahrenholz, F., and Postina, R. (2006) Alpha-secretase activation--an approach to Alzheimer's disease therapy, *Neuro-degenerative diseases* 3, 255-261.
119. De Strooper, B., Annaert, W., Cupers, P., Saftig, P., Craessaerts, K., Mumm, J. S., Schroeter, E. H., Schrijvers, V., Wolfe, M. S., Ray, W. J., Goate, A., and Kopan, R. (1999) A presenilin-1-dependent gamma-secretase-like protease mediates release of Notch intracellular domain, *Nature* 398, 518-522.
120. Schenk, D., Barbour, R., Dunn, W., Gordon, G., Grajeda, H., Guido, T., Hu, K., Huang, J., Johnson-Wood, K., Khan, K., Kholodenko, D., Lee, M., Liao, Z., Lieberburg, I., Motter, R., Mutter, L., Soriano, F., Shopp, G., Vasquez, N., Vandeventer, C., Walker, S., Wogulis, M., Yednock, T., Games, D., and Seubert, P. (1999) Immunization with amyloid-beta attenuates Alzheimer-disease-like pathology in the PDAPP mouse, *Nature* 400, 173-177.
121. Bard, F., Cannon, C., Barbour, R., Burke, R. L., Games, D., Grajeda, H., Guido, T., Hu, K., Huang, J., Johnson-Wood, K., Khan, K., Kholodenko, D., Lee, M., Lieberburg, I., Motter, R., Nguyen, M., Soriano, F., Vasquez, N., Weiss, K., Welch, B., Seubert, P., Schenk, D., and Yednock, T. (2000) Peripherally administered antibodies against amyloid beta-peptide enter the central nervous system and reduce pathology in a mouse model of Alzheimer disease, *Nature medicine* 6, 916-919.
122. DeMattos, R. B., Bales, K. R., Cummins, D. J., Dodart, J. C., Paul, S. M., and Holtzman, D. M. (2001) Peripheral anti-A beta antibody alters CNS and plasma A beta clearance and decreases brain A beta burden in a mouse model of Alzheimer's disease, *Proceedings of the National Academy of Sciences of the United States of America* 98, 8850-8855.
123. Rogers, J., Webster, S., Lue, L. F., Brachova, L., Civin, W. H., Emmerling, M., Shivers, B., Walker, D., and McGeer, P. (1996) Inflammation and Alzheimer's disease pathogenesis, *Neurobiology of aging* 17, 681-686.
124. Wolozin, B., Kellman, W., Ruosseau, P., Celesia, G. G., and Siegel, G. (2000) Decreased prevalence of Alzheimer disease associated with 3-hydroxy-3-methylglutaryl coenzyme A reductase inhibitors, *Archives of neurology* 57, 1439-1443.
125. Refolo, L. M., Pappolla, M. A., LaFrancois, J., Malester, B., Schmidt, S. D., Thomas-Bryant, T., Tint, G. S., Wang, R., Mercken, M., Petanceska, S. S., and Duff, K. E. (2001) A cholesterol-lowering drug reduces beta-amyloid pathology in a transgenic mouse model of Alzheimer's disease, *Neurobiology of disease* 8, 890-899.
126. Bush, A. I., Pettingell, W. H., Multhaup, G., d Paradis, M., Vonsattel, J. P., Gusella, J. F., Beyreuther, K., Masters, C. L., and Tanzi, R. E. (1994) Rapid induction of Alzheimer A beta amyloid formation by zinc, *Science* 265, 1464-1467.
127. Cherny, R. A., Atwood, C. S., Xilinas, M. E., Gray, D. N., Jones, W. D., McLean, C. A., Barnham, K. J., Volitakis, I., Fraser, F. W., Kim, Y., Huang, X., Goldstein, L. E., Moir, R. D., Lim, J. T., Beyreuther, K., Zheng, H., Tanzi, R. E., Masters, C. L., and Bush, A. I. (2001) Treatment with a copper-zinc

- chelator markedly and rapidly inhibits beta-amyloid accumulation in Alzheimer's disease transgenic mice, *Neuron* 30, 665-676.
128. Mangialasche, F., Solomon, A., Winblad, B., Mecocci, P., and Kivipelto, M. (2010) Alzheimer's disease: clinical trials and drug development, *The Lancet. Neurology* 9, 702-716.
 129. Kuzuhara, S. (2010) [Treatment strategy of Alzheimer's disease: pause in clinical trials of Abeta vaccine and next steps], *Brain and nerve = Shinkei kenkyu no shinpo* 62, 659-666.
 130. Iqbal, K., Gong, C. X., and Liu, F. (2013) Hyperphosphorylation-induced tau oligomers, *Frontiers in neurology* 4, 112.
 131. Kremer, A., Louis, J. V., Jaworski, T., and Van Leuven, F. (2011) GSK3 and Alzheimer's Disease: Facts and Fiction, *Frontiers in molecular neuroscience* 4, 17.
 132. Engel, T., Goni-Oliver, P., Lucas, J. J., Avila, J., and Hernandez, F. (2006) Chronic lithium administration to FTDP-17 tau and GSK-3beta overexpressing mice prevents tau hyperphosphorylation and neurofibrillary tangle formation, but pre-formed neurofibrillary tangles do not revert, *Journal of neurochemistry* 99, 1445-1455.
 133. Sereno, L., Coma, M., Rodriguez, M., Sanchez-Ferrer, P., Sanchez, M. B., Gich, I., Agullo, J. M., Perez, M., Avila, J., Guardia-Laguarta, C., Clarimon, J., Lleo, A., and Gomez-Isla, T. (2009) A novel GSK-3beta inhibitor reduces Alzheimer's pathology and rescues neuronal loss in vivo, *Neurobiology of disease* 35, 359-367.
 134. Lovestone, S., Boada, M., Dubois, B., Hull, M., Rinne, J. O., Huppertz, H. J., Calero, M., Andres, M. V., Gomez-Carrillo, B., Leon, T., del Ser, T., and investigators, A. (2015) A phase II trial of tideglusib in Alzheimer's disease, *Journal of Alzheimer's disease : JAD* 45, 75-88.
 135. Yoshiyama, Y., Lee, V. M., and Trojanowski, J. Q. (2013) Therapeutic strategies for tau mediated neurodegeneration, *Journal of neurology, neurosurgery, and psychiatry* 84, 784-795.
 136. Gong, C. X., Shaikh, S., Wang, J. Z., Zaidi, T., Grundke-Iqbal, I., and Iqbal, K. (1995) Phosphatase activity toward abnormally phosphorylated tau: decrease in Alzheimer disease brain, *Journal of neurochemistry* 65, 732-738.
 137. Gong, C. X., Singh, T. J., Grundke-Iqbal, I., and Iqbal, K. (1993) Phosphoprotein phosphatase activities in Alzheimer disease brain, *Journal of neurochemistry* 61, 921-927.
 138. Vogelsberg-Ragaglia, V., Schuck, T., Trojanowski, J. Q., and Lee, V. M. (2001) PP2A mRNA expression is quantitatively decreased in Alzheimer's disease hippocampus, *Experimental neurology* 168, 402-412.
 139. Liu, F., Grundke-Iqbal, I., Iqbal, K., and Gong, C. X. (2005) Contributions of protein phosphatases PP1, PP2A, PP2B and PP5 to the regulation of tau phosphorylation, *The European journal of neuroscience* 22, 1942-1950.
 140. Gong, C. X., Lidsky, T., Wegiel, J., Zuck, L., Grundke-Iqbal, I., and Iqbal, K. (2000) Phosphorylation of microtubule-associated protein tau is regulated by protein phosphatase 2A in mammalian brain. Implications for neurofibrillary degeneration in Alzheimer's disease, *The Journal of biological chemistry* 275, 5535-5544.
 141. van Eersel, J., Ke, Y. D., Liu, X., Delerue, F., Kril, J. J., Gotz, J., and Ittner, L. M. (2010) Sodium selenate mitigates tau pathology, neurodegeneration, and functional deficits in Alzheimer's disease models, *Proceedings of the National Academy of Sciences of the United States of America* 107, 13888-13893.
 142. Chohan, M. O., Khatoun, S., Iqbal, I. G., and Iqbal, K. (2006) Involvement of I2PP2A in the abnormal hyperphosphorylation of tau and its reversal by Memantine, *FEBS letters* 580, 3973-3979.

143. Degerman Gunnarsson, M., Kilander, L., Basun, H., and Lannfelt, L. (2007) Reduction of phosphorylated tau during memantine treatment of Alzheimer's disease, *Dementia and geriatric cognitive disorders* 24, 247-252.
144. Cash, A. D., Aliev, G., Siedlak, S. L., Nunomura, A., Fujioka, H., Zhu, X., Raina, A. K., Vinters, H. V., Tabaton, M., Johnson, A. B., Paula-Barbosa, M., Avila, J., Jones, P. K., Castellani, R. J., Smith, M. A., and Perry, G. (2003) Microtubule reduction in Alzheimer's disease and aging is independent of tau filament formation, *The American journal of pathology* 162, 1623-1627.
145. Zhang, B., Maiti, A., Shively, S., Lakhani, F., McDonald-Jones, G., Bruce, J., Lee, E. B., Xie, S. X., Joyce, S., Li, C., Toleikis, P. M., Lee, V. M., and Trojanowski, J. Q. (2005) Microtubule-binding drugs offset tau sequestration by stabilizing microtubules and reversing fast axonal transport deficits in a tauopathy model, *Proceedings of the National Academy of Sciences of the United States of America* 102, 227-231.
146. Yenjerla, M., LaPointe, N. E., Lopus, M., Cox, C., Jordan, M. A., Feinstein, S. C., and Wilson, L. (2010) The neuroprotective peptide NAP does not directly affect polymerization or dynamics of reconstituted neural microtubules, *Journal of Alzheimer's disease : JAD* 19, 1377-1386.
147. Zhang, B., Carroll, J., Trojanowski, J. Q., Yao, Y., Iba, M., Potuzak, J. S., Hogan, A. M., Xie, S. X., Ballatore, C., Smith, A. B., 3rd, Lee, V. M., and Brunden, K. R. (2012) The microtubule-stabilizing agent, epothilone D, reduces axonal dysfunction, neurotoxicity, cognitive deficits, and Alzheimer-like pathology in an interventional study with aged tau transgenic mice, *The Journal of neuroscience : the official journal of the Society for Neuroscience* 32, 3601-3611.
148. Barten, D. M., Fanara, P., Andorfer, C., Hoque, N., Wong, P. Y., Husted, K. H., Cadelina, G. W., Decarr, L. B., Yang, L., Liu, V., Fessler, C., Protassio, J., Riff, T., Turner, H., Janus, C. G., Sankaranarayanan, S., Polson, C., Meredith, J. E., Gray, G., Hanna, A., Olson, R. E., Kim, S. H., Vite, G. D., Lee, F. Y., and Albright, C. F. (2012) Hyperdynamic microtubules, cognitive deficits, and pathology are improved in tau transgenic mice with low doses of the microtubule-stabilizing agent BMS-241027, *The Journal of neuroscience : the official journal of the Society for Neuroscience* 32, 7137-7145.
149. Petrucelli, L., Dickson, D., Kehoe, K., Taylor, J., Snyder, H., Grover, A., De Lucia, M., McGowan, E., Lewis, J., Prihar, G., Kim, J., Dillmann, W. H., Browne, S. E., Hall, A., Voellmy, R., Tsuboi, Y., Dawson, T. M., Wolozin, B., Hardy, J., and Hutton, M. (2004) CHIP and Hsp70 regulate tau ubiquitination, degradation and aggregation, *Human molecular genetics* 13, 703-714.
150. Luo, W., Dou, F., Rodina, A., Chip, S., Kim, J., Zhao, Q., Moulick, K., Aguirre, J., Wu, N., Greengard, P., and Chiosis, G. (2007) Roles of heat-shock protein 90 in maintaining and facilitating the neurodegenerative phenotype in tauopathies, *Proceedings of the National Academy of Sciences of the United States of America* 104, 9511-9516.
151. Derisbourg, M., Leghay, C., Chiappetta, G., Fernandez-Gomez, F. J., Laurent, C., Demeyer, D., Carrier, S., Buee-Scherrer, V., Blum, D., Vinh, J., Sergeant, N., Verdier, Y., Buee, L., and Hamdane, M. (2015) Role of the Tau N-terminal region in microtubule stabilization revealed by new endogenous truncated forms, *Scientific reports* 5, 9659.
152. Wang, Y., Martinez-Vicente, M., Kruger, U., Kaushik, S., Wong, E., Mandelkow, E. M., Cuervo, A. M., and Mandelkow, E. (2009) Tau fragmentation, aggregation and clearance: the dual role of lysosomal processing, *Human molecular genetics* 18, 4153-4170.
153. Schaeffer, V., Lavenir, I., Ozcelik, S., Tolnay, M., Winkler, D. T., and Goedert, M. (2012) Stimulation of autophagy reduces neurodegeneration in a mouse model of human tauopathy, *Brain : a journal of neurology* 135, 2169-2177.
154. Dolan, P. J., and Johnson, G. V. (2010) A caspase cleaved form of tau is preferentially degraded through the autophagy pathway, *The Journal of biological chemistry* 285, 21978-21987.

155. Frost, B., Jacks, R. L., and Diamond, M. I. (2009) Propagation of tau misfolding from the outside to the inside of a cell, *The Journal of biological chemistry* 284, 12845-12852.
156. Clavaguera, F., Bolmont, T., Crowther, R. A., Abramowski, D., Frank, S., Probst, A., Fraser, G., Stalder, A. K., Beibel, M., Staufenbiel, M., Jucker, M., Goedert, M., and Tolnay, M. (2009) Transmission and spreading of tauopathy in transgenic mouse brain, *Nature cell biology* 11, 909-913.
157. Asuni, A. A., Boutajangout, A., Quartermain, D., and Sigurdsson, E. M. (2007) Immunotherapy targeting pathological tau conformers in a tangle mouse model reduces brain pathology with associated functional improvements, *The Journal of neuroscience : the official journal of the Society for Neuroscience* 27, 9115-9129.
158. Chai, X., Wu, S., Murray, T. K., Kinley, R., Cella, C. V., Sims, H., Buckner, N., Hanmer, J., Davies, P., O'Neill, M. J., Hutton, M. L., and Citron, M. (2011) Passive immunization with anti-Tau antibodies in two transgenic models: reduction of Tau pathology and delay of disease progression, *The Journal of biological chemistry* 286, 34457-34467.
159. Bi, M., Ittner, A., Ke, Y. D., Gotz, J., and Ittner, L. M. (2011) Tau-targeted immunization impedes progression of neurofibrillary histopathology in aged P301L tau transgenic mice, *PLoS one* 6, e26860.
160. Wischik, C. M., Harrington, C. R., and Storey, J. M. (2014) Tau-aggregation inhibitor therapy for Alzheimer's disease, *Biochemical pharmacology* 88, 529-539.
161. Quideau, S., Deffieux, D., Douat-Casassus, C., and Pouysegu, L. (2011) Plant polyphenols: chemical properties, biological activities, and synthesis, *Angewandte Chemie* 50, 586-621.
162. Taniguchi, S., Suzuki, N., Masuda, M., Hisanaga, S., Iwatsubo, T., Goedert, M., and Hasegawa, M. (2005) Inhibition of heparin-induced tau filament formation by phenothiazines, polyphenols, and porphyrins, *The Journal of biological chemistry* 280, 7614-7623.
163. Bieschke, J., Russ, J., Friedrich, R. P., Ehrnhoefer, D. E., Wobst, H., Neugebauer, K., and Wanker, E. E. (2010) EGCG remodels mature alpha-synuclein and amyloid-beta fibrils and reduces cellular toxicity, *Proceedings of the National Academy of Sciences of the United States of America* 107, 7710-7715.
164. Meng, X., Munishkina, L. A., Fink, A. L., and Uversky, V. N. (2010) Effects of Various Flavonoids on the alpha-Synuclein Fibrillation Process, *Parkinson's disease* 2010, 650794.
165. Daccache, A., Lion, C., Sibille, N., Gerard, M., Slomianny, C., Lippens, G., and Cotelle, P. (2011) Oleuropein and derivatives from olives as Tau aggregation inhibitors, *Neurochemistry international* 58, 700-707.
166. Pickhardt, M., Gazova, Z., von Bergen, M., Khlistunova, I., Wang, Y., Hascher, A., Mandelkow, E. M., Biernat, J., and Mandelkow, E. (2005) Anthraquinones inhibit tau aggregation and dissolve Alzheimer's paired helical filaments in vitro and in cells, *The Journal of biological chemistry* 280, 3628-3635.
167. Howlett, D. R., George, A. R., Owen, D. E., Ward, R. V., and Markwell, R. E. (1999) Common structural features determine the effectiveness of carvedilol, daunomycin and rolitetracycline as inhibitors of Alzheimer beta-amyloid fibril formation, *The Biochemical journal* 343 Pt 2, 419-423.
168. Bulic, B., Pickhardt, M., Khlistunova, I., Biernat, J., Mandelkow, E. M., Mandelkow, E., and Waldmann, H. (2007) Rhodanine-based tau aggregation inhibitors in cell models of tauopathy, *Angewandte Chemie* 46, 9215-9219.
169. Fatouros, C., Pir, G. J., Biernat, J., Koushika, S. P., Mandelkow, E., Mandelkow, E. M., Schmidt, E., and Baumeister, R. (2012) Inhibition of tau aggregation in a novel *Caenorhabditis elegans* model of tauopathy mitigates proteotoxicity, *Human molecular genetics* 21, 3587-3603.

170. Messing, L., Decker, J. M., Joseph, M., Mandelkow, E., and Mandelkow, E. M. (2013) Cascade of tau toxicity in inducible hippocampal brain slices and prevention by aggregation inhibitors, *Neurobiology of aging* 34, 1343-1354.
171. Larbig, G., Pickhardt, M., Lloyd, D. G., Schmidt, B., and Mandelkow, E. (2007) Screening for inhibitors of tau protein aggregation into Alzheimer paired helical filaments: a ligand based approach results in successful scaffold hopping, *Current Alzheimer research* 4, 315-323.
172. Pickhardt, M., Larbig, G., Khlistunova, I., Coksezen, A., Meyer, B., Mandelkow, E. M., Schmidt, B., and Mandelkow, E. (2007) Phenylthiazolyl-hydrazide and its derivatives are potent inhibitors of tau aggregation and toxicity in vitro and in cells, *Biochemistry* 46, 10016-10023.
173. Bulic, B., Pickhardt, M., and Mandelkow, E. (2013) Progress and developments in tau aggregation inhibitors for Alzheimer disease, *Journal of medicinal chemistry* 56, 4135-4155.
174. Pickhardt, M., Biernat, J., Khlistunova, I., Wang, Y. P., Gazova, Z., Mandelkow, E. M., and Mandelkow, E. (2007) N-phenylamine derivatives as aggregation inhibitors in cell models of tauopathy, *Current Alzheimer research* 4, 397-402.
175. Klunk, W. E., Wang, Y., Huang, G. F., Debnath, M. L., Holt, D. P., and Mathis, C. A. (2001) Uncharged thioflavin-T derivatives bind to amyloid-beta protein with high affinity and readily enter the brain, *Life sciences* 69, 1471-1484.
176. Necula, M., Chirita, C. N., and Kuret, J. (2005) Cyanine dye N744 inhibits tau fibrillization by blocking filament extension: implications for the treatment of tauopathic neurodegenerative diseases, *Biochemistry* 44, 10227-10237.
177. Crowe, A., Huang, W., Ballatore, C., Johnson, R. L., Hogan, A. M., Huang, R., Wichterman, J., McCoy, J., Hurn, D., Auld, D. S., Smith, A. B., 3rd, Inglese, J., Trojanowski, J. Q., Austin, C. P., Brunden, K. R., and Lee, V. M. (2009) Identification of aminothienopyridazine inhibitors of tau assembly by quantitative high-throughput screening, *Biochemistry* 48, 7732-7745.
178. Crowe, A., James, M. J., Lee, V. M., Smith, A. B., 3rd, Trojanowski, J. Q., Ballatore, C., and Brunden, K. R. (2013) Aminothienopyridazines and methylene blue affect Tau fibrillization via cysteine oxidation, *The Journal of biological chemistry* 288, 11024-11037.
179. Noble, W., Hanger, D. P., Miller, C. C., and Lovestone, S. (2013) The importance of tau phosphorylation for neurodegenerative diseases, *Frontiers in neurology* 4, 83.
180. Arai, T., Ikeda, K., Akiyama, H., Nonaka, T., Hasegawa, M., Ishiguro, K., Iritani, S., Tsuchiya, K., Iseki, E., Yagishita, S., Oda, T., and Mochizuki, A. (2004) Identification of amino-terminally cleaved tau fragments that distinguish progressive supranuclear palsy from corticobasal degeneration, *Annals of neurology* 55, 72-79.
181. Anderson, J. P., Walker, D. E., Goldstein, J. M., de Laat, R., Banducci, K., Caccavello, R. J., Barbour, R., Huang, J., Kling, K., Lee, M., Diep, L., Keim, P. S., Shen, X., Chataway, T., Schlossmacher, M. G., Seubert, P., Schenk, D., Sinha, S., Gai, W. P., and Chilcote, T. J. (2006) Phosphorylation of Ser-129 is the dominant pathological modification of alpha-synuclein in familial and sporadic Lewy body disease, *The Journal of biological chemistry* 281, 29739-29752.
182. Igaz, L. M., Kwong, L. K., Xu, Y., Truax, A. C., Uryu, K., Neumann, M., Clark, C. M., Elman, L. B., Miller, B. L., Grossman, M., McCluskey, L. F., Trojanowski, J. Q., and Lee, V. M. (2008) Enrichment of C-terminal fragments in TAR DNA-binding protein-43 cytoplasmic inclusions in brain but not in spinal cord of frontotemporal lobar degeneration and amyotrophic lateral sclerosis, *The American journal of pathology* 173, 182-194.
183. Guo, H., Albrecht, S., Bourdeau, M., Petzke, T., Bergeron, C., and LeBlanc, A. C. (2004) Active caspase-6 and caspase-6-cleaved tau in neuropil threads, neuritic plaques, and neurofibrillary tangles of Alzheimer's disease, *The American journal of pathology* 165, 523-531.

184. Vechterova, L., Kontsekova, E., Zilka, N., Ferencik, M., Ravid, R., and Novak, M. (2003) DC11: a novel monoclonal antibody revealing Alzheimer's disease-specific tau epitope, *Neuroreport* 14, 87-91.
185. Braak, E., Braak, H., and Mandelkow, E. M. (1994) A sequence of cytoskeleton changes related to the formation of neurofibrillary tangles and neuropil threads, *Acta neuropathologica* 87, 554-567.
186. Guillozet-Bongaarts, A. L., Garcia-Sierra, F., Reynolds, M. R., Horowitz, P. M., Fu, Y., Wang, T., Cahill, M. E., Bigio, E. H., Berry, R. W., and Binder, L. I. (2005) Tau truncation during neurofibrillary tangle evolution in Alzheimer's disease, *Neurobiology of aging* 26, 1015-1022.
187. de Calignon, A., Fox, L. M., Pitstick, R., Carlson, G. A., Bacskai, B. J., Spires-Jones, T. L., and Hyman, B. T. (2010) Caspase activation precedes and leads to tangles, *Nature* 464, 1201-1204.
188. Filipcik, P., Zilka, N., Bugos, O., Kucerak, J., Koson, P., Novak, P., and Novak, M. (2012) First transgenic rat model developing progressive cortical neurofibrillary tangles, *Neurobiology of aging* 33, 1448-1456.
189. Zilka, N., Stozicka, Z., Kovac, A., Pilipcinec, E., Bugos, O., and Novak, M. (2009) Human misfolded truncated tau protein promotes activation of microglia and leukocyte infiltration in the transgenic rat model of tauopathy, *Journal of neuroimmunology* 209, 16-25.
190. Cente, M., Filipcik, P., Pevalova, M., and Novak, M. (2006) Expression of a truncated tau protein induces oxidative stress in a rodent model of tauopathy, *The European journal of neuroscience* 24, 1085-1090.
191. Zilka, N., Kovacech, B., Barath, P., Kontsekova, E., and Novak, M. (2012) The self-perpetuating tau truncation circle, *Biochemical Society transactions* 40, 681-686.
192. Horowitz, P. M., LaPointe, N., Guillozet-Bongaarts, A. L., Berry, R. W., and Binder, L. I. (2006) N-terminal fragments of tau inhibit full-length tau polymerization in vitro, *Biochemistry* 45, 12859-12866.
193. Wischik, C. M., Novak, M., Thogersen, H. C., Edwards, P. C., Runswick, M. J., Jakes, R., Walker, J. E., Milstein, C., Roth, M., and Klug, A. (1988) Isolation of a fragment of tau derived from the core of the paired helical filament of Alzheimer disease, *Proceedings of the National Academy of Sciences of the United States of America* 85, 4506-4510.
194. Rankin, C. A., Sun, Q., and Gamblin, T. C. (2005) Pseudo-phosphorylation of tau at Ser202 and Thr205 affects tau filament formation, *Brain research. Molecular brain research* 138, 84-93.
195. Gamblin, T. C., King, M. E., Dawson, H., Vitek, M. P., Kuret, J., Berry, R. W., and Binder, L. I. (2000) In vitro polymerization of tau protein monitored by laser light scattering: method and application to the study of FTDP-17 mutants, *Biochemistry* 39, 6136-6144.
196. Morris, A. M., Watzky, M. A., Agar, J. N., and Finke, R. G. (2008) Fitting neurological protein aggregation kinetic data via a 2-step, minimal/"Ockham's razor" model: the Finke-Watzky mechanism of nucleation followed by autocatalytic surface growth, *Biochemistry* 47, 2413-2427.
197. Ghoshal, N., Garcia-Sierra, F., Fu, Y., Beckett, L. A., Mufson, E. J., Kuret, J., Berry, R. W., and Binder, L. I. (2001) Tau-66: evidence for a novel tau conformation in Alzheimer's disease, *Journal of neurochemistry* 77, 1372-1385.
198. Fasulo, L., Ugolini, G., Visintin, M., Bradbury, A., Brancolini, C., Verzillo, V., Novak, M., and Cattaneo, A. (2000) The neuronal microtubule-associated protein tau is a substrate for caspase-3 and an effector of apoptosis, *Journal of neurochemistry* 75, 624-633.
199. Friedhoff, P., von Bergen, M., Mandelkow, E. M., Davies, P., and Mandelkow, E. (1998) A nucleated assembly mechanism of Alzheimer paired helical filaments, *Proceedings of the National Academy of Sciences of the United States of America* 95, 15712-15717.

200. Combs, B., and Gamblin, T. C. (2012) FTDP-17 tau mutations induce distinct effects on aggregation and microtubule interactions, *Biochemistry* 51, 8597-8607.
201. Lee, V. M., Goedert, M., and Trojanowski, J. Q. (2001) Neurodegenerative tauopathies, *Annual review of neuroscience* 24, 1121-1159.
202. von Bergen, M., Barghorn, S., Biernat, J., Mandelkow, E. M., and Mandelkow, E. (2005) Tau aggregation is driven by a transition from random coil to beta sheet structure, *Biochimica et biophysica acta* 1739, 158-166.
203. Khlistunova, I., Biernat, J., Wang, Y., Pickhardt, M., von Bergen, M., Gazova, Z., Mandelkow, E., and Mandelkow, E. M. (2006) Inducible expression of Tau repeat domain in cell models of tauopathy: aggregation is toxic to cells but can be reversed by inhibitor drugs, *The Journal of biological chemistry* 281, 1205-1214.
204. Crowe, A., Ballatore, C., Hyde, E., Trojanowski, J. Q., and Lee, V. M. (2007) High throughput screening for small molecule inhibitors of heparin-induced tau fibril formation, *Biochemical and biophysical research communications* 358, 1-6.
205. Oakley, C. E., Edgerton-Morgan, H., and Oakley, B. R. (2012) Tools for manipulation of secondary metabolism pathways: rapid promoter replacements and gene deletions in *Aspergillus nidulans*, *Methods in molecular biology* 944, 143-161.
206. Szewczyk, E., Nayak, T., Oakley, C. E., Edgerton, H., Xiong, Y., Taheri-Talesh, N., Osmani, S. A., and Oakley, B. R. (2006) Fusion PCR and gene targeting in *Aspergillus nidulans*, *Nature protocols* 1, 3111-3120.
207. Nayak, T., Szewczyk, E., Oakley, C. E., Osmani, A., Ukil, L., Murray, S. L., Hynes, M. J., Osmani, S. A., and Oakley, B. R. (2006) A versatile and efficient gene-targeting system for *Aspergillus nidulans*, *Genetics* 172, 1557-1566.
208. Soukup, A. A., Chiang, Y. M., Bok, J. W., Reyes-Dominguez, Y., Oakley, B. R., Wang, C. C., Strauss, J., and Keller, N. P. (2012) Overexpression of the *Aspergillus nidulans* histone 4 acetyltransferase EsaA increases activation of secondary metabolite production, *Molecular microbiology* 86, 314-330.
209. Yeh, H. H., Chiang, Y. M., Entwistle, R., Ahuja, M., Lee, K. H., Bruno, K. S., Wu, T. K., Oakley, B. R., and Wang, C. C. (2012) Molecular genetic analysis reveals that a nonribosomal peptide synthetase-like (NRPS-like) gene in *Aspergillus nidulans* is responsible for microperfurane biosynthesis, *Applied microbiology and biotechnology* 96, 739-748.
210. Lo, H. C., Entwistle, R., Guo, C. J., Ahuja, M., Szewczyk, E., Hung, J. H., Chiang, Y. M., Oakley, B. R., and Wang, C. C. (2012) Two separate gene clusters encode the biosynthetic pathway for the meroterpenoids austinol and dehydroaustinol in *Aspergillus nidulans*, *Journal of the American Chemical Society* 134, 4709-4720.
211. Somoza, A. D., Lee, K. H., Chiang, Y. M., Oakley, B. R., and Wang, C. C. (2012) Reengineering an azaphilone biosynthesis pathway in *Aspergillus nidulans* to create lipoxygenase inhibitors, *Organic letters* 14, 972-975.
212. Sanchez, J. F., Chiang, Y. M., Szewczyk, E., Davidson, A. D., Ahuja, M., Elizabeth Oakley, C., Woo Bok, J., Keller, N., Oakley, B. R., and Wang, C. C. (2010) Molecular genetic analysis of the orsellinic acid/F9775 gene cluster of *Aspergillus nidulans*, *Molecular bioSystems* 6, 587-593.
213. Sanchez, J. F., Entwistle, R., Hung, J. H., Yaegashi, J., Jain, S., Chiang, Y. M., Wang, C. C., and Oakley, B. R. (2011) Genome-based deletion analysis reveals the prenyl xanthone biosynthesis pathway in *Aspergillus nidulans*, *Journal of the American Chemical Society* 133, 4010-4017.
214. Chiang, Y. M., Szewczyk, E., Davidson, A. D., Keller, N., Oakley, B. R., and Wang, C. C. (2009) A gene cluster containing two fungal polyketide synthases encodes the biosynthetic pathway for a

- polyketide, asperfuranone, in *Aspergillus nidulans*, *Journal of the American Chemical Society* **131**, 2965-2970.
215. Chiang, Y. M., Szewczyk, E., Davidson, A. D., Entwistle, R., Keller, N. P., Wang, C. C., and Oakley, B. R. (2010) Characterization of the *Aspergillus nidulans* monodictyphenone gene cluster, *Applied and environmental microbiology* **76**, 2067-2074.
216. Ahuja, M., Chiang, Y. M., Chang, S. L., Praseuth, M. B., Entwistle, R., Sanchez, J. F., Lo, H. C., Yeh, H. H., Oakley, B. R., and Wang, C. C. (2012) Illuminating the diversity of aromatic polyketide synthases in *Aspergillus nidulans*, *Journal of the American Chemical Society* **134**, 8212-8221.
217. Bok, J. W., Chiang, Y. M., Szewczyk, E., Reyes-Dominguez, Y., Davidson, A. D., Sanchez, J. F., Lo, H. C., Watanabe, K., Strauss, J., Oakley, B. R., Wang, C. C., and Keller, N. P. (2009) Chromatin-level regulation of biosynthetic gene clusters, *Nature chemical biology* **5**, 462-464.
218. Carlson, S. W., Branden, M., Voss, K., Sun, Q., Rankin, C. A., and Gamblin, T. C. (2007) A complex mechanism for inducer mediated tau polymerization, *Biochemistry* **46**, 8838-8849.
219. LoPresti, P., Szuchet, S., Papasozomenos, S. C., Zinkowski, R. P., and Binder, L. I. (1995) Functional implications for the microtubule-associated protein tau: localization in oligodendrocytes, *Proceedings of the National Academy of Sciences of the United States of America* **92**, 10369-10373.
220. Keller, N. P., Turner, G., and Bennett, J. W. (2005) Fungal secondary metabolism - from biochemistry to genomics, *Nature reviews. Microbiology* **3**, 937-947.
221. Sanchez, J. F., Somoza, A. D., Keller, N. P., and Wang, C. C. (2012) Advances in *Aspergillus* secondary metabolite research in the post-genomic era, *Natural product reports* **29**, 351-371.
222. Gao, J. M., Yang, S. X., and Qin, J. C. (2013) Azaphilones: chemistry and biology, *Chemical reviews* **113**, 4755-4811.
223. Chu, J., and Pratico, D. (2011) Pharmacologic blockade of 5-lipoxygenase improves the amyloidotic phenotype of an Alzheimer's disease transgenic mouse model involvement of gamma-secretase, *The American journal of pathology* **178**, 1762-1769.
224. Hyman, B. T., Phelps, C. H., Beach, T. G., Bigio, E. H., Cairns, N. J., Carrillo, M. C., Dickson, D. W., Duyckaerts, C., Frosch, M. P., Masliah, E., Mirra, S. S., Nelson, P. T., Schneider, J. A., Thal, D. R., Thies, B., Trojanowski, J. Q., Vinters, H. V., and Montine, T. J. (2012) National Institute on Aging-Alzheimer's Association guidelines for the neuropathologic assessment of Alzheimer's disease, *Alzheimer's & dementia : the journal of the Alzheimer's Association* **8**, 1-13.
225. Montine, T. J., Phelps, C. H., Beach, T. G., Bigio, E. H., Cairns, N. J., Dickson, D. W., Duyckaerts, C., Frosch, M. P., Masliah, E., Mirra, S. S., Nelson, P. T., Schneider, J. A., Thal, D. R., Trojanowski, J. Q., Vinters, H. V., Hyman, B. T., National Institute on, A., and Alzheimer's, A. (2012) National Institute on Aging-Alzheimer's Association guidelines for the neuropathologic assessment of Alzheimer's disease: a practical approach, *Acta neuropathologica* **123**, 1-11.
226. Mitchell, T. W., Nissanov, J., Han, L. Y., Mufson, E. J., Schneider, J. A., Cochran, E. J., Bennett, D. A., Lee, V. M., Trojanowski, J. Q., and Arnold, S. E. (2000) Novel method to quantify neuropil threads in brains from elders with or without cognitive impairment, *The journal of histochemistry and cytochemistry : official journal of the Histochemistry Society* **48**, 1627-1638.
227. Holmes, B. B., and Diamond, M. I. (2014) Prion-like properties of Tau protein: the importance of extracellular Tau as a therapeutic target, *The Journal of biological chemistry* **289**, 19855-19861.
228. Mocanu, M. M., Nissen, A., Eckermann, K., Khlistunova, I., Biernat, J., Drexler, D., Petrova, O., Schonig, K., Bujard, H., Mandelkow, E., Zhou, L., Rune, G., and Mandelkow, E. M. (2008) The potential for beta-structure in the repeat domain of tau protein determines aggregation, synaptic decay, neuronal loss, and coassembly with endogenous Tau in inducible mouse models

- of tauopathy, *The Journal of neuroscience : the official journal of the Society for Neuroscience* 28, 737-748.
229. Iqbal, K., Gong, C. X., and Liu, F. (2014) Microtubule-associated protein tau as a therapeutic target in Alzheimer's disease, *Expert opinion on therapeutic targets* 18, 307-318.
 230. Paranjape, S. R., Chiang, Y. M., Sanchez, J. F., Entwistle, R., Wang, C. C., Oakley, B. R., and Gamblin, T. C. (2014) Inhibition of Tau aggregation by three *Aspergillus nidulans* secondary metabolites: 2,omega-dihydroxyemodin, asperthecin, and asperbenzaldehyde, *Planta medica* 80, 77-85.
 231. Vishniac, W., and Santer, M. (1957) The thiobacilli, *Bacteriological reviews* 21, 195-213.
 232. Ward, S. M., Himmelstein, D. S., Ren, Y., Fu, Y., Yu, X. W., Roberts, K., Binder, L. I., and Sahara, N. (2014) TOC1: a valuable tool in assessing disease progression in the rTg4510 mouse model of tauopathy, *Neurobiology of disease* 67, 37-48.
 233. Kanaan, N. M., Morfini, G. A., LaPointe, N. E., Pigino, G. F., Patterson, K. R., Song, Y., Andreadis, A., Fu, Y., Brady, S. T., and Binder, L. I. (2011) Pathogenic forms of tau inhibit kinesin-dependent axonal transport through a mechanism involving activation of axonal phosphotransferases, *The Journal of neuroscience : the official journal of the Society for Neuroscience* 31, 9858-9868.
 234. Chang, E., and Kuret, J. (2008) Detection and quantification of tau aggregation using a membrane filter assay, *Analytical biochemistry* 373, 330-336.
 235. Akoury, E., Gajda, M., Pickhardt, M., Biernat, J., Soraya, P., Griesinger, C., Mandelkow, E., and Zweckstetter, M. (2013) Inhibition of tau filament formation by conformational modulation, *Journal of the American Chemical Society* 135, 2853-2862.
 236. Bhat, R. V., Budd Haeberlein, S. L., and Avila, J. (2004) Glycogen synthase kinase 3: a drug target for CNS therapies, *Journal of neurochemistry* 89, 1313-1317.
 237. Lagoja, I., Pannecouque, C., Griffioen, G., Wera, S., Rojadelaparra, V. M., and Van Aerschot, A. (2011) Substituted 2-aminothiazoles are exceptional inhibitors of neuronal degeneration in tau-driven models of Alzheimer's disease, *European journal of pharmaceutical sciences : official journal of the European Federation for Pharmaceutical Sciences* 43, 386-392.
 238. Brunden, K. R., Yao, Y., Potuzak, J. S., Ferrer, N. I., Ballatore, C., James, M. J., Hogan, A. M., Trojanowski, J. Q., Smith, A. B., 3rd, and Lee, V. M. (2011) The characterization of microtubule-stabilizing drugs as possible therapeutic agents for Alzheimer's disease and related tauopathies, *Pharmacological research : the official journal of the Italian Pharmacological Society* 63, 341-351.
 239. Ballatore, C., Brunden, K. R., Huryn, D. M., Trojanowski, J. Q., Lee, V. M., and Smith, A. B., 3rd. (2012) Microtubule stabilizing agents as potential treatment for Alzheimer's disease and related neurodegenerative tauopathies, *Journal of medicinal chemistry* 55, 8979-8996.
 240. Chang, E., Congdon, E. E., Honson, N. S., Duff, K. E., and Kuret, J. (2009) Structure-activity relationship of cyanine tau aggregation inhibitors, *Journal of medicinal chemistry* 52, 3539-3547.
 241. Honson, N. S., Jensen, J. R., Darby, M. V., and Kuret, J. (2007) Potent inhibition of tau fibrillization with a multivalent ligand, *Biochemical and biophysical research communications* 363, 229-234.
 242. Chirita, C., Necula, M., and Kuret, J. (2004) Ligand-dependent inhibition and reversal of tau filament formation, *Biochemistry* 43, 2879-2887.
 243. Wischik, C. M., Edwards, P. C., Lai, R. Y., Roth, M., and Harrington, C. R. (1996) Selective inhibition of Alzheimer disease-like tau aggregation by phenothiazines, *Proceedings of the National Academy of Sciences of the United States of America* 93, 11213-11218.
 244. Dickey, C. A., and Petrucelli, L. (2006) Current strategies for the treatment of Alzheimer's disease and other tauopathies, *Expert opinion on therapeutic targets* 10, 665-676.

245. Lansbury, P. T., and Lashuel, H. A. (2006) A century-old debate on protein aggregation and neurodegeneration enters the clinic, *Nature* 443, 774-779.
246. Paranjape, S. R., Riley, A. P., Somoza, A. D., Oakley, C. E., Wang, C. C., Prisinzano, T. E., Oakley, B. R., and Gamblin, T. C. (2015) Azaphilones inhibit tau aggregation and dissolve tau aggregates in vitro, *ACS chemical neuroscience* 6, 751-760.
247. Necula, M., and Kuret, J. (2004) A static laser light scattering assay for surfactant-induced tau fibrillization, *Analytical biochemistry* 333, 205-215.
248. Jeganathan, S., von Bergen, M., Brutlach, H., Steinhoff, H. J., and Mandelkow, E. (2006) Global hairpin folding of tau in solution, *Biochemistry* 45, 2283-2293.
249. Forlenza, O. V., Diniz, B. S., Stella, F., Teixeira, A. L., and Gattaz, W. F. (2013) Mild cognitive impairment. Part 1: clinical characteristics and predictors of dementia, *Revista brasileira de psiquiatria* 35, 178-185.
250. Selkoe, D. J. (2004) Cell biology of protein misfolding: the examples of Alzheimer's and Parkinson's diseases, *Nature cell biology* 6, 1054-1061.
251. Cardinale, A., Chiesa, R., and Sierks, M. (2014) Protein misfolding and neurodegenerative diseases, *International journal of cell biology* 2014, 217371.
252. Romero, D., Sanabria-Valentin, E., Vlamakis, H., and Kolter, R. (2013) Biofilm inhibitors that target amyloid proteins, *Chemistry & biology* 20, 102-110.